

COMPUTER AIDED DESIGN OF THE
SELF OSCILLATING MICROWAVE MESFET MIXER

M.S. THESIS

Ahmad Hakimi DARSINOOIEH, B.S.

Date of Submission : 4 June 1990

Date of Approval : 21 June 1990

Examination Committee :

Supervisor : Prof.Dr.Osman PALAMUTÇUOĞULLARI

Member : Prof.Dr.Bingül YAZGAN

Member : Prof.Dr.Eşref ADALI

W. E.

Teknik Doktora İmza Kurulu
Doktora İmza Kurulu

JUNE 1990

ACKNOWLEDGEMENTS

I wish to thank my supervisor, Prof.Dr. Osman PALAMUTÇUOĞULLARI for his guidance with this research work and his efforts in the preparation of the thesis. His continuous cooperation throughout my work is highly appreciated.

I would also like to thank Dr. F. Acar SAVACI for his consultancy, which enabled me to complete of this work. His guidance is also would be much appreciated.

June, 1990

Ahmad Hakimi DARSINOOTEH

CONTENTS

SUMMARY	v
ÖZET	vi
CHAPTER 1. INTRODUCTION	1
1.1. The Criteria For Oscillation	2
1.2. Basic Mixer Theory	5
1.3. Theory Of Self Oscillating Mixer	11
1.4. General GaAs FET Characteristics	12
1.4.1. Small-Signal Equivalent Circuit For The Single Gate GaAs MESFET	13
1.4.2. Dual Gate MESFET	15
1.4.3. Equivalent Circuit of GaAs Dual Gate MESFETs	16
1.4.4. Dual Gate MESFET As Three Port Device	20
CHAPTER 2. DIELECTRIC RESONATOR OSCILLATORS	23
2.1. Introduction	23
2.2. Oscillation And Stability Conditions ..	24
2.3. Microwave Dielectric Resonator	33
2.4. Coupling of a Dielectric Resonator With a Microstrip Line	37
2.5. Circuit Realization of Dielectric Resonator MESFET Oscillator	42
CHAPTER 3. COMPUTER AIDED DESIGN OF DUAL GATE MESFET OSCILLATOR	53
3.1. 3-Port s-Parameters From 2-Port Device.	55
3.2. Conditions For Oscillations And Unconditionally Stability In A Cascade Circuit	57
3.2.1. Unconditional Stability Conditions Of Gate 1	57
3.2.2. Oscillation Conditions	63
3.3. Investigating Oscillation Conditions ..	68
3.3.1. Oscillator Stability Criterion	69
CHAPTER 4. DUAL-GATE MESFET MIXERS	85
4.1. High-Frequency Model Of The Dual-Gate MESFET Mixer	87
4.2. The DC Analysis Of The Dual-Gate MESFET	88
4.3. Numerical Analysis Of Nonlinear Model Of The Dual-Gate MESFET Mixer	97
4.3.1. Describing The Method	98
4.3.2. Nonlinear Analysis Of Dual-Gate MESFET Mixer Under Large Signal Excitation	102

4.4. Small Signal Analysis Of The Mixer ..	108
CHAPTER 5. RESULTS AND CONCLUSION	114
REFERENCES	119
APPENDIX-A: PROGRAMS	121
APPENDIX-B: OUTPUTS FOR PROGRAMS	140
BIOGRAPHY	159

SUMMARY

A small signal equivalent circuit for GaAs dual gate MESFETs, valid for 2-11 GHz, is presented. And also a large signal equivalent-circuit model of a GaAs dual-gate mixer containing twelve elements, of which six are voltage dependent, is solved for local oscillator and signal frequencies of 11 and 12 GHz, respectively.

A new method for determining the steady-state response of nonlinear microwave circuits with periodic excitation is described. The method minimizes time-domain calculations by introducing a criterion for selecting the variables to be considered as unknowns and for solving the resulting nonlinear system by a new and efficient algorithm.

Investigation of the oscillation conditions is done by using 2-port S-parameters. In the case of a dielectric resonator coupled to a microstrip line, the methods for determination of the reflection coefficient at the resonant frequency have been represented.

ÖZET

KENDİNDEN UYARMALI ÇİFT GEÇİTLİ GaAs MESFET KARIŞTIRICININ BİLGİSAYAR DESTEKLİ TASARIMI

GaAs Alan-Etkili Tranzistor'lar ve mikrodalga tüm-devre teknolojisindeki (MIC) yeni gelişmeler sonucunda osilatör, kuvvetlendirici ve karıştırıcıları X bandının üzerinde tasarlamak olanlığı ortaya çıkmıştır [1].

Bir çift-geçitli GaAs FET'in X bandında belli bir kazançla Kendinden Uyarmalı Karıştırıcı (SOM) olarak kullanılabileceği gösterilmiştir.

Kendinden uyarmalı karıştırıcı FET'li bir alıcı ön-katında da kullanıldığından, ön-katın tüm işlevi sadece üç FET'le gerçekleştirilecektir.

Bu durum GaAs'in yapı malzemesinde ekonomik bakım-dan verim sağlanması yönünden önem taşımaktadır. Bu yüzden iki katlı tek geçitli FET'li kuvvetlendirici ve bir çift geçitli FET'li kendinden uyarmalı karıştırıcı herhangi bir hibrid alıcı için gerekli elemanlardır[10].

GaAs çift-geçitli MESFET tek bir eleman olarak ön kuvvetlendirici, karıştırıcı ve lokal osilatörün yeri tutar. Birinci geçitteki giriş işaretini (ω_{RF}) için çift geçitli FET, ortak geçitli MESFET'e seri olarak bağlı ortak-kaynaklı MESFET kuvvetlendirici olarak tanımlanabilir. Tüm FET'in geçiş iletkenliği FET'in ikinci geçidindeki osilasyon sonucu oluşan lokal osilatör gerilimi (ω_{LO}) ile modüle edilir. Çıkış akımı $\omega_{If} = |\omega_{RF} - \omega_{LO}|$ açısal frekanslı spektral bileşenleri içerir.

Tek geçitli FET yerine çift geçitli FET'leri kullanmanın yararı, tek geçitli FET karıştırıcılara ait olan dönüşüm kazancı ve düşük gürültü özelliklerinin dışında, işaret ve lokal osilatör kısımlarının ayrı olması ve ayrı empedans uydurma olanağının bulunmasının yanısıra oluşan güçlerin doğrudan birbirlerine eleman içinde eklenebilmesidir. Çift geçitli FET'lerin çalışma karakteristikleri, iki tek geçitli FET'in analizi birleştirilerek analiz edilebilir. Genellikle kaynağı toprağa bağlanmış 3-kapılı devre olarak da karakterize edilir [11].

Birinci bölümde tek ve çift geçitli FET'lere ilişkin daha fazla bilgi verilmiştir. Yine bu bölümde her iki FET içinde küçük ve büyük işaret eşdeğer devreleri

incelemiştir. Çift geçitli FET için iki tek geçitli FET'in eşdeğer devresinden meydana gelen, eşdeğer devre önerilmiştir. Son zamanlarda çift geçitli FET eşdeğer devresi, iki adet birbirine eş tek geçitli FET varsayılarak ölçülen S-parametrelerinden belirlenmiştir. GaAs çift geçitli MESFET'in eşdeğer devresi ölçülen 3-kapılı S-parametrelerinden elde edilebilir. Bu devre 28 elemanlı olup, 2-11 GHz frekans aralığında geçerlidir ve tel dirençleri, bağlantı endüktansları ve elektrodlar arası kapasiteler gibi parazitik elemanları da kapsamaktadır.

Daha önce de belirtildiği gibi GaAs MESFET kullanarak osilasyon oluşturmak olasıdır. Mikrodalga osilatörleri için frekans kararlılığı, kararlı çıkış gücü gibi elektriksel özelliklerin yanısıra, yüksek güvenililik ve düşük maliyette önemli unsurlardır. Bunun yanı sıra haberleşme cihazları küçülürken, osilatöründe az yer kaplaması istenilen bir başka özellikledir. Osilatörün elektriksel karakteristik, maliyet ve büyülüğünü belirleyen unsurlar, osilasyon için kullanılan aktif eleman ile osilasyon frekansının kontrolunda kullanılan rezonatördür. Son zamanlarda X bandının üzerinde çalışan osilatörler, Silisyum bipolar tranzistor ve GaAs FET'lerdeki gelişmeler sonucunda tasarılmaktadır. Bu aktif elemanların yanısıra, osilasyon frekansının kontrolunda dielektrik rezonatörler kullanılarak daha kaliteli ve az yer kaplayan osilatörlerin gerçekleştirilmesi mümkün olmuştur. İkinci bölümde söz edildiği gibi, mikrodalga osilatörlerinde kullanılan dielektrik rezonatörlerin elektriksel karakteristikleri hakkında şunlara dikkat edilmelidir:[7].

- 1) Rezonatörün boyutlarının küçük olması için yüksek bağıl dielektrik sabiti (ϵ_r),
- 2) Kararlı osilasyon frekansında osilasyon güç kaybını azaltmak ve frekans kararlılığını iyileştirmek için yüksek Q_0 ,
- 3) Osilasyon frekans kararlılığını iyileştirmek için rezonans frekansının ısiyla değişme katsayısı T_f küçük olmalıdır.

Dielektrik rezonatörler bu koşulları sağlayacak biçimde kullanılmaktadır. Örnek olarak Q_0 'ı 10 GHz de 5000, $\epsilon_r = 28 \sim 30$ ve $T_f = +1 \text{ ppm}/^\circ\text{C}$ olan tipik bir dielektrik rezonatör ($\text{Ba}(\text{Zn}_{1/3}\text{Ta}_{2/3})_{03} - \text{Ba}(\text{Zn}_{1/3}\text{Nb}_{2/3})_{03}$) verilebilir.

Osilatör gibi mikrodalga tümleşik devre uygulamalarında dielektrik rezonatörün mikroşerit hatlarla bağlanması gereklidir. Bağlama faktörü β , sabit koruyucu ortamda dielektrik rezonatör ile mikroşerit hatlar arasındaki uzaklığın bir fonksiyonu olup, rezonans bağlanma direncinin rezonatör dışı dirence oranı olarak tanımlanır.

$$\beta = \frac{R}{R_{ext}} = \frac{R}{2Z_0}$$

β aynı zamanda çeşitli iyilik faktörlerine aşağıdaki ifade ile bağlıdır.

$$Q_u = Q_L(1+\beta) = \beta \cdot Q_{ex}$$

Q_u , Q_L ve Q_{ex} sırasıyla yüksüz, yüklü ve dış iyilik faktörlerini göstermektedir.

Osilasyon frekansı, gereksinime bağlı olan farklı yaklaşımlar kullanılarak dar bir frekans aralığında ayarlanabilir. Tranzistorlu dielektrik rezonatörlü osilatörün frekans ayarı mekanik veya elektriksel olarak yapılabilir.

Mekanik ayar durumunda, ayar vidası kutunun üst kısmına dielektrik rezonatörün üzerine gelecek şekilde yerleştirilir.

Ayar vidasının derinliğinin (d) arttırılması genellikle TE₀₁₀ modunda kullanılan dielektrik rezonatörün rezonans frekansını artıracaktır. Dielektrik rezonatörden geri besleme elemanı olarak hem seri hem de paralel geribeslemede yararlanılabilir. Seri geri besleme için aşağıdaki yol izlenmelidir: Tranzistor üç kapılı bir eleman olarak düşünülür, üç kapılı S-parametreleri ölçülü veya ortak-kaynaklı iki kapılı S-parametrelerinden hesaplanabilir. Üç kapılı S-parametrelerini kullanmanın yolları şöyle ifade edilebilir:

- (i) Geribesleme analizi için, devreye geribesleme empedansı eklemeden önce S-parametrelerini Z veya Y parametrelerine dönüştürme gereksinimini ortadan kaldırır.
- (ii) Bir MESFET'in üç kapılı S-matrisinin satır ve sütunlarının toplamı 1'e eşittir.

Bu çalışmanın üçüncü bölümü çift geçitli MESFET için iki kapılı S-parametrelerini oluşturmaya ve osilasyon koşullarını belirlemeye ayrılmıştır. Çift geçitli bir FET yerine aynı özellikte iki FET kullanılmıştır. İki ayrı FET'in (AVANTEK 10650 ve AVANTEK 11671) dağılıma parametreleri, çift geçitli FET'in S-parametrelerini elde etmede kullanılabilir. İki geçitli elemanın, ortak kaynaklı birinci FET ve ortak geçitli ikinci FET'in ard arda bağlanmasıyla oluşturduğu düşünülebilir. Çift geçitli FET'in iki kapılı S-parametrelerini hesaplamada şu yöntem izlenebilir:

- 1) Mevcut 2-kapılı ortak kaynaklı S-parametrelerinden 3-kapılı S-parametrelerinin elde edilmesi.
- 2) Geçit veya savağı gerekli yük veya empedansla kapatarak 3-kapılı elemanın S-parametrelerinden 2-kapılı elemanın S-parametrelerinin hesaplanması.

- 3) Ortak kaynak ve ortak geçitli veya ortak savaklı FET'in zincir dağılma (ϕ_1 , ϕ_2) parametrelerinin elde edilmesi.
- 4) ϕ_1 ve ϕ_2 yi çarparak çift geçitli FET'in dağılma matrisinin ($\Phi = \phi_1 \cdot \phi_2$) elde edilmesi.
- 5) Φ matrisinden S matrisine dönüşüm yaparak çift geçitli elemanın dağılma parametrelerinin bulunması.

FET'in ikinci geçidi, rezonans frekansında Γ yansıtma katsayılı mikroşerit hatla kuple olan dielektrik rezonatörle sonlandırıldığı için iki osilasyon koşulu sağlanmalıdır [16].

$$|1/s_{11}| \leq |\Gamma|$$

$$\text{açı } (1/s_{11}) = \text{açı } (\Gamma)$$

Bu koşullar $1/s_{11}$ in cinsinden düşünüldüğünden osilatör tasarımında oldukça yararlıdır. $(1/s_{11})$ Smith abağında çizildiğinde R ve X in değerleri okunup negatif direnç ve reaktans değerlerini elde etmek için -1 ile çarpılır.

Birinci osilasyon koşulunun ($|1/s_{11}| \leq |\Gamma|$) sağlanığı bölgede sadece bir frekansta ikinci koşul ($\text{açı } (1/s_{11}) = \text{açı } (\Gamma)$) sağlandığında kararlı bir osilasyon oluşacaktır. Grafik olarak, şayet $1/s_{11}$ ve Γ nin fazları değişen frekansla zıt açısal yönlerde değişiyor ise kararlı bir osilasyon meydana gelecektir. Diğer bir deyişle, $1/s_{11}$ rezonans çevrimini kesmeli ve frekansla değişimi gösteren yön zıt olmalıdır.

Çift geçitli MESFET'in diğer bir uygulama alanı da karıştırıcılardır. Bu tür uygulamalarda çift geçitli MESFET'in büyük işaret eşdeğer devre modeli dördüncü bölümde gösterilmiştir. Schottky-engel kapasitesinin gerilime bağımlılığını veren ifadeler ve dc karakteristikleri kullanılarak, model zaman domeninde çözülmüş ve meydana gelen frekans bileşenlerini belirlemek için sonlu Fourier Analizi uygulanmıştır. Bu bölümde de gösterildiği gibi yüksek frekanslarda FET'in eşdeğer devresinde ilk FET'in birinci geçit ve kaynağı arasında, diğer FET'in ikinci geçit ve savaşı arasındaki kapasitelein gerilimleri $V_1(t)$, $V_2(t)$ ile kontrol edilen lineer olmayan elemanlar vardır.

Lineer olmayan katı hal, mikrodalga devrelerinin optimum tasarımı lineer olmayan performanslarını belirlemede doğru bir teknik gerektirir.

Bu tür lineer olmayan sistemlerin çözümünde değişik nümerik teknikler kullanılmaktadır. Newton-Raphson yöntemi lineer olmayan devrelerin çözümünde en çok kullanılan nümerik tekniktir. Bununla beraber türev değerlerini hesaplamadaki bilgisayar süresinin fazlalığı sebebiyle, harmonik değerler ve nonlineariteler düşünüldüğünde pratik bir yöntem olmamaktadır [13].

Bu çalışmada bilinmeyenler olarak düşünülen değişkenleri seçmek için bir kriter veren analiz yöntemi açıklanmıştır.

CARLOS CMACHO-PENALOSA [13] tarafından önerilen yeni yöntemi kullanarak lineer olmayan sistemin çözümü zaman-domeni analizini lineer olmayan elemanların akım ve gerilimlerini hesaplamaya indirgemistiştir.

Büyük işaret sürme durumunda devredeki bütün akım ve gerilimler zamanın peryodik fonksiyonu olduklarından Fourier serileri ile gösterilirler:

$$X(t) = \sum_{k=-\infty}^{\infty} X_k \exp(jk\omega_0 t)$$

İlgilenilen bütün fonksiyonlar gerçek olduklarından ve yerel osilatör frekansı

$$f_o = \frac{\omega_o}{2\pi} \text{ olduğundan } X_{-k} = X_k^* \text{ olur.}$$

Herhangi bir lineer olmayan sistem lineer olmayan gerçek denklem sistemi $X=f(X)$ biçiminde yazılabilir ve çözümü dördüncü bölümde anlatılan iterasyon tekniği kullanılarak nümerik yolla bulunabilir. Akım veya gerilimlerin Fourier katsayıları kolaylıkla bulunamadığından, bu katsayılar bağıntısı aşağıda verilen ayrik Fourier dönüşümü (DFT) kullanılarak belirlenir.

$$X_n = \frac{1}{N} \sum_{k=0}^{N-1} X_s(k\Delta t) e^{-j2\pi nk/N} \quad n=0, 1, \dots, N-1$$

$X_s(k\Delta t)$; $X(t)$ fonksiyonunun örneklenmiş durumu; N ; örnek sayısı, $\Delta t=T/N$, $f_o=1/T$.

Sonuç olarak eşdeğer devredeki çıkış akımları lineer olmayan elemanların Fourier katsayılarını kullanılarak ve devrenin lineer analizi yardımıyla bulunabilir.

Küçük RF işaretinde karıştırıcılardaki frekans değerleri $f_{s,k}=kf_o+sf_s$ bağıntısıyla verilir. Burada $-\infty \leq k \leq \infty$, $s=0$ ve ± 1 , f_o ve f_s sırasıyla yerel osilatör ve RF frekanslarıdır. Buna göre devredeki tüm genlik değerleri,

$$X(t) = \sum_{k=-\infty}^{\infty} \sum_{s=0, \pm 1} X_{k,s} \exp[j(k\omega_0 + s\omega_s)t]$$

birimindedir [14]. $k=\pm 5$ ve $s=0, \pm 1$, $N=10$, $f_o=11$ GHz, $f_s=12$ GHz için çıkış akımı, değişik V_{LO} genliği ve besleme değerlerinde hesaplanmıştır.

CHAPTER 1

INTRODUCTION

The development of GaAs MESFET devices in the early 70's has significantly influenced system designer to consider it as a multi purpose microwave active device.

The transferred electron or the Gunn oscillator, which has been the main selection for low power solid-state oscillator applications, suffers from two main drawbacks. One is the low d.c to r.f conversion efficiency and the other is the threshold current requirement.

The GaAs FET oscillator provides a higher d.c to r.f conversion efficiency ($> 10\%$) and does not have any threshold current requirements.

Being a three terminal structure the GaAs FET is an extremely versatile active oscillator circuit element and by making use of this feature it is possible to control the behaviour of the oscillator to provide modulation, compensation and stabilisation, etc.

The GaAs FET oscillator activity has received much attention in the recent years. High efficiency fixed frequency oscillators have been reported in the literature for frequencies up to 25 GHz and beyond.

Electronic tuning of FET oscillators by YIG resonators and varactor diodes has been extensively researched. Although most of the GaAs FET oscillators are realised in low Q microstrip circuits, efforts have also been directed towards improving their carrier noise and temperature stability by employing stabilisation techniques.

Other applications like monolithic oscillators and pulsed RF oscillators etc. have also been extensively researched.

In this chapter GaAs FET microwave oscillator design and the techniques for frequency stabilisation of these oscillators using dielectric resonators reviewed.

1.1. The Criteria For Oscillation

The criteria for osillation may be stated in several rigorous and equivalent ways:

First an oscillator containing a two part active device must provide a feedback path where by part of the output is fed back to the input. If the feedback signal is larger than, and in phase with the input, osillating begin and grow in amplitude until saturation reduces the gain around the feedback to unity. Therefore criterion one is that, a circuit will oscillate when a feedback path is present providing at least unity loop gain with zero phase shift. Conceptually, a circuit containing such a feedback path is an amplifier that can generate its own input.

Hence a second criterion for oscillation is that the stability factor (K) of an oscillator circuit must be less than 1.

When a circuit meets either of the first two oscillation criteria, that determinant of its node voltage or mesh current equation goes to zero, and this is a third criterion for oscillation.

Equivalent circuits and most of the analytical tools of circuit analysis are based upon linearity, a condition that does not exist in most oscillators. This means that the steady state operating conditions of an oscillator in general cannot be predicted accurately by

simple mathematical techniques.

The circuits reach steady-state operation only when a transistor has been driven into nonlinear operation that its gain averaged over each output cycle drops to a small fraction of the nominal small signal value.

Data sheet tabulations of transistor parameters define only the initial conditions of an oscillator circuit, the transitional and final value are usually unknown.

In order for oscillations to start, the output of an amplifying device must be feedback to the input with gain greater than unity and with a phase shift of 0° or some multiple of 360° . In an ideal oscillator circuit this can occur at only one frequency, this will be the frequency of oscillation.

If the phase shift through the feedback network and active device is independent of the transistor operation conditions, the frequency of oscillation will be the same at steady state as it was when oscillations began and it may be predicted accurately by small signal analysis of the initial circuit.

It is also possible to predict the minimum transistor gain that will initiate oscillation, but this and the operating frequency are about all that small signal analysis can yield.

Frequency dependence of passive component values is another complicating factor. Capacitors larger than a few hundred picofarads tend to look inductive above about 10 megaherts, and stray capacitance between turns may cause inductors to become capacitive. These effects are difficult to model in conventional circuit theory and they may allow a circuit to satisfy the conditions

for oscillation at frequencies that are not predicted by circuit analysis.

Circuit analysis of an oscillator is thus only the beginning of the design process. It will yield values for perhaps all of the frequency-determining components in the circuit, but it can say little or nothing about such things as power output, efficiency, waveform purity, frequency stability, and sensitivity to temperature and supply voltage variations.

These points are most often resolved by taking the small signal computations as a starting point, and then building. The circuit and adjusting component values until the desired performance is achieved.

Microwave oscillator for the communication and radar systems must satisfy the following characteristics:

- 1) Good frequency stability:
 - a) Temperature stability
 - b) Load variation stability
- 2) Good output power stability
- 3) Low thermal noise of the active device
- 4) Small dimension and low cost
- 5) Reliable operation characteristics.

In microwave oscillators the dielectric resonators have recently become very popular as a feedback element. In general two type of feedback configurations are used.

- 1) Dielectric resonator as a series feedback element
- 2) Dielectric resonator as a parallel feedback element.

Figure 1.1 presents these possibilities. Where in Fig 1.1.a and c DR is placed as series element and in (b) DR provides parallel feedback between drain and gate terminals.

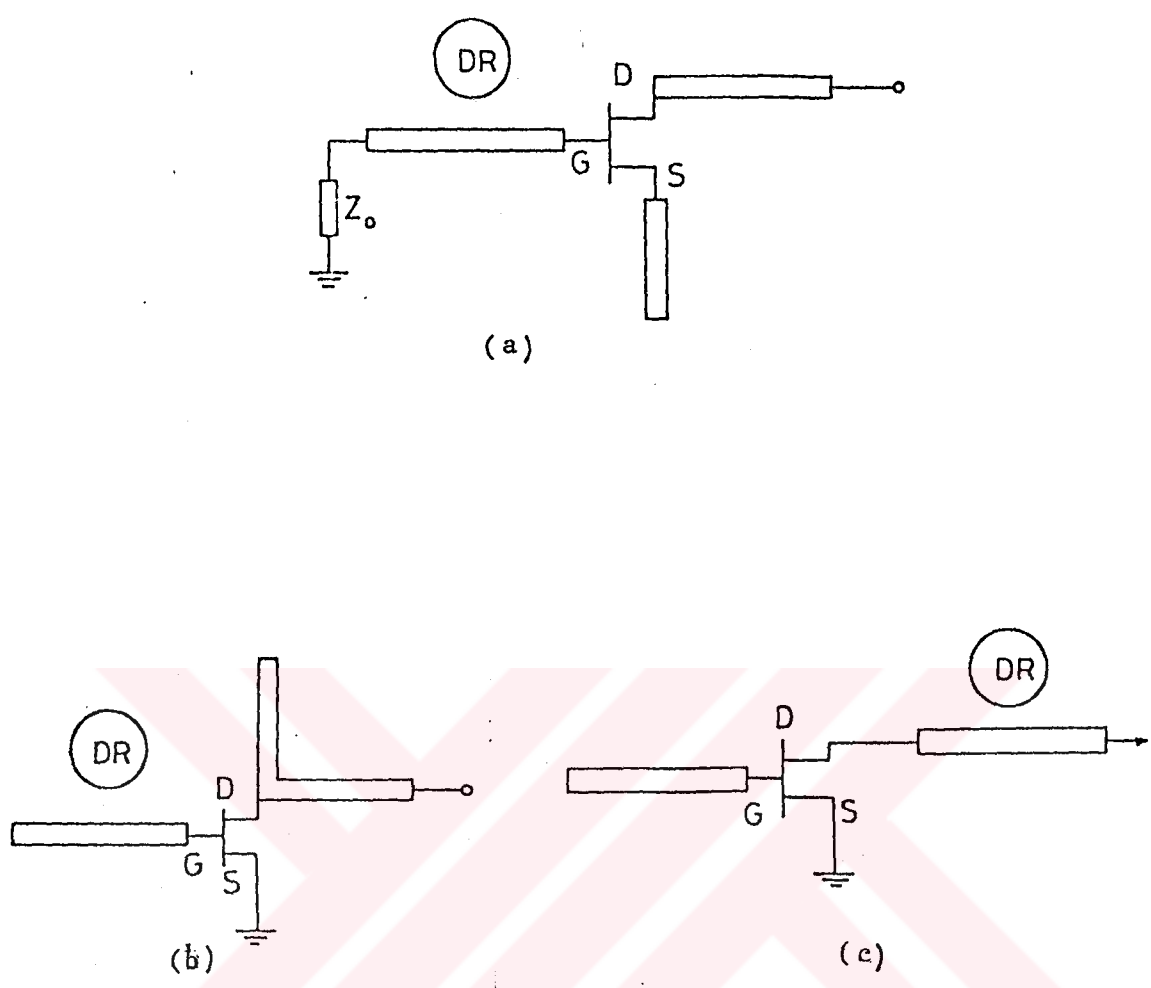


Fig. 1.1 Different configurations showing how the dielectric resonator may be used as a feedback element.

1.2. Basic Mixer Theory

Any nonlinear device can serve as a mixer. Nonlinearity is required for the production of frequencies which are not present in the input. Thus mixers may utilize diodes, FETs, BJTs.

The design choices hinge upon considerations of gain (or loss), noise figure, stability, dynamic range, and possible generation of undesired frequency components that produce intermodulation and cross-modulation distortion.

Figure 1.2 illustrates a simple mixer that consists of a nonlinear device with two input voltages $v_1(t)$ and $v_2(t)$ of different frequencies f_1 and f_2 , respectively.

If the device were perfectly linear, the output voltage or current would contain frequencies f_1 and f_2 only.

The nature of the nonlinearity will dictate what other frequencies are generated.

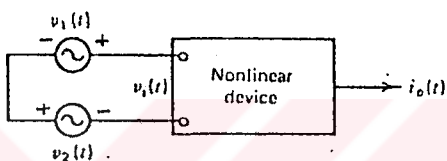


Fig. 1.2 Nonlinear device used as a mixer.

In general, the input-output relationship of a memoryless system in the time domain can be expressed by a Taylor series.

$$i_o(t) = I_0 + a v_i(t) + b [v_i(t)]^2 + c [v_i(t)]^3 + \dots \quad (1.1)$$

In which I_0 is the quiescent output current and $v_i(t)$ represents the summation of the effects of all input signals. If the input contains only one frequency, the nonlinearity will generate harmonics of this frequency and will alter the direct-current component. If several input frequencies are present, sum and difference frequencies as well as harmonics will be generated.

The sum and difference frequencies generated by the square term in (1.1) are called second-order intermodulation products; those generated by the cubed term are third-order products.

A square-law device is ideal as a mixer element, since the least number of undesired frequencies are produced.

If the device has the transfer characteristic

$$i_0(t) = a v_i(t) + b [v_i(t)]^2 \quad (1.2)$$

and input

$$v_i(t) = V_1 \cos \omega_1 t + V_2 \cos \omega_2 t \quad (1.3)$$

the output current becomes

$$\begin{aligned} i_0(t) = & a V_1 \cos \omega_1 t + a V_2 \cos \omega_2 t + b V_1^2 \cos^2 \omega_1 t + \\ & b V_2^2 \cos^2 \omega_2 t + 2b V_1 V_2 \cos \omega_1 t \cos \omega_2 t \end{aligned} \quad (1.4)$$

The first two terms in (1.4) are of no interest for mixer action, except that in a practical circuit it may be necessary to filter them out. By the use of the trigonometric identity

$$b V_1^2 \cos^2 \omega_1 t = \frac{b}{2} V_1^2 (1 + \cos 2\omega_1 t)$$

the third and fourth terms are seen to represent a dc component and second harmonics of the input frequencies. The final term in (1.4) called the product term, yields the desired output, that is

$$2b V_1 V_2 \cos \omega_1 t \cos \omega_2 t = b V_1 V_2 [\cos(\omega_1 - \omega_2)t + \cos(\omega_1 + \omega_2)t] \quad (1.5)$$

Note that the amplitudes of the sum and difference frequency components are proportional to the product $V_1 V_2$ of the input-signal amplitudes.

Usually, in receiver mixers, only the difference-frequency output component is desired, so the original frequencies, their harmonics, and their sum must be

removed by filtering or other means.

A general mathematical treatment of the spectral analysis of mixer output is necessary. This is desirable because the approach given in the preceding paragraph would be very cumbersome if it were extended to modulated input signals and nonlinearities of higher order.

By mean of Fourier transform theory, a time function $f(t)$ and its transform $G(f)$ in the frequency domain are related by

$$f(t) = \int_{-\infty}^{\infty} G(f) e^{j2\pi ft} df \quad (1.6)$$

and

$$G(f) = \int_{-\infty}^{\infty} f(t) e^{-j2\pi ft} dt \quad (1.7)$$

Now, if $G_0(f)$, $G_1(f)$ and $G_2(f)$ are the Fourier transforms of $f_0(t)$, $f_1(t)$, and $f_2(t)$ respectively, and if

$$f_0(t) = f_1(t) \cdot f_2(t) \quad (1.8)$$

the convolution theorem states that

$$G_0(f) = \int_{-\infty}^{\infty} G_1(\lambda) \cdot G_2(f-\lambda) d\lambda \quad (1.9)$$

in which λ is a dummy frequency variable. Although the integration of (1.9) may be formidable in general, it can be done easily by a graphical process for problems that involve discrete frequencies.

For an example of graphical convolution, let $f_1(t)$ and $f_2(t)$ be given by

$$f_1(t) = \cos(\omega_1 t + \theta_1) \quad (1.10)$$

and

$$f_2(t) = \cos(\omega_2 t + \theta_2) \quad (1.11)$$

By the use of a trigonometric identity, the product function is found to be

$$f_0(t) = f_1(t) \cdot f_2(t) = \frac{1}{2} \{ \cos[(\omega_1 + \omega_2)t + (\theta_1 + \theta_2)] + \cos[(\omega_1 + \omega_2)t + (\theta_1 - \theta_2)] \} \quad (1.12)$$

The same result is obtained by graphical convolution in Fig.1.3 the spectrum of $G_2(\lambda)$, the Fourier transform of $f_2(t)$, is shown in Fig.1.3a as two impulse functions at $\pm f_2$.

The impulses have areas or weights of 0.5 and phase angle as shown on the diagram.

To obtain the spectrum $G_2(-\lambda)$ as in Fig.1.3b all components of the $G_2(\lambda)$ spectrum are inverted or folded with respect to the origin; that is, each component appears at the negative of its original frequency. The $G_2(f-\lambda)$ spectrum of Fig.1.3c is produced by sliding the $G_2(-\lambda)$ spectrum to the right by the amount f , which can be chosen arbitrarily.

Multiplication of the spectrum of $G_2(f-\lambda)$ by that of $G_1(\lambda)$ (shown in Fig.1.3d) yields the spectrum of $G_0(f)$ according to the convolution integral (1.9).

The infinite integration is easily performed because the two spectra in the product contain only weighted impulse functions, and a product term will result only if lines in the two spectra coincide. For the spectra shown in Fig.1.3c and d, $G_0(f)=0$, because f was chosen such that no lines in the two spectra are coincide.

Now let f decrease, which will slide the lines in Fig.1.3c to the left, until line A corresponds with line D of the $G_1(\lambda)$ spectrum.

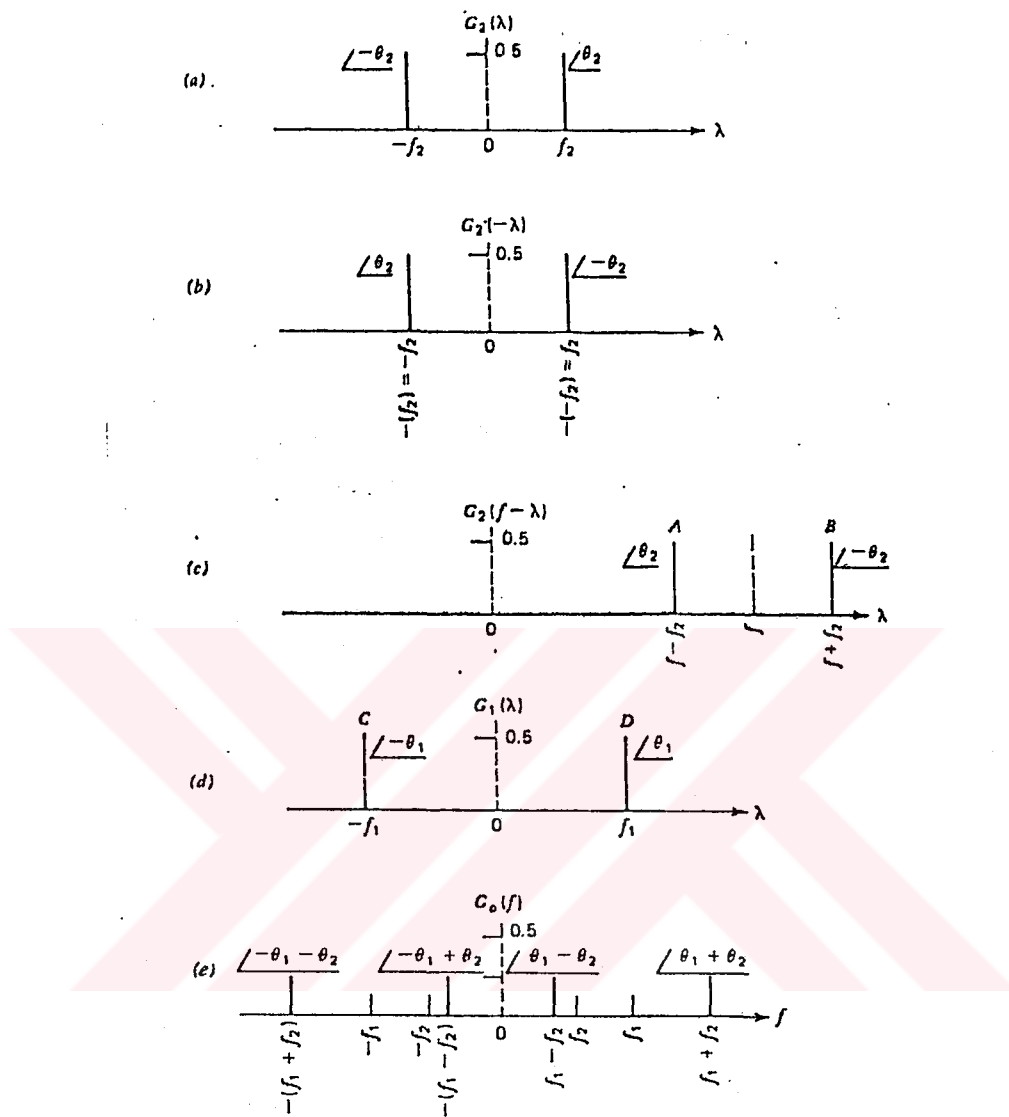


Fig.1.3. Illustration of graphical convolution.
 (a) spectrum of $f_2(t) = \cos(\omega_2 t + \theta_2)$; (b) inverted spectrum of $f_2(t)$ obtained by folding or inverting the components of (a) with respect to the origin; (c) the $G_2(-\lambda)$ spectrum is shifted to the right by the value of variable f to obtain the spectrum of $G_2(f-\lambda)$ shown here; (d) spectrum of $f_1(t) = \cos(\omega_1 t + \theta_1)$ and (e) spectrum of the product $f_0(t) = f_1(t) \cdot f_2(t)$.

Integration over the entire λ axis will now yield a value for $G_0(f)$; that is, it will be the product of the two impulse functions A and D, the product of their weights and the sum of their angles.

The value of f where all this happens is $f=f_1+f_2$, and the resulting value of G_0 is $0.25|\theta_1+\theta_2|$. The other lines in the G_0 spectrum are obtained in the same way.

1.3. Theory Of Self Oscillating Mixer:

It has been shown that a dual-gate GaAs FET can be used as a self oscillating mixer with gain in the X-band implanted in to an FET receiver.

In this work two identical FET's in cascode connection will be used instead of a dual gate FET as the self oscillating mixer element.

As shown in Fig.1.4 The RF signal is injected at the gate of first FET and the second FET acts as local oscillator.

An open microstrip line which its lengths it $\lambda/4$ would be short circuit at resonance frequency and short circuits the pump signal at the output.

So, the conditions for oscillating and mixing for these two FET's must be provided. In Chapter these conditions by using two computer programs will be discussed.

In Chapter 4 more rigorous analysis of a dual gate MESFET mixer is presented which takes into account the nonlinear components in the actual circuits. Nonlinearities in a dual gate MESFET, requirs an extremly complicated circuit analysis methods which can not be solved without resorting to numerical methods.

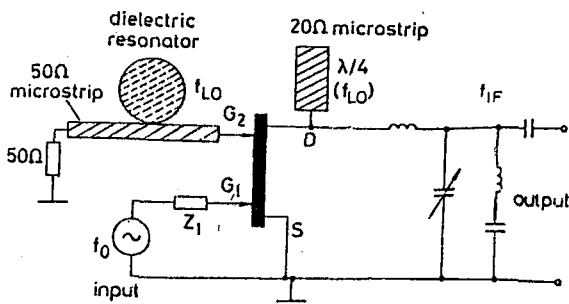


Fig.1.4. Equivalent circuit of a dual gate FET self oscillating mixer.

1.4. General GaAs FET Characteristics:

A MESFET consists of a semi-insulating GaAs substrate on which an n-type epitaxial layer (also called a channel) of about $0.2 \mu\text{m}$ thickness is deposited by epitaxial growth. Sometimes a buffer layer is introduced between the epi-layer and semi-insulating substrate. The buffer layer restricts the diffusion of impurities from the substrate. The source and the drain electrodes are deposited on the active layer using photolithography technique.

Another contact, a metal-semiconductor Schottky junction is added between the source and the drain. This is called the "gate". The gate length is typically 0.5 to $0.7 \mu\text{m}$ and source-drain spacing is about $2 \mu\text{m}$.

Metal-semiconductor FET's (MESFET's) find applications as low noise amplifiers, power amplifiers, oscillators, mixers, modulators, and in logic circuits. For all these applications the device should be characterized, accurately and equivalent circuits must be obtained.

1.4.1. Small-Signal Equivalent Circuit For The Single Gate GaAs MESFET:

For CS configuration the small signal equivalent circuit of a GaAs MESFET can be represented accurately by lumped elements up to 12 GHz for the extrinsic and 14 GHz for the intrinsic FET as is shown in Fig.1.5.

In the intrinsic model, the depletion layer capacitance under the gate electrode is denoted by the source gate capacitance C_i and its charging resistance in the channel by R_i , C_f represents the fringing capacitance between the drain and the gate, and R_0 shows the effect of drain-source channel resistance. $R_s, R_g, R_d, L_s, L_i, C_0$, and L_o represent the extrinsic parasitic elements.

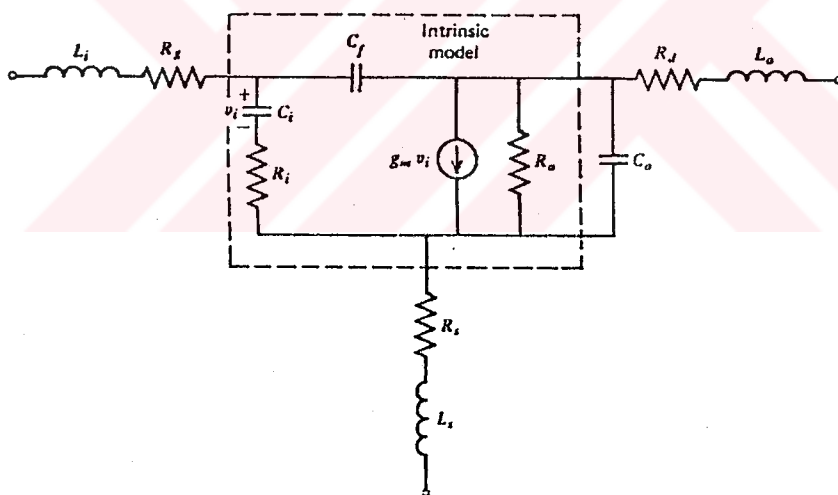


Fig. 1.5 A GaAs FET small-signal equivalent circuit.

For a 0.5μ gate GaAs MESFET, $\tau_0 = L_g / v_s = 2.5 \text{ psec}$. The activity of the FET is determined by its maximum frequency of oscillation ω_{\max} where the FET becomes passive. Consider the intrinsic model of the FET in Fig. 1.5. Its admittance matrix $Y = [Y_{ij}]$ is given as:

$$Y = \begin{bmatrix} \frac{\omega^2 \tau_i C_i}{1 + \omega^2 \tau_i^2} + j\omega(C_i + C_f) & \frac{g_m}{1 + \omega^2 \tau_i^2} - j\omega(g_m \tau_i + C_f) \\ -j\omega C_f & G_0 + j\omega C_f \end{bmatrix} \quad (1.13)$$

where $\tau_i = C_i R_i$ and $G_0 = 1/R_0$. When the FET is passive we get $Y+Y^T \geq 0$,

hence

$$Y+Y^T = \begin{bmatrix} \frac{2\omega^2 \tau_i C_i}{1 + \omega^2 \tau_i^2} & \frac{g_m}{1 + \omega^2 \tau_i^2} - j\omega g_m \tau_i \\ \frac{g_m}{1 + \omega^2 \tau_i^2} + j\omega g_m \tau_i & 2G_0 \end{bmatrix} \geq 0 \quad (1.14)$$

implies that the determinant of $Y+Y^T$ is none negative, that is,

$$\frac{4\omega^2 \tau_i C_i G_0}{1 + \omega^2 \tau_i^2} - \frac{g_m^2}{(1 + \omega^2 \tau_i^2)^2} - \omega^2 g_m^2 \tau_i^2 \geq 0 \quad (1.15)$$

in practice $\omega_{\max}^{-1} \gg \tau_i$, and (1.15) can be approximated as

$$4\omega_{\max}^2 \tau_i C_i G_0 - g_m^2 - \omega_{\max}^2 g_m^2 \tau_i^2 \geq 0 \quad (1.16)$$

which yields

$$\omega_{\max} \approx g_m (4\tau_i C_i G_0 - g_m^2 \tau_i^2)^{-1/2} \quad (1.17)$$

For a GaAs MESFET with a 1μ gate length, the maximum frequency of oscillation is about 30-40 GHz.

For the extrinsic FET, the parasitic elements reduce ω_{\max} considerably. The maximum available power gain $G_{a,\max}$ of the extrinsic model can be approximated by

$$G_{a,\max} \approx \alpha \left(\frac{\omega_T}{\omega} \right)^2 \quad (1.18)$$

where

$$\omega_T = g_m / (C_i + C_f) \quad (1.19)$$

and

$$\alpha = \left[4G_0(R_i + R_s + \frac{1}{2}\omega_T L_s) + 2\omega_T C_f(R_i + R_s + \omega_T L_s) \right]^{-1} \quad (1.20)$$

From (1.18) we see that the FET has a gain roll-off of about 6 dB/octave. This is true for most microwave GaAs MESFETs.

Furthermore, in the operating range the feedback capacitance C_f is very small compared to C_i , and the reverse transmission scattering parameter S_{12} of the GaAs FET is very small in magnitude compared to S_{21} [4].

1.4.2. Dual Gate MESFET

Although the single gate structure has become the most widely manufactured and used device the dual gate FET has the advantages of an increased capability due to the ability of the two independent gates to perform such functions as gain control and mixing as well as reduced feedback and improvement in signal gain. The dual gate FET, however, is in general much less well understood than the single gate FET mainly due to the r.f interaction which can occur between its three accessible ports when it is used in a particular configuration, usually common source.

The applications of the dual gate FET are numerous. It has been used in up and down converters, modulators, and pulse regenerators as well as in oscillator applications.

The dual gate device can be considered as two separate FETs connected in cascode as shown in Fig.1.6a where the current characteristics of the bottom FET are determined by the top device. Fig.1.6b. shows a representation of a dual-gate device where the first and second Schottky gates G_1 and G_2 are formed between the source and drain ohmic contacts [5].

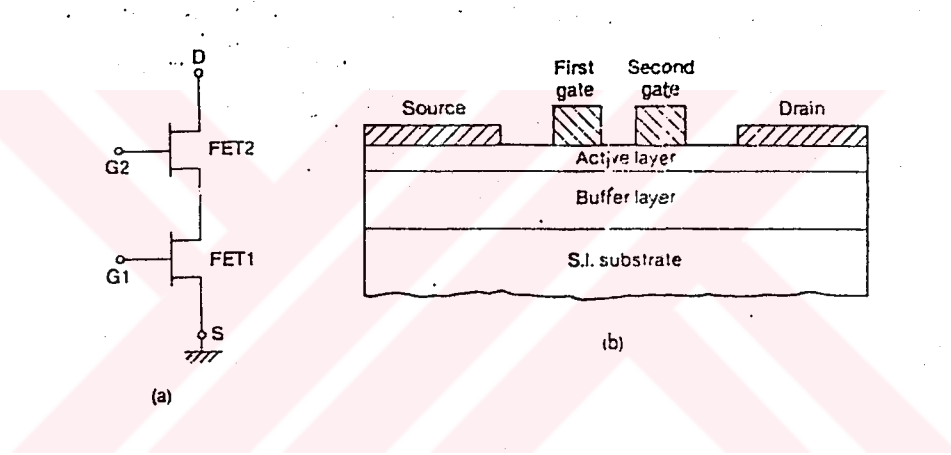


Fig.1.6 (a) Equivalent circuit configuration of two single gated FETs,
(b) Cross section of dual-gate MESFET.

The operation and characteristics of the dual-gate FET can be analysed by combining the analyses of the two single gate FETs.

1.4.3. Equivalent Circuit of GaAs Dual Gate MESFETs:

An equivalent circuit for GaAs dual gate MESFETs valid for 2-11 GHz, and including 28 elements, has been derived from measured 3-port s-parameters. The bi-dimensional transfer characteristic of the device made possible separate microwave measurement of each FET part and determination of precise starting value for the optimisation.

For a certain number of applications of the GaAs dual gate MESFET (AGC amplifier, mixer, phase shifter and detector, oscillator, self-oscillating mixer and power divider), there is a need for well founded knowledge of its RF behaviour, that can be described more efficiently by an equivalent circuit than by S or Y parameters.

Wideband small-signal equivalent circuits are determined by curve fitting between measured and calculated s-parameters. For a large number of elements, however, the error function EF to be minimised may have several local minima and makes a straight forward optimisation procedure senseless.

Precise starting values are necessary in order to find the global minimum. This is pronounced valid for dual-gate MESFETs with a number of 25-28 circuit elements.

For the internal parameters (transconductance, input, output, and feedback capacitance and channel resistance) of each FET-part, little can be said, especially since the internal biases of the FETs are not known. The bidimensional transfer characteristic, $I_D(V_{G1S}, V_{G2S}/V_{DS}=\text{constant})$ of the dual gate FET given in Fig.1.7 [6].

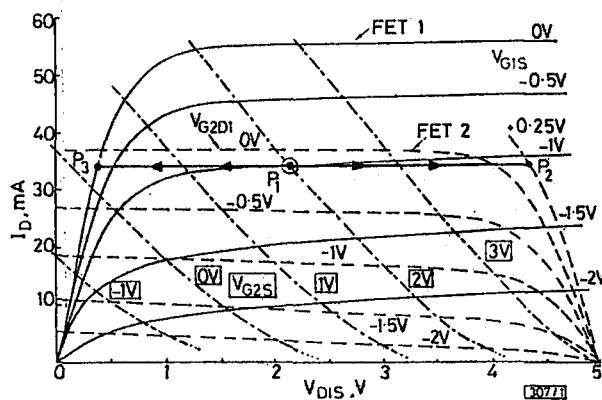


Fig.1.7 Bidimensional transfer characteristics of dual-gate MESFET.

In Fig.1.7, V_{G2D1} is the effective gate 2 to channel (D1) voltage and vertical broken lines (---) correspond to $V_{G2}=\text{constant}$ [6].

This diagram can be constructed by appropriate combination of the output characteristics of the two single gate FETs comprising the dual gate FET. It gives the values of all internal voltages of the DG FET:

- (a) Intrinsic gate 2 to channel voltage V_{G2D1}
- (b) Voltage across FET1: V_{D1S} and FET2: V_{DD1} .

For external bias: $V_{DS}=5\text{ V}$, $V_{G1S}=-1\text{ V}$, $V_{G2S}=12\text{ V}$ (point P1).

We find: $V_{D1S}=2,15\text{ V}$, $V_{DD1}=2,85\text{ V}$, $V_{G2D1}=-0,15\text{ V}$, $I_D=34\text{ mA}$.

New bias conditions can now be defined in order to keep the bias of one of the two FETs as before and drive the other one in the ohmic region: For bias point P_2 ($V'_{DS}=2,8\text{ V}$, $V'_{G1S}=-1\text{ V}$, $V'_{G2S}=2,5\text{ V}$) FET 1 is biased as in P_1 whereas FET 2 is nonsaturated and represents a resistive load ($V_{DD1}=0,65\text{ V}$, $V_{G2D1}=0,25\text{ V}$).

The S-parameters of FET 1 can now be measured and its equivalent circuit can be determined giving starting values of the intrinsic FET 1 (Fig.1.8).

External bias:

$$V_{DS}=5\text{ V}, V_{G1S}=1\text{ V}, V_{G2S}=+2\text{ V}, I_D=34\text{ mA}.$$

Internal bias:

$$\text{FET 1: } V_{D1S}=2,15\text{ V}, V_{G1S}=-1\text{ V}, I_D=34\text{ mA}$$

$$\text{FET 2: } V_{DD1}=2,85\text{ V}, V_{G2D1}=-0,15\text{ V}, I_D=34\text{ mA} \quad [6]$$

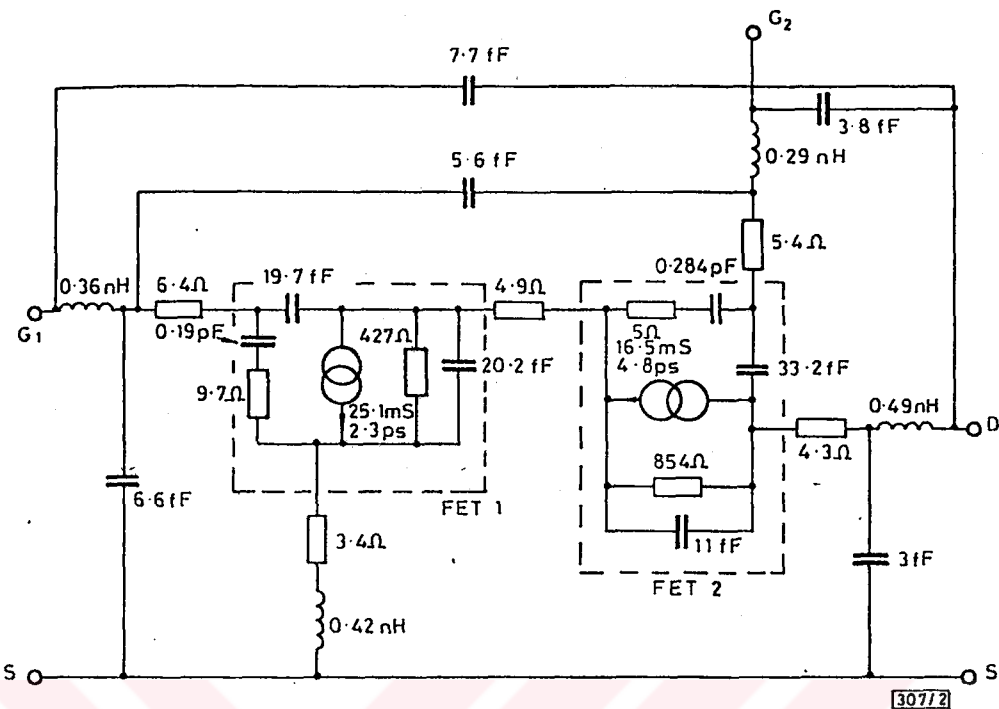


Fig. 1.8 Equivalent circuit of GaAs dual-gate MESFET valid from 2 to 11 GHz.

The same can be done for FET 2 at the bias point P_3 in Fig. 1.7. The external bias is now $V_{DS}''=3.2$ V, $V_{G1S}''=0$ V, $V_{G2S}''=0.2$ V. FET 1 is non saturated and the s-parameters of FET 2 can be measured, and give, after optimisation, the starting values of the second intrinsic FET in Fig. 1.8.

A comparison between measured and calculated 3-port s-parameters is given in Fig. 1.9.

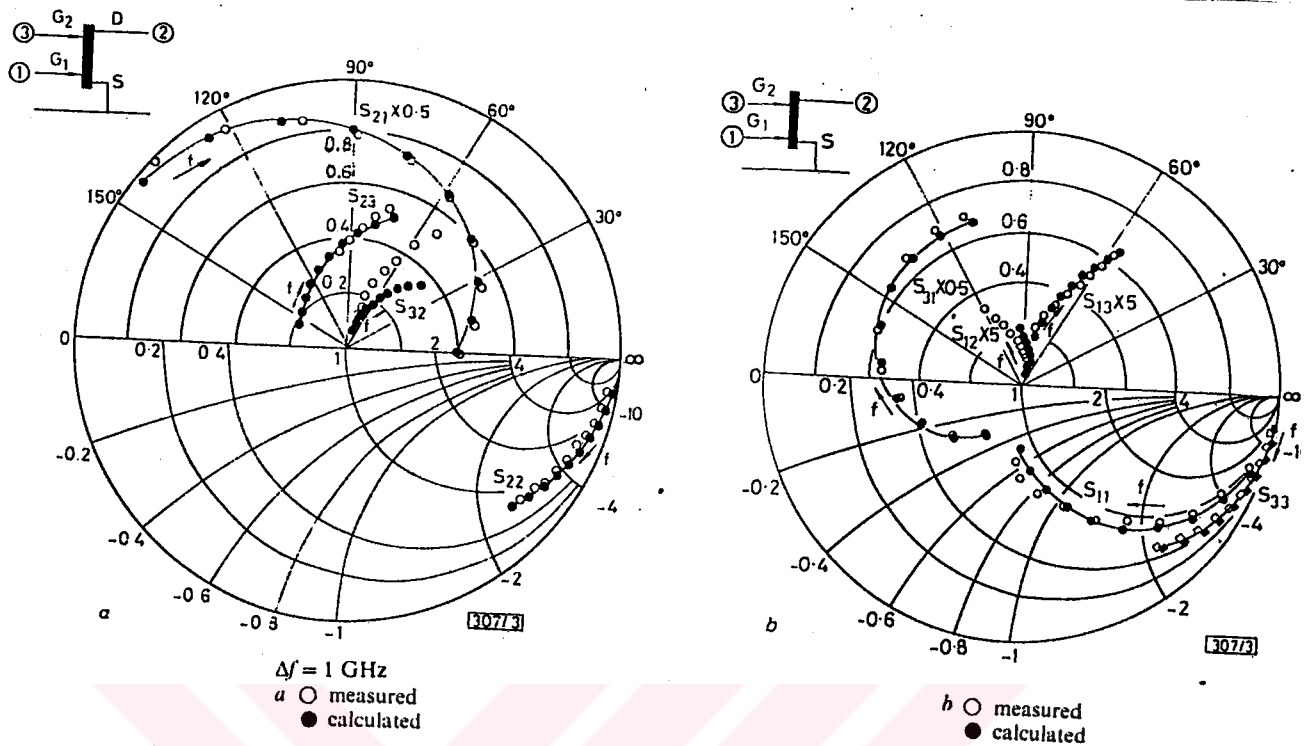


Fig. 1.9 Comparison between measured and calculated 3-port s-parameters of GaAs dual-gate MESFET for 2 to 11 GHz.

1.4.4. Dual Gate MESFET As Three Port Device

The dual gate MESFET is characterized as a three-port device with the source as a common terminal.

The source pads are grounded in this fixture with negligible lead inductance.

S-parameters measured at 10 GHz in a 50Ω system are illustrated in the signal flow graph of Fig. 1.11.

The reference plane for port 1 and port 2 is located at the first gate, and the reference plane for port 3 runs through the center of the chip perpendicular to the gates.

The dc bias has been chosen to yield high gain and allow a simultaneous image match at port 1 and port 2

for a 50Ω termination at port 3. As expected, strong signal coupling is experienced from gate 1 to drain. But, in addition, nearly the same amount of power is feed from the first gate to the second gate.

The reverse couplings are weak, especially S_{12} . The forward coupling from port 3 to port 2 is less pronounced because the output impedance Z_{01} connected in series with the second-gate capacitance (Fig. 1.10b), keeps the extrinsic transconductance of the second low.

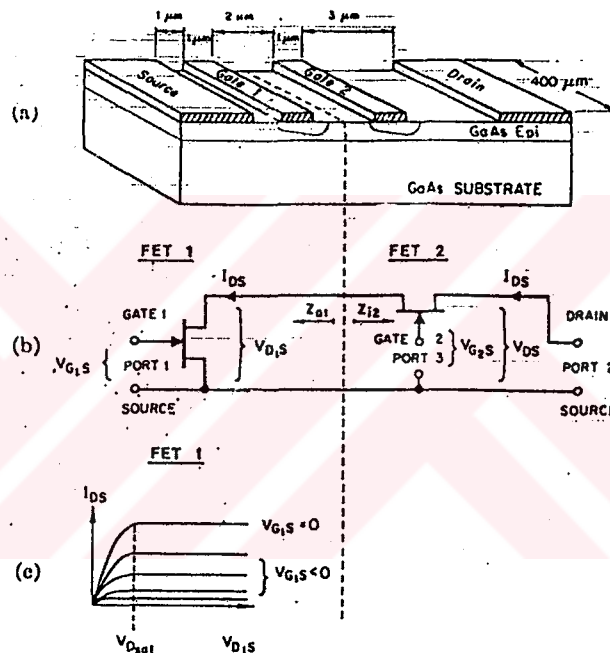


Fig. 1.10 The dual MESFET is modeled as two single-gate MESFET's connected in cascade. The first MESFET is operated with a common source. Its drain current feeds the source of the second MESFET. The drain current versus drain voltage of the first MESFET is shown in (c).

Z_{01} , acting also a series feedback impedance, enhances the reverse signal flow from port 2 to port 3.

In comparison, the parameters S_{11}, S_{12}, S_{21} , and S_{22} of a single-gate MESFET with the same geometry are listed in parentheses in Fig. 1.11 [15].

The three port s-parameters fully describe the dual-gate MESFET's small signal behavior.

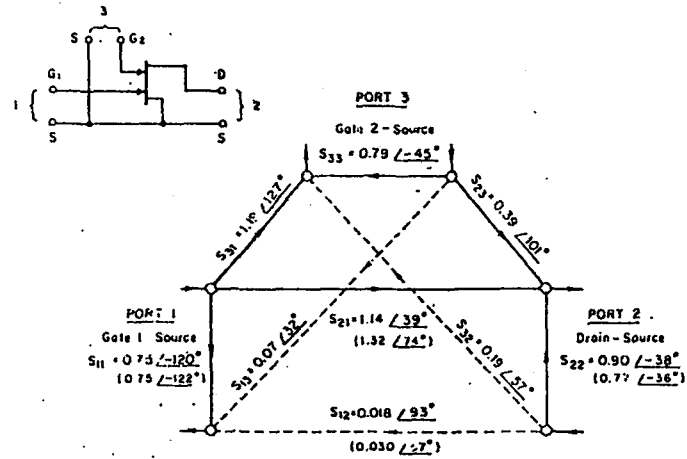


Fig. 1.11 Three port signal flow graph of the dual-gate MESFET at 10 GHz, operating conditions:
 $V_{DS} = 4.5$ V, $V_{G1S} = 0$ V, $V_{G2S} = 20$ V, $I_{DSS} = 46$ mA;
 $Z_0 = 50 \Omega$, $f = 10$ GHz. The s-parameter of a comparable single-gate MESFET are listed in parentheses.

CHAPTER 2

DIELECTRIC RESONATOR OSCILLATORS

2.1. Introduction

The microwave oscillator is one of the important devices in microwave communication equipment. It is necessary for microwave oscillators used in those systems not only to have good electrical characteristics, such as frequency stability, stable output power, low thermal noise, etc., but also to have high reliability and low cost. It is also required for the oscillator to be compact in size, as communication equipment is getting smaller.

Electrical characteristics, cost and size of the oscillator are determined mainly by the active device for oscillating and the resonator for controlling the oscillating frequency.

Until around the 1970's, F_{\max} (The highest frequency able to oscillate) had been limited to about 2 GHz, because of the electrical characteristics of the silicon bipolar transistor. Consequently, for oscillators required for oscillating at higher frequencies than 2 GHz, it was necessary to use frequency multipliers. Cavity and coaxial resonators have mainly been used for the resonator. Accordingly, the oscillator size was rather large because of the resonator size, and use of the frequency multiplier. At frequencies higher than the X-band, the Gunn diode and the IMPATT diode have been used as the active device. However, oscillators with those active devices have had some problems, such as complexity of mechanical parts in constructing, the oscillating circuits, large oscillator size and high oscillator cost.

Recently, direct oscillators at higher than the X-band without frequency multipliers have been designed by active device development of Si bipolar transistor and GaAs FET.

By using a dielectric resonator for controlling the oscillating frequency addition with those active devices, it is possible to produce high stable, low cost and small size oscillators.

In this chapter the coupling parameters between a dielectric resonator and a microstrip line is investigated. Additionally oscillating circuits controlled by dielectric resonators and stabilization of the oscillator stabilized with dielectric resonators are also presented.

2.2. Oscillation And Stability Conditions:

A GaAs MESFET oscillator can be represented in an arbitrary plane on the output line by a nonlinear impedance, Z_{NL} , having a negative real part with a load impedance Z_C . In certain case, load impedance can also be non-linear (e.g., when the oscillator is directly connected to a mixer diode).

In the analysis it is assumed that this circuit has a sufficiently high Q for neglecting harmonic currents. We also assume that if the amplitude and the angular frequency of current varies in the circuit, this variation take place slowly, so that a quasi-stationary approximation may be applied to the circuit.

Taking these hypotheses into account, suppose that a current $I_0 \cos \omega_0 t$ exist in the circuit (Fig. 2.1). We can apply the Kirchoff law and write in plane π .

$$(Z_{NL} + Z_C)I_0 = 0 \quad \text{at } \omega = \omega_0 \quad (2.1)$$

where ω_0 is resonate frequency.

Now let

$$Z_{NL} + Z_C = Z_T = R_T + j X_T$$

Since I_0 is supposed to be different from zero, the Equation (2.1) is satisfied by:

$$R_T \Big|_{\omega=\omega_0} = 0$$

$$X_T \Big|_{\omega=\omega_0} = 0 \quad (2.2)$$

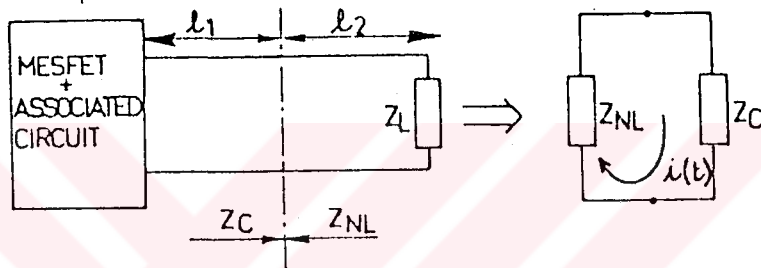


Fig. 2.1 Oscillator circuit.

Since $R_e(Z_C) > 0$, equation (2.1) necessarily implies that $R_e(Z_{NL}) < 0$. In the following paragraphs the methods which permit this condition to be realized using a GaAs MESFET will be reviewed.

Oscillation conditions in terms of reflection coefficient can be determined as follows:

Calling Γ_{NL} the reflection coefficient represented by the output line, the preceding conditions of oscillation become

$$\Gamma_{NL} \cdot \Gamma_C = 1$$

that is,

$$|\Gamma_{NL}| \cdot |\Gamma_C| = 1$$

$$\angle \Gamma_{NL} + \angle \Gamma_C = 2K\pi, \quad K=0, 1, 2, \dots \quad (2.3)$$

For investigating the oscillation conditions in general case first we consider generalized oscillation conditions for n-port active device.

A MESFET oscillator can also be considered as a combination of an active multiport (the MESFET) and a passive network as shown in Figure 2.2.

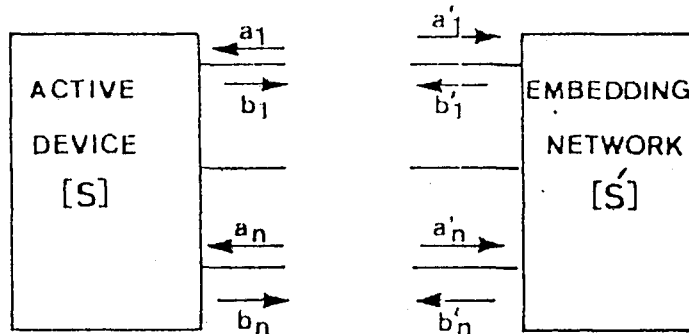


Fig. 2.2 N-port device/load interface for active oscillation.

Suppose the active device and the passive circuit characterized by their scattering matrix; for the active device

$$\begin{bmatrix} b_1 \\ \vdots \\ b_n \end{bmatrix} = \begin{bmatrix} S_{11} & \dots & S_{1n} \\ \vdots & & \vdots \\ S_{n1} & & S_{nn} \end{bmatrix} \begin{bmatrix} a_1 \\ \vdots \\ a_n \end{bmatrix} \quad (2.4)$$

or $[b] = [S][a]$

and for the passive network

$$\begin{bmatrix} b'_1 \\ \vdots \\ b'_n \end{bmatrix} = \begin{bmatrix} S'_{11} & \dots & S'_{1n} \\ \vdots & & \vdots \\ S'_{n1} & & S'_{nn} \end{bmatrix} \begin{bmatrix} a'_1 \\ \vdots \\ a'_n \end{bmatrix} \quad (2.5)$$

or $[b'] = [S'][a']$

To make an oscillator, the active device and the passive network are connected such that corresponding i ports are connected together so that we have

$$[b'] = [a]$$

and

$$[b] = [a']$$

we can then write

$$a' = [S][S'][a']$$

or

$$\{[S][S'] - [I]\} [a'] = 0 \quad (2.6)$$

where I is a unit matrix.

Since $[a'] \neq 0$

$$[M] = [S][S'] - [I]$$

is a singular matrix

or

$$\text{Det}[M] = 0 \quad (2.7)$$

This expression represents the generalized oscillation condition for a n active-ports oscillator.

In fact the scattering matrix of the active device is only defined at small signal levels, so oscillations will start if

$$|\text{Det}[M]| > 0 \quad (2.8)$$

and

$$\text{Arg Det}[M] = 0$$

Then they build up until device non-linearities cause a steady state to be reached.

Now if the active device and the circuit are

defined by their Z matrix we have

for the active device $[V] = [Z][i]$

for the passive circuit $[V'] = [Z'][i']$

and by connecting the port i to i' we have

$$[i] = [i']$$

$$[V] = [V']$$

so that

$$\{[Z] + [Z']\}[i] = 0$$

Since $[i] \neq 0$

The matrix $[Z] + [Z']$ is singular, or

$$\text{Det}\{[Z] + [Z']\} = 0 \quad (2.9)$$

similarly if the multiport is defined by its admittance matrix

$$\text{Det}\{[Y] + [Y']\} = 0 \quad (2.10)$$

for this work the two port GaAs MESFET will be used, so we consider the oscillation conditions for a two port active device.

At the first we consider a two port active device which connected to a generator as shown in Figure 2.3.

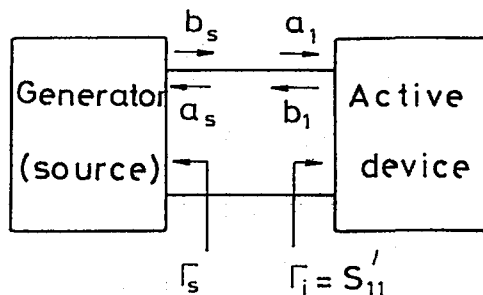


Fig. 2.3. Tow Port Active Device

By using Mason's gain formula for signal flow graphs and drawing the signal flow graph for above circuit we have:

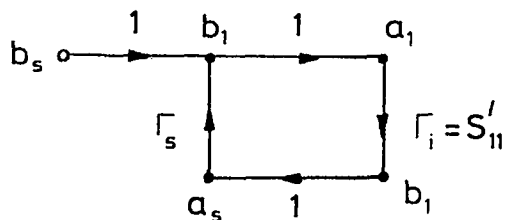


Fig. 2.4. Signal Flow Graph For Fig. 2.3.

$$\frac{a_1}{b_s} = \frac{1}{1 - \Gamma_s \Gamma_i}$$

$$b_s = a_1 (1 - \Gamma_s \Gamma_i)$$

$$= \frac{b_1}{\Gamma_i} (1 - \Gamma_s \Gamma_i)$$

$$\Gamma_i = S'_{11} = \frac{b_1}{a_1}$$

$$\frac{b_1}{b_s} = \frac{\Gamma_i}{1 - \Gamma_s \Gamma_i} = \frac{S'_{11}}{1 - \Gamma_s S'_{11}}$$

If there is not any source at the input port then $b_s = 0$ and we have

$$1 - \Gamma_s S'_{11} = 0$$

$$\text{or } \Gamma_s S'_{11} = 0 \quad (2.11)$$

this is a condition for oscillation at the input port.

For showing the oscillation condition at the output port a theorem can be used as follows:

Theorem:

Consider the two-port in Fig. 2.5 represented by an S matrix whose elements are S_{11} , S_{12} , S_{21} , and S_{22} .

Let a reflection coefficient Γ_1 placed at port 1 result in a port 2 input reflection coefficient of s'_{22} , and a reflection coefficient Γ_2 placed at port 2 result in a port 1 input reflection coefficient of s'_{11} . Then the oscillation conditions $s'_{11}\Gamma_1=1$ and $s'_{22}\Gamma_2=1$ simultaneously represent boundary conditions for the two-port to generate oscillations. That is:

$$s'_{11}\Gamma_1 = 1 \iff s'_{22}\Gamma_2 = 1 \quad (2.12)$$

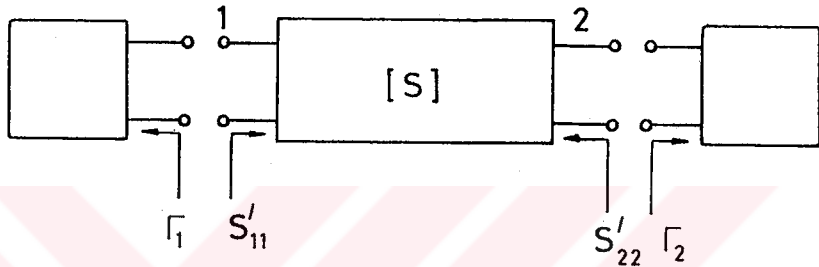


Fig. 2.5 Theorem block diagram.

Proof:

If $[s]$ and $[s']$ be the scattering matrix for active device and passive circuit connected at the input and output port respectively, Then we have

$$S = \begin{bmatrix} s_{11} & s_{12} \\ s_{21} & s_{22} \end{bmatrix}, \quad S' = \begin{bmatrix} s'_{11} & s'_{12} \\ s'_{21} & s'_{22} \end{bmatrix} \quad \text{or} \quad S' = \begin{bmatrix} \Gamma_1 & 0 \\ 0 & \Gamma_2 \end{bmatrix}$$

as we showed before, $\det\{|s||s'|-I\}$ must be equal to zero. Therefore we have

$$(s_{11}\Gamma_1-1)(s_{22}\Gamma_2-1) - s_{12}s_{21}\Gamma_1\Gamma_2 = 0 \quad (2.13)$$

From

$$s'_{22} = s_{22} + \frac{s_{12}s_{21}\Gamma_1}{1-s_{11}\Gamma_1}$$

We can show that

$$\frac{1}{s'_{22}} = \frac{1-s_{11}\Gamma_1}{s_{22}-|s|\Gamma_1}$$

where $|s|$ is the determinat of the S matrix. Substituting for s_{11} from

$$s_{11} = s'_{11} - \frac{s_{12}s_{21}\Gamma_2}{1-s_{22}\Gamma_2}$$

we have

$$\frac{1}{s'_{22}} = \frac{(1-s'_{11}\Gamma_1) + \frac{s_{12}s_{21}\Gamma_1\Gamma_2}{1-s_{22}\Gamma_2}}{s_{22}(1-s'_{11}\Gamma_1) + \frac{s_{12}s_{21}\Gamma_1}{1-s_{22}\Gamma_2}}$$

by using $s'_{11}\Gamma_1=1$ (threshold of oscillations); then we have

$$\frac{1}{s'_{22}} = \frac{s_{12}s_{21}\Gamma_1\Gamma_2}{s_{12}s_{21}\Gamma_1} = \Gamma_2$$

That is

$$s'_{22}\Gamma_2 = 1 \quad (2.14)$$

Similarly, we can show that if $s'_{22}\Gamma_2=1$, then $s'_{11}\Gamma_1=1$.

Let's consider the implications of the theorem. For every Γ_2 there corresponds some s'_{11} and, for the case where the Γ_2 chosen results in oscillations, there exists some value of Γ_1 such that $\Gamma_1 s'_{11}=1$.

Moreover, this value of Γ_1 corresponds to a value of s'_{22} such that $\Gamma_2 s'_{22}=1$.

In the design of oscillators, there are the following questions.

- 1) Is there a set of loads that can be placed at port 1 that will have the effect of causing oscillations?
- 2) If so, are there loads that can be placed at port 2 that will enhance or can inhibit such oscillations?
- 3) What, in fact, would be the loads at ports 1 and 2 that give the desired performance?

One way to proceeding to obtain answers would be as follows. We assume that we can synthesize any passive load placed at port 2; i.e we can generate any load such that $|\Gamma_2| \leq 1$ ($|\Gamma_2|=1$ represents a boundry circle for the load at port 2).

Since the S matrix is a bilinear transformation that maps the circle in the s'_{11} plane into a circle in the Γ_1 plane defined by $\Gamma_1 = 1/s'_{11}$.

Thus $|\Gamma_2| \leq 1$ and the condition $\Gamma_1 s'_{11} = 1$ represents a further bilinear transformation that maps the circle in the s'_{11} plane into a circle in the Γ_1 plane defined by $\Gamma_1 = 1/s'_{11}$. Thus $|\Gamma_2| \leq 1$ and the condition $\Gamma_1 s'_{11} = 1$ combine to generate a circle in the Γ_1 plane, which represents the boundry conditions for oscillations.

Let this circle be represented by the equation $|\Gamma_1 - a| = b$ where b is the redius of the mapped circle and a its vector offset from the origin.

Consider first the case where the area defined by $|\Gamma_2| \leq 1$ maps within this circle. Then for any point $X \in |\Gamma_2| < 1$, there exists a point $Y \in |\Gamma_1 - a| < b$, such that $\Gamma_1 s'_{11} = 1$.

To answer question 1, Then, we have only to investigate whether $|\Gamma_1 - a| = b$ intersects, contains, falls within or outside of $|\Gamma_1| \leq 1$. If it intersects or falls

within, a passive $|\Gamma_1| < 1$ exists such that $\Gamma_1 s'_{11} = 1$, so a load Z_1 can be synthesized that will cause oscillations at ω_0 . The area within the intersection of the two circles in fact denotes the impedances Z_1 that make oscillations at port 1 possible.

If $|\Gamma_1 - a| = b$ falls outside of $|\Gamma_1| \leq 1$, however, it would require a negative resistance load of sufficient magnitude and phase to create oscillations at port 1.

Now consider the case where $|\Gamma_2| \leq 1$ maps outside the circle $|\Gamma_1 - a| \leq b$, then any Γ_1 outside the circle $|\Gamma_1 - a| \leq b$ will cause oscillation at port 1.

For there to exist passive loads such that oscillations are possible, It is only necessary that $|\Gamma_1 - a| \leq b$ not enclose the area $|\Gamma_1| \leq 1$.

For second questions, we determine the map of the $|\Gamma_1| \leq 1$ into the Γ_2 plane, given by, say, $|\Gamma_2 - c| \leq d$.

As in the previous case, the relation between this circle and $|\Gamma_2| \leq 1$ determines the oscillation condition at port 2.

The third question is answered by the use of the actual Γ_1 chosen at port 1, for example, and by designing the proper match at port 2 for desired performance.

2.3. Microwave Dielectric Resonator

Previously, cavities were used in microwave oscillators for controlling the oscillating frequency. Cavity sizes are uniquely determined by the wavelength of the desired frequency, so it is difficult to make it smaller. Microstrip line resonators ($1/4\lambda$, or $1/2\lambda$ length) have been considered instead of cavities to reduce the resonator size, but it has a major defect

in the electrical characteristics, so that Q_o (unloaded quality factor of resonators) is reduced.

Dielectric resonators have begun to be used instead of the resonators previously used. The following items must be considered for dielectric resonator electrical characteristics as used in microwave oscillators.

- 1) High ϵ_r (relative dielectric constant)

To make the resonator size small.

- 2) High Q_o

To reduce oscillating power loss for stabilizing oscillating frequency and to improve the frequency stability.

- 3) Small T_f (coefficient of resonant frequency drift Vs temperature)

To improve the oscillator frequency stability.

At the present time, dielectric resonators can be used to meet the three conditions mentioned above.

The resonator mode for the dielectric resonator, which is used in the oscillator, is $TE_{01\delta}$, which refers to resonant mode TE_{011} in the cavity.

Accordingly, as the dielectric resonator's Q_o is becoming lower by its radiation loss, in case it is mounted in free air, it is necessary to surround it with a metallic case. When the metallic wall of the case closes, the dielectric resonator Q_o becomes lower by the conduction loss in the metallic surface. To reduce this loss, it is required that the metallic case size be about three times larger than the dielectric resonator size [7].

In Fig. 2.6 measurement values, Q_o Vs the metal case width, are shown. In these data, Q_o values $\epsilon_r=30$ and $\epsilon_r=39$ are becoming the breakdown at a point lower

than $W/D=3$, and $W/D=2$, respectively [7].

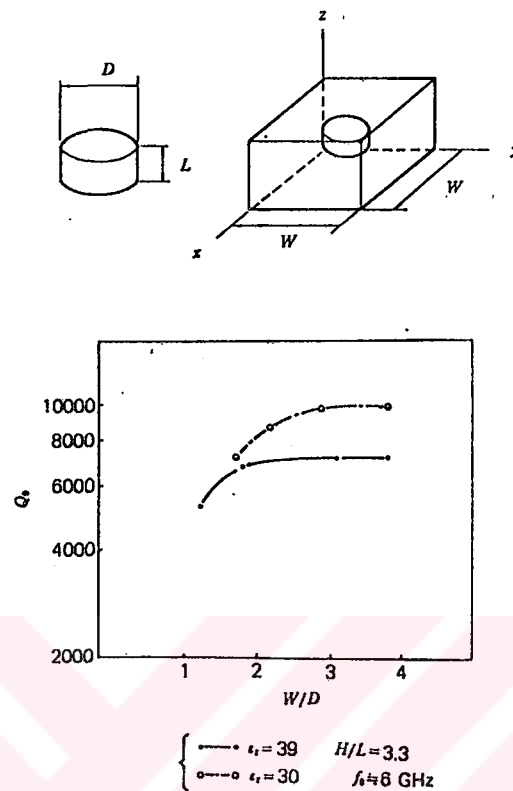


Fig. 2.6 Q_0 Vs metal case size.

To a first approximation, a dielectric resonator is the dual of a metallic cavity. The radiation losses of the dielectric resonators with the commonly used permittivities, however, are generally much greater than the energy losses in the metallic cavities, which makes proper shielding of the dielectric resonator a necessity. The shape of a dielectric resonator is usually a solid cylinder, but one can also find tubular and spherical shapes.

A commonly used resonant mode in cylindrical resonators is denoted by $TE_{01\delta}$. The magnetic field lines are contained in the meridian plane, while the electric field lines are concentric circles around the z axis, as shown in Fig. 2.7.

For a distant observer, this mode appears as a magnetic dipole and for this reason sometimes this mode is referred to as a magnetic dipole mode.

When the relative dielectric constant is around 40, more than 95 % of the stored electric energy of the $TE_{01\delta}$ mode, as well as more than 60 % of the stored magnetic energy are located within the cylinder. The remaining energy is distributed in the air around the resonator, decaying rapidly with distance away from the resonator surface.

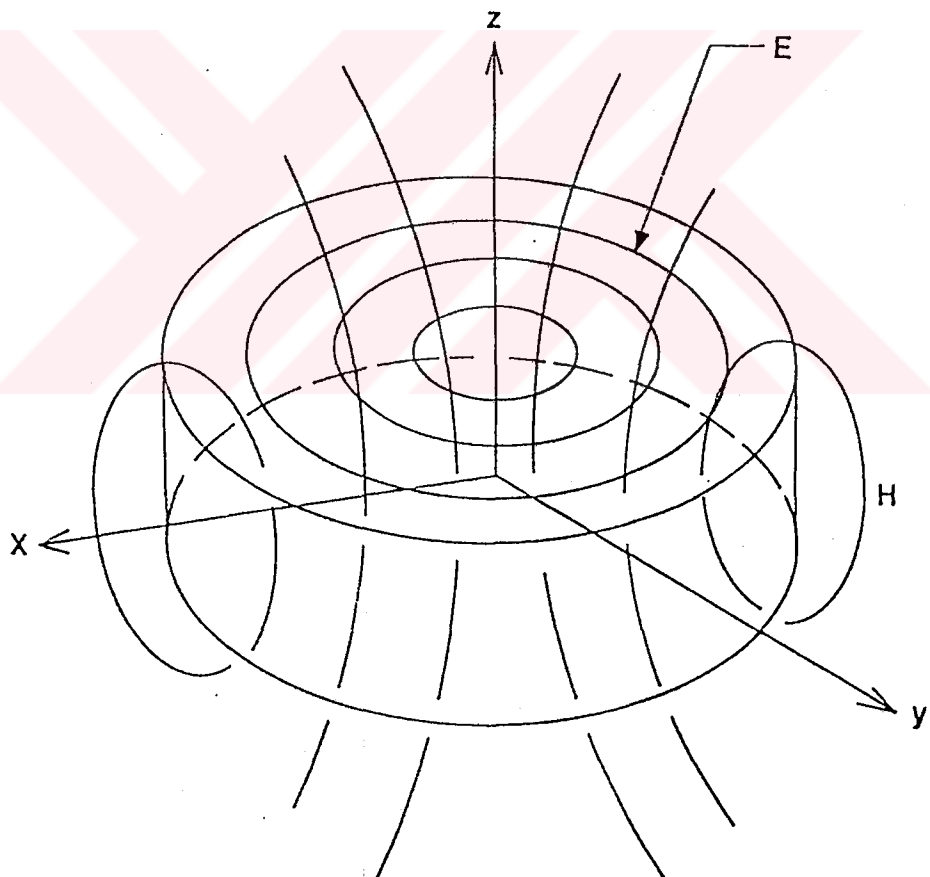


Fig. 2.7 Field lines of the resonant mode $TE_{01\delta}$ in an isolated dielectric resonator.

2.4. Coupling of a Dielectric Resonator With a Microstrip

Line:

The dielectric resonator is used in a number of different configurations depending upon the application. In order to effectively use dielectric resonators in microwave circuits, it is necessary to have an accurate knowledge of the coupling between the resonator and different transmission lines. The $TE_{01\delta}$ mode of the cylindrical resonator can be easily coupled to microstrip-line, fin-line, magnetic-loop, metallic, and dielectric wave guides.

In this section the most commonly used configuration of the dielectric resonator, that is $TE_{01\delta}$ mode coupling with a microstrip line will be discussed.

Figure 2.8 shows the magnetic coupling between a dielectric resonator and microstrip. The resonator is placed on the top of the microstrip substrate. The lateral distance between the resonator and the microstrip conductor primarily determines the amount of coupling between the resonator and the microstrip transmission line. Proper metallic shielding required to minimize the radiation losses (hence to increase Q) also effects the resonant frequency of the $TE_{01\delta}$ mode. The reason for the modification of the resonant frequency can be explained by the cavity perturbation theory.

Namely when a metal wall of a resonant cavity is moved inwards, the resonant frequency will decrease if the stored energy of the displaced field is predominately electric. Otherwise, when the stored energy close to the metal wall is mostly magnetic, as in the case of the shielded $TE_{01\delta}$ dielectric resonator considered here, the resonant frequency will increase when the wall moves inwards.

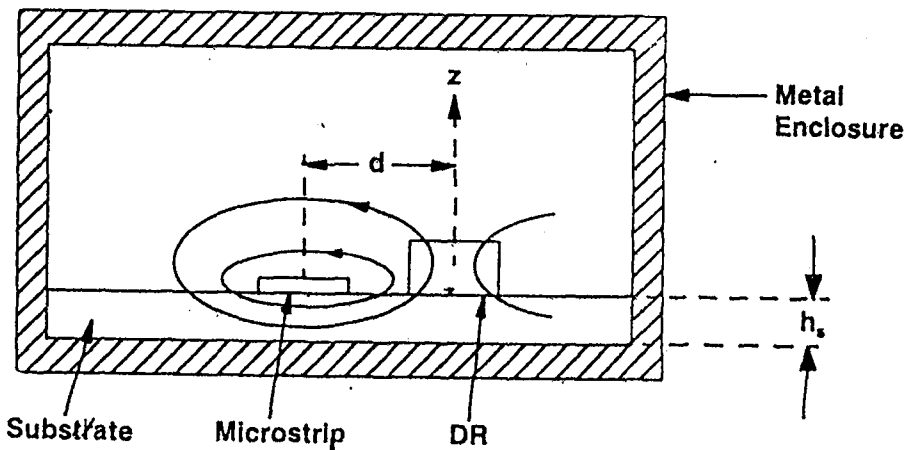


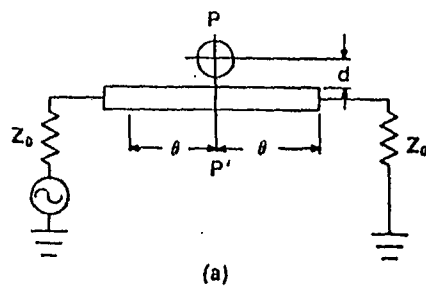
Fig. 2.8 Coupling between a microstrip line and a dielectric resonator.

The $TE_{01\delta}$ mode in a dielectric resonator can be approximated by a magnetic dipole of moment M . The coupling between the line and the resonator is accomplished by orienting the magnetic moment of the resonator perpendicular to the microstrip plane. So that the magnetic lines of the resonator link with those of the microstrip line, as shown in Fig. 2.8.

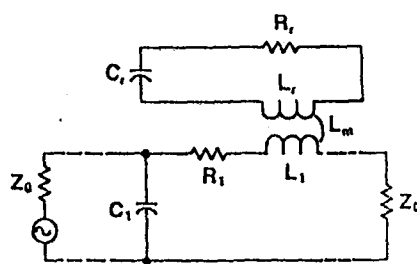
The dielectric resonator placed adjacent to the microstrip line operates like a reaction cavity that reflects the RF energy at the resonant frequency.

The equivalent circuit of the resonator coupled to a microstrip line is shown in Fig. 2.9.

In this Figure L_r , C_r , R_r are the equivalent parameters of the dielectric resonator, L_1 , C_1 , and R_1 are the equivalent parameters of the microstrip line, and L_m characterizes the magnetic coupling.



(a)



(b)

Fig. 2.9 Equivalent circuit of the dielectric resonator coupled with a line.

The transformed resonator impedance Z in series with the transmission line is easily determined to be

$$Z = j\omega L_1 + \frac{\omega^2 L_m^2}{R_r + j\omega(L_r - 1/\omega^2 C_r)} \quad (2.15)$$

Around the center frequency, ωL_1 can be neglected and Z becomes

$$Z = \omega \cdot Q_u \cdot \frac{L_m^2}{L_r} \cdot \frac{1}{1+jX} \quad (2.16)$$

Where $X = 2Q_u(\Delta\omega/\omega)$, and unloaded Q and the resonant frequency of the resonator are given by

$$Q_u = \frac{\omega_o L_r}{R_r} \quad (2.17)$$

$$\omega_o = \frac{1}{\sqrt{L_r C_r}} \quad (2.18)$$

At the resonance frequency, $X=0$ and

$$Z = R = \omega_0 Q_u \frac{L_m^2}{L_r} \quad (2.19)$$

Equation (2.19) indicates that the circuit shown in Fig. 2.9 can be represented by the simple parallel tuned circuit as shown in Fig. 2.10, where L, R, C satisfy the following equations [3].

$$L = \frac{L_m^2}{L_r} \quad (2.20)$$

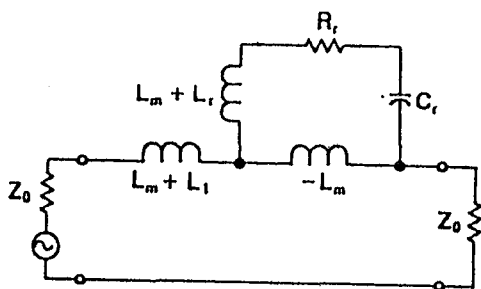
$$C = \frac{L_r}{\omega_0^2 L_m^2}$$

and

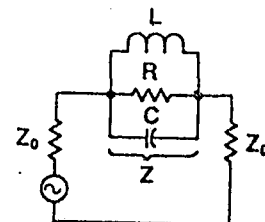
$$R = \omega_0 Q_u \frac{L_m^2}{L_r}$$

The couplingling coefficient β at the resonant frequency ω_0 is defined by.

$$\beta = \frac{R}{R_{ext}} = \frac{\omega_0 Q_u}{2Z_0} \cdot \frac{L_m^2}{L_r} \quad (2.21)$$



(a)



(b)

Fig. 2.10 (a) Simplified equivalent circuit,
 (b) Final equivalent of dielectric resonator coupled with a microstrip line.

The quantity L_m^2/L_r in (2.21) is a strong function of the distance between the resonator and the microstrip line for given shielding conditions and substrait thickness and permittivity. The analysis of β involves the use of known electromagnetic concepts and finite-element techniques.

The relation between different quality factor is well and given by

$$Q_u = Q_L(1+\beta) = Q_{ex}\beta \quad (2.22)$$

where Q_L and Q_{ex} represent loaded and external quality factor [8].

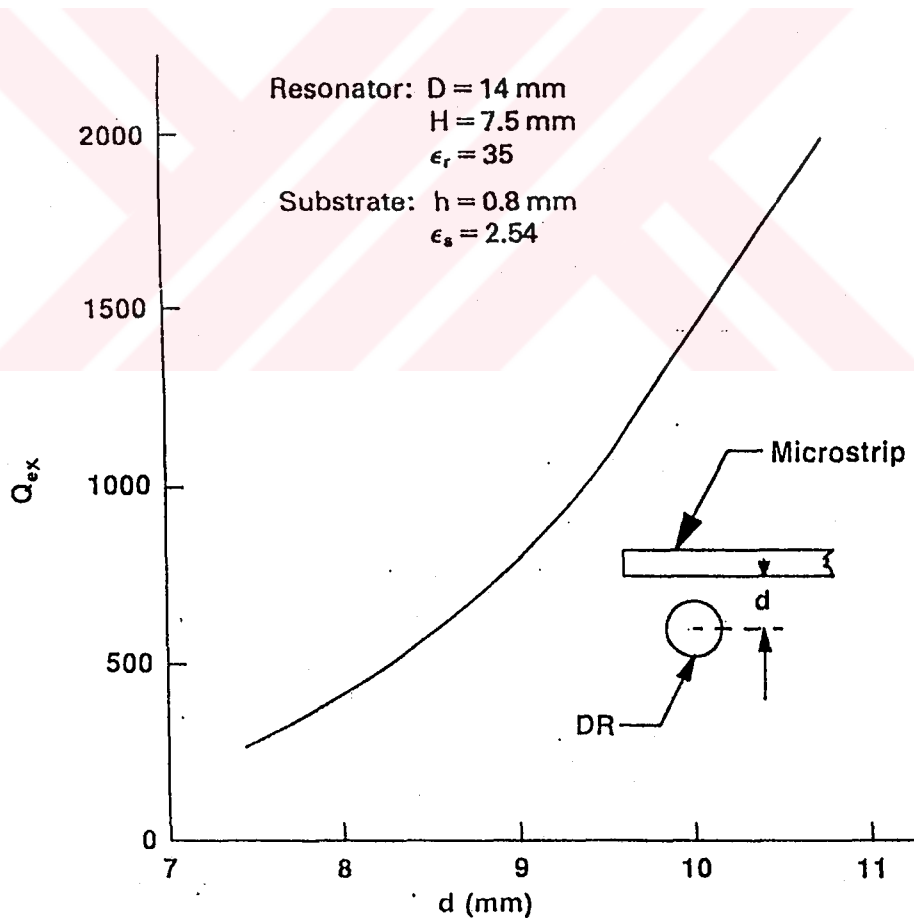


Fig. 2.11 External Q factor as a function of d .

The external quality factor Q_{ex} ($= Q_u / \beta$) is generally used to characterize the coupling. Fig. 2.11 shows an example of the variation of Q_{ex} with the distance between the resonator and line.

The S-parameters of the dielectric resonator coupled to a microstrip with the lengths of transmission lines on input and output, as shown in Fig. 2.9 are given by [8].

$$S = \begin{bmatrix} \frac{\beta}{\beta + 1 + jQ_u \Delta\omega/\omega_o} e^{-2j\theta} & \frac{1 + jQ_u \Delta\omega/\omega_o}{\beta + 1 + jQ_u \Delta\omega/\omega_o} e^{-j2\theta} \\ \frac{1 + jQ_u \Delta\omega/\omega_o}{\beta + 1 + jQ_u \Delta\omega/\omega_o} e^{-2j\theta} & \frac{\beta}{\beta + 1 + jQ_u \Delta\omega/\omega_o} e^{-2j\theta} \end{bmatrix} \quad (2.23)$$

where 2θ is the electrical line length between the input and output planes.

2.5. Circuit Realization of Dielectric Resonator MESFET Oscillator:

Fig. 2.12 shows a dielectric resonator oscillator circuits. In this figure Z_1 and Z_m would be used as series feedback element and output matching network.

The represented symbol in Fig. 2.12 are defined as follows.

Γ_i : represents the reflection coefficient from the right hand side of A-A' to the input of DR.

Γ'_i : represents the reflection coefficient from the left hand side of A-A' to the output.

Γ_L : represent, the reflection coefficient of output matching network and load.

and Γ_0 is the reflection coefficient at port 2 of MESFET. as mentioned before for oscillation conditions at port 1 the following condition must be satisfied.

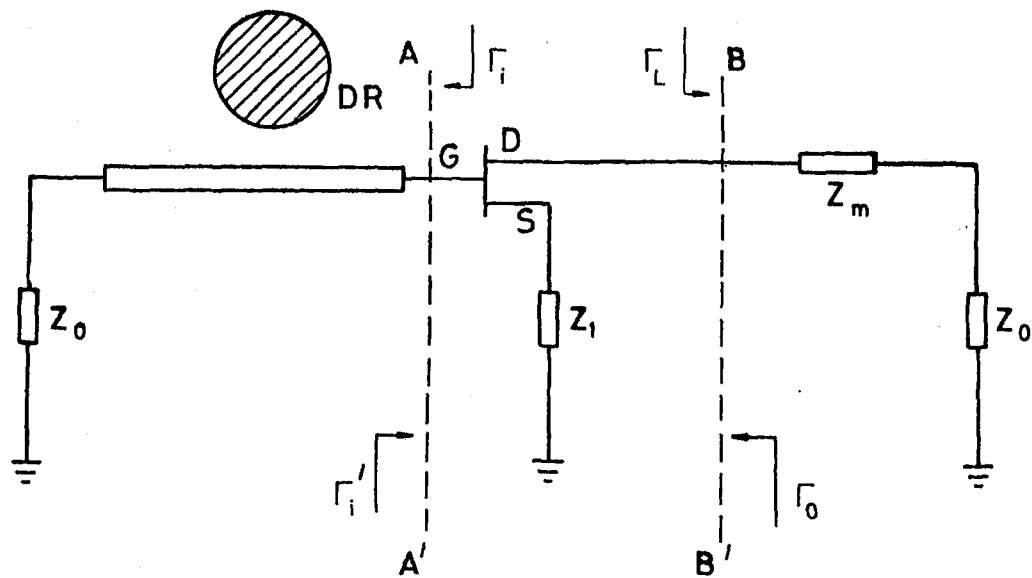


Fig. 2.12 DR oscillator circuit.

$$\Gamma_i \cdot \Gamma_i' > 1 \quad (2.24)$$

or

$$|\Gamma_i| |\Gamma_i'| > 1 \quad (2.25)$$

$$\text{and } \arg(\Gamma_i) + \arg(\Gamma_i') = \pm 2K\pi, \quad K=1, 2, \dots \quad (2.26)$$

to find Γ_i Fig. 2.13 can be used.

$$Z_{i1} = Z(\omega) + Z_0 \quad (2.27)$$

at oscillation frequency $\omega = \omega_0$ and the equivalent circuit of parallel resonant circuit reduces to R_0 then

$$Z_{i1} = Z(\omega_0) + Z_0 = R_0 + Z_0 \quad (2.28)$$

and normalized impedans, is equal to

$$Z_{i1} = r_0 + 1 \quad (2.29)$$

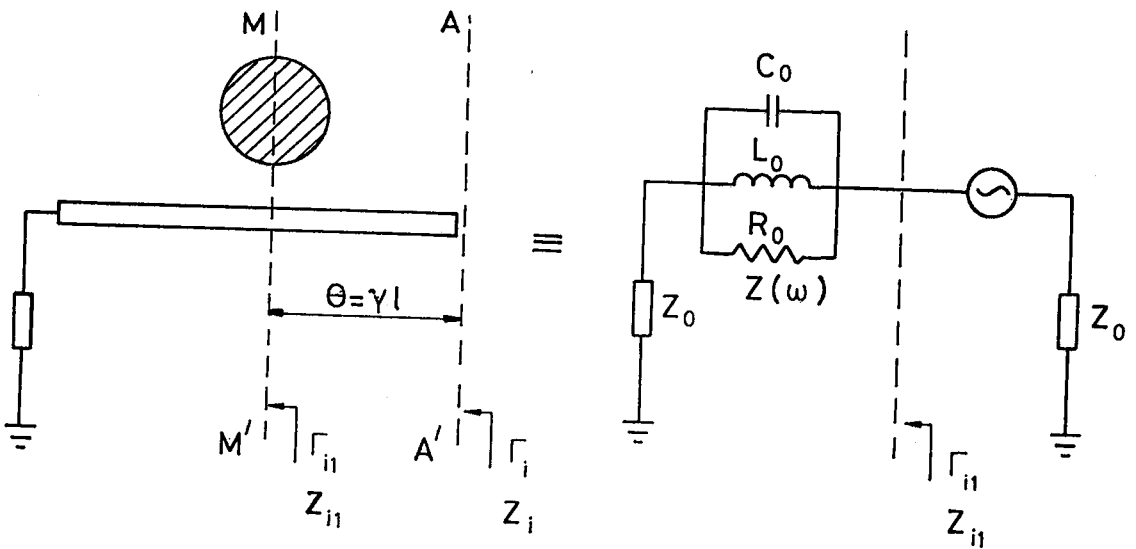


Fig. 2.13 DR coupled to a microstrip line and equivalent circuit.

Now we can determine the reflection coefficient at the left hand of M-M' and gives:

$$\Gamma_{i1} = \frac{Z_{i1}-1}{Z_{i1}+1}$$

at the oscillation frequency this reflection coefficient would be as:

$$\Gamma_{i1} = \frac{Z_{i1}(\omega_o)-1}{Z_{i1}(\omega_o)+1} = \frac{r_o+1-1}{r_o+1+1} = \frac{r_o}{r_o+2} \quad (2.30)$$

at any frequency other than ω_o (oscillation frequency) we need to determine the input impedance at the left side of M-M'.

In Fig. 2.13, Z_{i1} in the plane MM' of the dielectric resonator is given by [8].

$$Z_{i1} = Z_0 + \frac{R}{1+j2Q_u \delta} \quad (2.31)$$

where $\delta = (f - f_o)/f_o$ is the normalized frequency deviation.

By using $\beta = R/R_{ext} = \frac{R}{2Z_0}$ and $Q_u = Q_L(1+\beta) = \beta Q_{ext}$ the normalized input impedance $z_{il} = Z_{il}/Z_0$ can be written as

$$z_{il} = 1 + \frac{2\beta}{1+j2Q_u\delta} = 1 + \frac{\beta}{1+j2Q_L(1+\beta)\delta} = 1 + \frac{2\beta}{1+j2Q_u\beta\delta} \quad (2.32)$$

from $\Gamma_{il} = \frac{z_{il}-1}{z_{il}+1}$ now we can write

$$\Gamma_{il} = \frac{1 + \frac{2\beta}{1+j2Q_u\delta} - 1}{1 + \frac{2\beta}{1+j2Q_u\delta} + 1} = \frac{\frac{2\beta}{1+j2Q_u\delta}}{\frac{2+j4Q_u\delta+2\beta}{1+j2Q_u\delta}} = \frac{\beta}{1+\beta+j2Q_u\delta} \quad (2.33)$$

If the electrical distance between MM' and AA' planes in Figure 2.13 be equal to θ then the reflection coefficient at the left side of AA' plane equals to

$$\Gamma_i(\omega) = \Gamma_{il}(\omega)e^{-j2\theta} = \frac{\beta e^{-j2\theta}}{1+\beta+j2Q_u\delta} \quad (2.34)$$

Using (2.24) and substituting for Γ_{il} from (2.34) gives

$$\frac{\beta}{1+\beta+j2Q_u\delta} e^{-j2\theta} \cdot |\Gamma'_i| e^{j\phi} \geq 1 \quad (2.35)$$

where ϕ is the phase of Γ'_i .

Two equations can be written from (2.35) as follows

$$\Gamma_i(\omega) = \frac{\beta}{[(1+\beta^2)+(2Q_u\delta)^2]^{1/2}} \geq \frac{1}{|\Gamma'_i(\omega)|} \quad (2.36)$$

and the other is

$$-2\theta - \arctan \left(\frac{2Q_u\delta}{1+\beta} \right) + \phi = 0 \quad (2.37)$$

at oscillation frequency (where $\omega = \omega_0$) using $\delta = (f - f_0)/f_0$, equation (2.36) and (2.37) give

$$|\Gamma_i(\omega_0)| = \frac{\beta_0}{1+\beta_0} \cdot \frac{1}{|\Gamma'_i(\omega_0)|} \quad (2.38)$$

and $\theta_0 = \phi_0 / 2 = \gamma_0 l$ (2.39)

where

β_0 : Coupling coefficient at resonans frequency ($\omega = \omega_0$)

γ_0 : Propagation constant at resonans frequency ($\omega = \omega_0$).

Using (2.38) we can find β_0 with respect to Γ'_i as follows

$$\beta_0 = \frac{1/|\Gamma'_i(\omega_0)|}{1-1/|\Gamma'_i(\omega_0)|} \quad (2.40)$$

as shown in Figure 2.12 $\Gamma'_i(\omega_0)$ depends on feedback element (Z_1), so we must investigate the oscillation conditions at port 2 of GaAs MESFET while Z_1 is used as series feedback element.

At the begining of this investigation, s-parameters for two port device from 3-port s-parameters while the third port terminated by impedance Z_1 will be used.

In Chapter 3 there is more information about s-parameters of 3-port device, and for this section we use from those relations.

Figure 2.14 shows two-port device while there is an impedance at source. If the s-parameters for this configuration denoted by S^T . Then we have

$$S^T = \begin{bmatrix} s_{11} + \frac{s_{31}s_{13}\Gamma_1}{1-s_{33}\Gamma_1} & s_{12} + \frac{s_{13}s_{32}\Gamma_1}{1-s_{33}\Gamma_1} \\ s_{21} + \frac{s_{31}s_{23}\Gamma_1}{1-s_{33}\Gamma_1} & s_{22} + \frac{s_{23}s_{32}\Gamma_1}{1-s_{33}\Gamma_1} \end{bmatrix} \quad (2.41)$$

where Γ_1 is the reflection coefficient related to Z_1 and equals to $Z_1 - Z_0 / Z_1 + Z_0$.

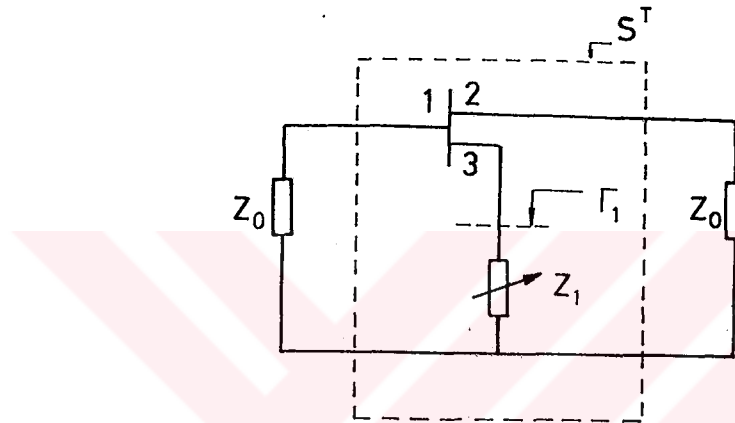


Fig. 2.14 Determination of Z_1 .

The aim is to determine the value of the series feedback impedance Z_1 that will result in the modulus of s_{11}^T and s_{22}^T being greater than unity and hence, create instability in the transistor, that is

$$|s_{11}^T| > 1 \quad \text{and} \quad |s_{22}^T| > 1 \quad (2.42)$$

The $|\Gamma_1|=1$ plane determines a circle when mapped in the input and output reflection coefficient planes using the mapping technique.

The following formulas can be used for mapping: any S^T parameter from S^T matrix can be written as

$$S = A + \frac{BC}{\frac{1}{\Gamma} - D} \quad (2.43)$$

where $\Gamma = \frac{Z-Z_0}{Z+Z_0}$

for drawing the results (2.43) has another form as

$$S = M + R \left(\frac{Z-NZ_0^*}{Z+N^*Z_0} \right) \quad (2.44)$$

where

$$M \hat{=} A + \frac{BC}{1-|D|^2} \cdot D^* \quad (2.45)$$

$$R \hat{=} \frac{BC}{1-|D|^2} \cdot \frac{1-D^*}{1-D} \quad (2.46)$$

$$N \hat{=} \frac{1+D^*}{1-D} \quad (2.47)$$

for mapping $|\Gamma_1|=1$ in s_{11}^T

$$A=s_{11}, B=s_{13}, C=s_{31}, D=s_{33}, Z=Z_1, \Gamma=\Gamma_1$$

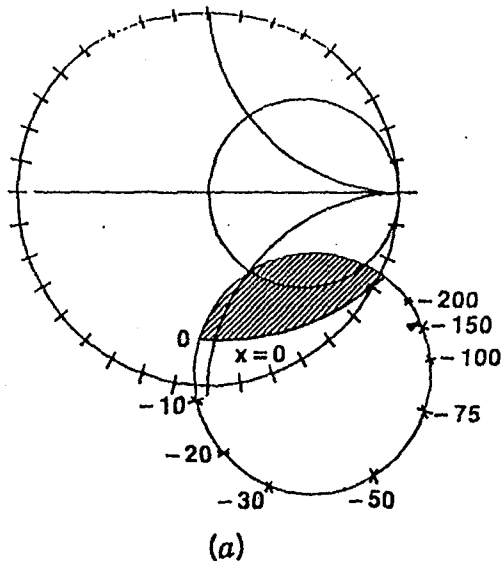
and for mapping $|\Gamma_1|=1$ in s_{22}^T

$$A=s_{22}, B=s_{23}, C=s_{32}, D=s_{31}$$

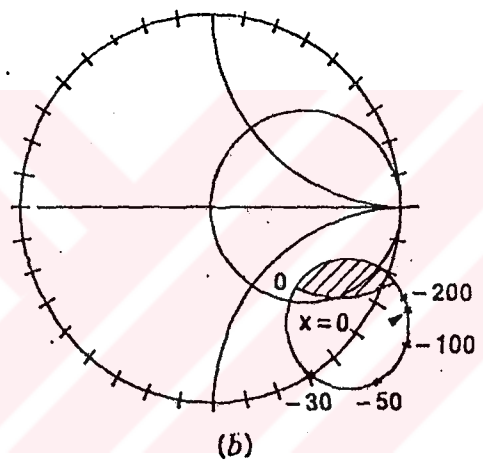
Figure 2.15 shows the $|\Gamma_1|=1$ plane mapped into the s_{11}^T and s_{22}^T planes for the half-micron GaAs FET at 10 GHz.

The shaded area represents inductive impedance and the unshaded area represents the capacitive impedance in the source.

From Figure 2.15 it may be noted that a negative reactance greater than 30Ω can be used to make both s_{11}^T and s_{22}^T greater than one [9].



(a)



(b)

Fig. 2.15 Mapping of $|\Gamma_1| \approx 1$ in (a) s_{11}^T and (b) s_{22}^T .

A dielectric resonator coupled to a microstrip line can also be used as impedance Z_1 in Fig. 2.14.

The reflection coefficient Γ_1 , in this case is a function of the coupling coefficient β and the distance θ between the transistor plane and the resonator plane.

After determining Z_1 for impedance matching at the output port Fig. 2.16 can be used.

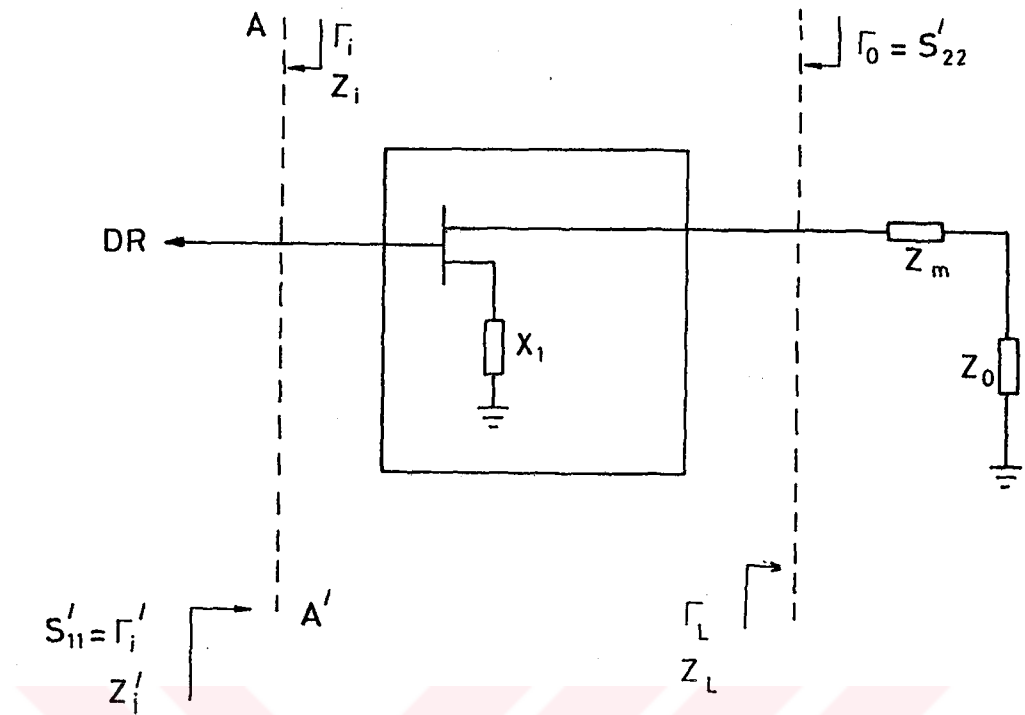


Fig. 2.16 Impedance matching conditions.

The impedance seen at the right side of BB' plane is

$$Z_L = Z_0 + Z_m \quad (2.48.a)$$

since Z_m for impedance matching selected as passive element then $Z_m = jX_m$, the normalize impedance equals to

$$z_L = (Z_0 + jX_m) / Z_0 = 1 + jX_m \quad (2.48.b)$$

for oscillation at port 2 of FET $\Gamma_L \cdot \Gamma_0 > 1$ must be satisfied, and,

$$Z_L + Z_0 = 0$$

or

$$Z_0 = -Z_L = -1 - jX_m \quad (2.49)$$

If the normalized impedance at the left side of AA' plane in Figure 2.16 represented by

$$z_i = r - jy$$

and oscillation condition at port 1 of FET be

$$\Gamma_i \Gamma'_i > 1$$

and also the sum of impedances at this port be equal to zero, Then we have

$$Z'_i + Z_i = 0$$

or

$$z'_i = -z_i = -r + jy \quad (2.50)$$

Then for reflection coefficient at these ports one obtains:

$$z_0 = \frac{1+s'_{22}}{1-s'_{22}} = -1-jX_m \quad (2.51)$$

$$z'_i = \frac{1+s'_{11}}{1-s'_{11}} = -r+jy \quad (2.52)$$

Since $s'_{11} = \Gamma'_i$ and $s'_{22} = \Gamma_0$, above equations obtained like this form.

Using (2.51) and (2.52) gives

$$s'_{22} = 1 + \frac{j_2}{X_m} \quad (2.53)$$

and

$$s'_{11} = \frac{1+r-jy}{r-1-jy} \quad (2.54)$$

s'_{11} and s'_{22} can be determined in another way by using S^T matrix. For two port FET which is loaded by Γ_L ,

That is

$$s'_{11} = s_{11}^T + \frac{s_{12}^T s_{21}^T \Gamma_L}{1-s_{22}^T \Gamma_L} \quad (2.55)$$

and

$$s'_{22} = s_{22}^T + \frac{s_{12}^T s_{21}^T \Gamma_i}{1 - s_{11}^T \Gamma_i} \quad (2.56)$$

For oscillation conditions at two ports the following relation must be satisfied.

$$s'_{11} = 1/\Gamma_i \quad (2.57)$$

$$\text{and } s'_{22} = 1/\Gamma_L \quad (2.58)$$

using (2.57) and (2.58) in (2.55) and (2.56) gives

$$\frac{1}{\Gamma_L} = s_{22}^T + \frac{s_{12}^T s_{21}^T \Gamma_i}{1 - s_{11}^T \Gamma_i} \quad (2.59)$$

$$\frac{1}{\Gamma_i} = s_{11}^T + \frac{s_{12}^T s_{21}^T \Gamma_L}{1 - s_{11}^T \Gamma_L} \quad (2.60)$$

from $z_L = 1 + jX_m$ for reflection coefficient we have

$$\Gamma_L = \frac{z_L - 1}{z_L + 1} = \frac{-jX_m}{2 + jX_m} \quad (2.61)$$

and for $z'_i = -r + jy$,

$$\Gamma'_i = \frac{z'_i - 1}{z'_i + 1} = \frac{-r - 1 + jy}{-r + 1 + jy} \quad (2.62)$$

Thus by satisfying (2.59) and (2.60) simultaneously X_m can be determined.

CHAPTER 3

COMPUTER AIDED DESIGN OF DUAL GATE MESFET OSCILLATOR

GaAs MESFET have been used for X-band mixer applications as externally driven and self oscillating mode operation. When low IF's are used the dual-gate MESFET is preferred because the isolation between RF and L_0 is readily accomplished.

It has been shown that a dual gate GaAs FET can also be used as a self oscillating mixer (SOM) with an appreciable amount of gain in the X-band. Implanted into a FET receiver, the self oscillating mixer will increase the degree of integration and all receiver functions will now need only three FETs. This will be important in order to economise wafer material of a monolithic GaAs front end and to choose the best architecture.

To find the best configuration for a self-oscillating mixer with a dual gate FET, a stability analysis using S-parameters has been carried out. It showed that for a short-circuit at the drain, the instability region of gate 1 covers the whole area of the smith chart ($R>0$), while at gate 2 the instability regions are located at the periphery [10].

This fact has essential advantages since gate 1 can be matched for maximum gain at 12 GHz without altering the oscillation conditions.

At gate 2 (near drain), on the other hand, the oscillation condition can be realised using a dielectric

resonator only at its resonance frequency in order to avoid parasitic oscillations.

In Fig. 1.4, a common source dual-gate FET operates as a dielectric resonator stabilised oscillator at the local oscillator frequency f_{L0} (≈ 11 GHz). The stabilisation circuit, using $\text{Ba}_2\text{Ti}_9\text{O}_{20}$ dielectric resonators, a 50Ω microstrip and a 50Ω damping load, is connected with gate 2 and imposes the frequency and temperature stability of the oscillation.

The requirements to the oscillator circuit are:

- (a) The circuit oscillates only in the presence of the dielectric resonator at the resonance frequency of the resonator.
- (b) The magnitude of the oscillation is sufficient for conversion gain of the circuit in mixer operation.
- (c) The oscillation frequency has low variation with temperature. All these conditions could be satisfied by the used stabilisation circuit.

For investigating the conditions for unconditional stability at gate 1 and oscillation condition at gate 2, we need the s-parameters for common gate and common drain FET configurations from the general scattering-parameters which are available for CS configuration.

For obtaining s-parameters for common gate and common drain FET, the s-parameters for 3-port device from 2-port FET are obtained and then these three-port s-parameters are changed to 2-port s-parameter according the condition at any time in the circuit.

3.1. 3-Port s-Parameters From 2-Port Device:

For a three-port device as shown in Fig. 3.1 we have:

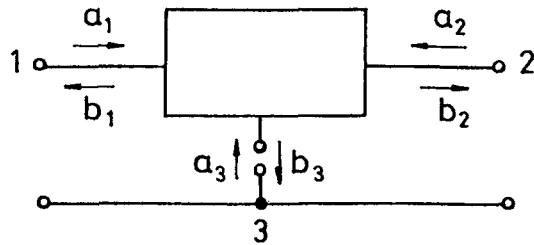


Fig. 3.1 3-port FET.

$$\begin{bmatrix} b_1 \\ b_2 \\ b_3 \end{bmatrix} = \begin{bmatrix} s_{11} & s_{12} & s_{13} \\ s_{21} & s_{22} & s_{23} \\ s_{31} & s_{32} & s_{33} \end{bmatrix} \begin{bmatrix} a_1 \\ a_2 \\ a_3 \end{bmatrix} \quad (3.1)$$

By using the property of S-matrix for three port device that states the summation of elements in any row or column is equal to 1 we have six equations as follows:

$$\sum_{j=1}^3 s(i,j) = 1 \quad i=1, 2, 3 \quad (3.2.a)$$

$$\sum_{i=1}^3 s(i,j) = 1 \quad j=1, 2, 3 \quad (3.2.b)$$

If the third port in Fig. 3.1 is grounded then we have $\Gamma_3 = b_3/a_3 = -1$ (Γ_3 is reflection coefficient at port-3).

By substituting instead of a_3 , b_3 in (3.1) we have:

$$b_1 = s_{11}a_1 + s_{12}a_2 + s_{13}a_3 \quad (a)$$

$$b_2 = s_{21}a_1 + s_{22}a_2 + s_{23}a_3 \quad (b) \quad (3.3)$$

$$b_3 = s_{31}a_1 + s_{32}a_2 + s_{33}a_3 \quad (c)$$

where $b_3/a_3 = -1$

and then in (3.3.c) we have

$$\begin{aligned} -a_3 &= s_{31}a_1 + s_{32}a_2 + s_{33}a_3 \\ -(1+s_{33})a_3 &= s_{31}a_1 + s_{32}a_2 \\ a_3 &= \frac{s_{31}a_1 + s_{32}a_2}{-(1+s_{33})} \end{aligned} \quad (3.4)$$

by substituting the value of a_3 in (3.3 a,b) we have:

$$b_1 = s_{11}a_1 + s_{12}a_2 + \frac{s_{13}s_{31}a_1}{-(1+s_{33})} + \frac{s_{13}s_{32}a_2}{-(1+s_{33})} \quad (3.5.a)$$

$$b_2 = s_{21}a_1 + s_{22}a_2 + \frac{s_{23}s_{31}a_1}{-(1+s_{33})} + \frac{s_{23}s_{32}a_2}{-(1+s_{33})}$$

or equivalently;

$$\begin{bmatrix} b_1 \\ b_2 \end{bmatrix} = \begin{bmatrix} s_{11} - \frac{s_{13}s_{31}}{1+s_{33}} & s_{12} - \frac{s_{13}s_{32}}{1+s_{33}} \\ s_{21} - \frac{s_{23}s_{31}}{1+s_{33}} & s_{22} - \frac{s_{23}s_{32}}{1+s_{33}} \end{bmatrix} \begin{bmatrix} a_1 \\ a_2 \end{bmatrix} \quad (3.5.b)$$

By defining the s-matrix for common source FET $S' \stackrel{\Delta}{=} [s'_{ij}]$ and using (3.2), (3.3), (3.4) after some manipulations we obtain:

$$1) s_{33} = \sum_{i,j=1,2} S'(i,j) / \left[4 - \sum_{i,j=1,2} S'(i,j) \right]$$

$$2) s_{32} = \frac{1+s_{33}}{2} (1-s'_{12}-s'_{22})$$

$$3) s_{23} = \frac{1+s_{33}}{2} (1-s'_{21}-s'_{12})$$

$$4) s_{22} = s'_{22} + \frac{s_{23}s_{32}}{1+s_{33}}$$

$$5) s_{13} = 1-s'_{23}-s'_{33}$$

- 6) $s_{31} = 1 - s_{33} - s_{32}$
 - 7) $s_{12} = 1 - s_{22} - s_{32}$
 - 8) $s_{21} = 1 - s_{22} - s_{23}$
 - 9) $s_{11} = 1 - s_{21} - s_{31}$
- (3.6)

3.2. Conditions For Oscillations And Unconditionally Stability In A Cascode Circuit:

Fig. 3.2 shows the dual-gate MESFET represented as a cascode of two single-gate FET's, FET 1 and FET 2. Terminal voltages and currents are defined in the figure.

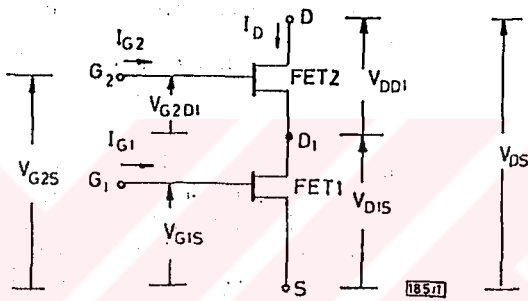


Fig. 3.2 Cascode equivalent of dual-gate MESFET.

As described before and shown in Fig. 1.4 for gate 1 the unconditional stability conditions for mixing function and for gate 2 the oscillation conditions must be provided.

In investigation of this conditions we will use the cascode equivalent circuit of dual-gate MESFET. At first the stability conditions for gate 1 will be considered.

3.2.1. Unconditional Stability Conditions Of Gate 1

Fig. 3.3 shows the equivalent circuit of dual gate FET where the gate of second FET is terminated with an impedance (Z_3) with reflection coefficient Γ_3 .

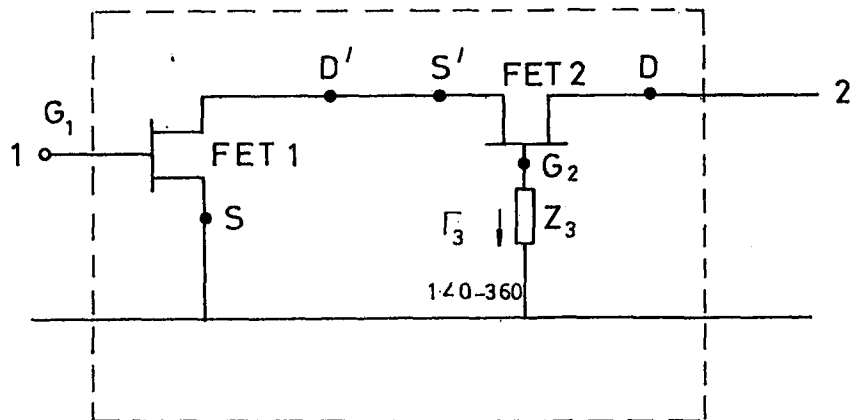


Fig. 3.3 Equivalent of dual-gate with an impedance between gate 2 and ground.

The following symbols will be used for this configuration:

$S' = [s'_{ij}; i, j=1, 2]$: S-matrix for single gate common source FET (FET 1)

$S = [s_{ij}; i, j=1, 2, 3]$: S-matrix for 3-port device from S'

$S_g = [s_g{}_{ij}; i, j=1, 2]$: S-matrix for common gate FET from 3-port device (FET 2)

$S_c = [s_c{}_{ij}; i, j=1, 2]$: S-matrix for two FET which are cascaded with each other

s'_{c11} : reflection coefficient at gate 1 of cascode circuit. with short circuit load at drain

$\phi_s' = [\phi_s{}_{ij}; i, j=1, 2]$: chain scattering matrix of FET 1

$\phi_g' = [\phi_g{}_{ij}; i, j=1, 2]$: chain scattering matrix of FET 2

$\phi_c' = [\phi_c{}_{ij}; i, j=1, 2]$: chain scattering matrix of cascode circuit

K: stern stability factor.

According to the defined symbols we have:

$$S' = \begin{bmatrix} s'_{11} & s'_{12} \\ s'_{21} & s'_{22} \end{bmatrix} : \text{given s-parameters for FET 1}$$

S'_{c11} can be determined by considering the cascode circuit step by step as is explained as follows:

Step 1: obtaining S-matrix for three port device from given S'-parameters which the third port is floating.

Step 2: by terminating the third port (gate of FET) with an impedance which its reflection coefficient is Γ_3 as shown in Fig. 3.3 we have

$$b_1/a_1 = \Gamma_3 \quad \text{or} \quad b_1 = \Gamma_3 a_1 \quad (3.7)$$

by substituting (3.7) in (3.3a) we have:

$$\Gamma_3 a_1 = s_{11} a_1 + s_{12} a_2 + s_{13} a_3$$

or

$$a_1 = \frac{s_{12} a_2 + s_{13} a_3}{\Gamma_3 - s_{11}}$$

as result we have:

$$b_3 = s_{11} \left(\frac{s_{12} a_2 + s_{13} a_3}{\Gamma_3 - s_{11}} \right) + s_{32} a_2 + s_{33} a_3 \quad (3.8.a)$$

$$b_2 = s_{21} \left(\frac{s_{12} a_2 + s_{13} a_3}{\Gamma_3 - s_{11}} \right) + s_{22} a_2 + s_{23} a_3 \quad (3.8.b)$$

for a common gate FET with source (port 3 of Fig. 3.1) as input and drain as output we have the matrix as:

$$\begin{bmatrix} b_3 \\ b_2 \end{bmatrix} = \begin{bmatrix} \frac{s_{31} s_{13}}{\Gamma_3 - s_{11}} + s_{33} & \frac{s_{31} s_{12}}{\Gamma_3 - s_{11}} + s_{32} \\ \frac{s_{21} s_{13}}{\Gamma_3 - s_{11}} + s_{23} & \frac{s_{21} s_{12}}{\Gamma_3 - s_{11}} + s_{22} \end{bmatrix} \begin{bmatrix} a_3 \\ a_2 \end{bmatrix} \quad (3.9)$$

and the configuration related to this matrix is shown in Fig. 3.4.

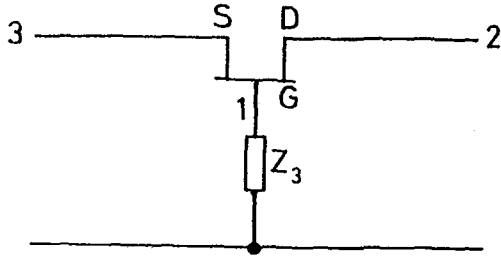


Fig. 3.4 Common gate FET.

Now we define the above matrix as S_g , that is:

$$\begin{bmatrix} b_3 \\ b_2 \end{bmatrix} = \begin{bmatrix} s_{g11} & s_{g12} \\ s_{g21} & s_{g22} \end{bmatrix} \begin{bmatrix} a_3 \\ a_2 \end{bmatrix}$$

where

$$\begin{aligned} s_{g11} &= \frac{s_{31}s_{13}}{\Gamma_3 - s_{11}} + s_{33} \\ s_{g12} &= \frac{s_{31}s_{12}}{\Gamma_3 - s_{11}} + s_{32} \\ s_{g21} &= \frac{s_{21}s_{13}}{\Gamma_3 - s_{11}} + s_{23} \\ s_{g22} &= \frac{s_{21}s_{12}}{\Gamma_3 - s_{11}} + s_{22} \end{aligned} \tag{3.10}$$

Step 3: obtaining chain scattering matrix for each FET.

For common source FET we defined S-matrix as S' , then we have

$$\phi_{S'} = \begin{bmatrix} s_{21}^{-1} & -s_{21}^{-1}s_{22}' \\ s_{11}'s_{21}^{-1} & s_{12}' - s_{11}'s_{21}^{-1}s_{22}' \end{bmatrix} \tag{3.11}$$

and for common gate:

$$\phi_g = \begin{bmatrix} s_{g21}^{-1} & -s_{g21}^{-1}s_{g22} \\ s_{g11}s_{g21}^{-1} & s_{g12}-s_{g11}s_{g21}^{-1}s_{g22} \end{bmatrix} \quad (3.12)$$

for cascode circuit these two ϕ matrices would be multiplied by each other. That is

$$\phi_c = \phi_s \cdot \phi_g$$

where

$$\begin{aligned} \phi_c &= \begin{bmatrix} s_{21}'^{-1} & -s_{21}'^{-1}s_{22}' \\ s_{11}'s_{21}'^{-1} & s_{12}'-s_{11}'s_{21}'^{-1}s_{22}' \end{bmatrix} \begin{bmatrix} s_{g21}^{-1} & -s_{g21}^{-1}s_{g22} \\ s_{g11}s_{g21}^{-1} & s_{g12}-s_{g11}s_{g21}^{-1}s_{g22} \end{bmatrix} \quad (3.13) \\ &= \begin{bmatrix} \phi_{c11} & \phi_{c12} \\ \phi_{c21} & \phi_{c22} \end{bmatrix} \end{aligned}$$

where

$$\begin{aligned} \phi_{c11} &= s_{21}'^{-1}s_{g21}^{-1} + s_{g11}s_{g21}^{-1} \cdot (-s_{21}'^{-1}s_{22}') \\ \phi_{c12} &= -s_{21}'^{-1}s_{g21}^{-1}s_{g22}' + (-s_{21}'^{-1}s_{22}') (s_{g12}-s_{g11}s_{g21}^{-1}s_{g22}) \\ \phi_{c21} &= s_{11}'s_{21}'^{-1}s_{g21}^{-1} + (s_{g11}s_{g21}^{-1})(s_{12}'-s_{11}'s_{21}'^{-1}s_{22}') \\ \phi_{c22} &= (s_{11}'s_{21}'^{-1})(-s_{g21}^{-1}s_{g22}') + (s_{g12}-s_{g11}s_{g21}^{-1}s_{g22}) (s_{12}'-s_{11}'s_{21}'^{-1}s_{22}') \end{aligned} \quad (3.14)$$

Step 4: Obtaining scattering matrix for cascode circuit from ϕ_c matrix

$$S_c = \begin{bmatrix} \phi_{c21}\phi_{c11}^{-1} & \phi_{c22} - \phi_{c21}\phi_{c11}^{-1}\phi_{c12} \\ \phi_{c11}^{-1} & -\phi_{c11}^{-1}\phi_{c12} \end{bmatrix} \quad (3.15)$$

$$= \begin{bmatrix} s_{c11} & s_{c12} \\ s_{c21} & s_{c22} \end{bmatrix}$$

If port 2 of cascode circuit (in Fig.3.3) terminated by a load which its reflection coefficient is equal to Γ_y then the reflection coefficient at port 1 of this circuit will be as:

$$s'_{c11} = s_{c11} + \frac{s_{c12}s_{c21}\Gamma_y}{1-s_{c22}\Gamma_y} \quad (3.16)$$

and stern stability factor (K) equals to:

$$K = \frac{1+|\Delta|^2 - |s_{c11}|^2 - |s_{c22}|^2}{2|s_{c12}s_{c21}|} \quad (3.17)$$

where $\Delta = s_{c11}s_{c22} - s_{c12}s_{c21}$

for unconditionally stability at gate 1 of Fig. 3.3 with a variable impedance Z_3 which its reflection coefficient changes as $1/0-360^\circ$ there are two conditions which must be satisfied together. These conditions are:

$$|s'_{c11}| < 1 \quad (3.18)$$

$$\text{and } K > 1 \quad (3.19)$$

By using a computer program as (cascade 1. For) program, these strains are investigated by changing the phase of Γ_3 from zero to 360 degree by step 5° .

As mentioned before for terminating gate 1 by RF signal, port 2 of this circuit must behaves as a short circuit that is, $\Gamma_y = 1$. Then we have

$$s'_{c11} = s_{c11} - \frac{s_{c12}s_{c21}}{1+s_{c22}} \quad (3.20)$$

in the next sections the results of this program will be considered.

3.2.2. Oscillation Conditions:

For self oscillating mixer at gate 2 (near drain) which is terminated with a dielectric resonator coupled to a microstrip line with 50Ω characteristic impedance, conditions for oscillation must be provided. These conditions are $K<1$ and $|s'_{c11}|>1$ (reflection coefficient at port 1 or gate 1).

Fig. 3.5 shows the cascode circuit for this type of conditions which will be used as local oscillator.

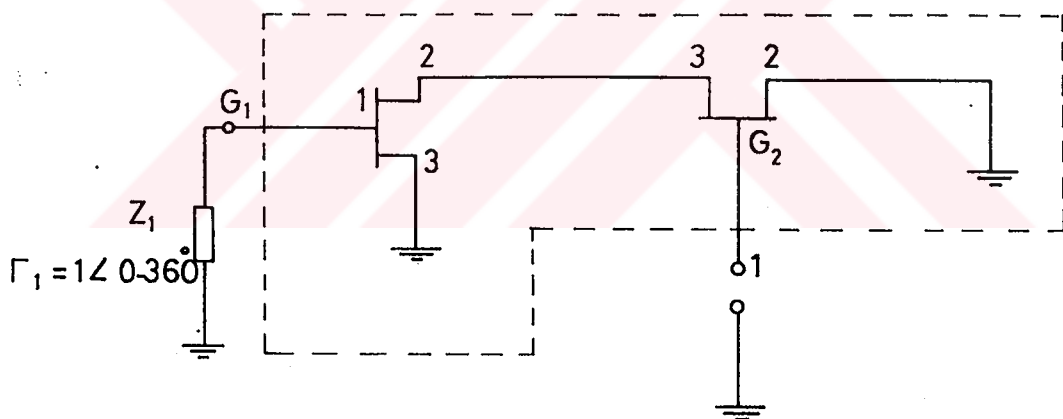


Fig. 3.5 Equivalent circuit of dual gate FET which gate 2 is as input and gate 1 is as output for cascode circuit.

The following symbols will be used for Fig. 3.5.

$S' = [s'_{ij}; i, j=1, 2]$: S-matrix for single gate common source (FET 1)

$S = [s_{ij}; i, j=1, 2, 3]$: S-matrix for 3-port device from S'

$S_d = [s_d{}_{ij}; i, j=1, 2]$: S-matrix for common drain (FET 2) from 3-port S-matrix

$S'_c = [s'_{cij}; i, j=1, 2]$: S-matrix for cascode circuit

s''_{c11} : Reflection coefficient at gate 2 of cascode circuit with terminating gate 1 by $\Gamma_1 = 1/0-360$

$\phi_s' = [\phi_{sij}; i, j=1, 2]$: chain scattering matrix of FET 1

$\phi_d' = [\phi_{dij}; i, j=1, 2]$: chain scattering matrix of FET 2

$\phi_c' = [\phi'_{cij}; i, j=1, 2]$: chain scattering matrix of cascode circuit

s'_{c11} can be determined by using Fig. 3.5. The steps for finding the reflection coefficient are:

Step 1: Obtaining 3-port s-parameters from given S' -matrix for common source FET which the third port is floating.

Step 2: Obtaining 2-port s-parameters for common drain FET from three port S-matrix by terminating drain with a short circuit load as shown in Figure 3.6.

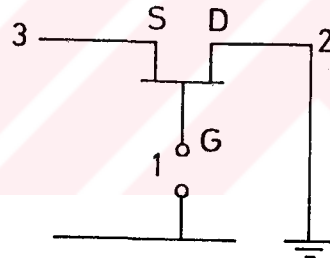


Fig. 3.6 Common drain FET.

with short circuit load at port 2 we have:

$$b_2/a_2 = -1 \quad \text{or} \quad b_2 = -a_2 \quad (3.21)$$

by substituting (3.21) in (3.3) we have:

$$b_1 = s_{11}a_1 + s_{12}a_2 + s_{13}a_3 \quad (a)$$

$$b_2 = -a_2 = s_{21}a_1 + s_{22}a_2 + s_{23}a_3 \quad (b) \quad (3.22)$$

$$b_3 = s_{31}a_1 + s_{32}a_2 + s_{33}a_3 \quad (c)$$

From (3.22.b) we obtain:

$$a_2 = \frac{s_{21}a_1 + s_{23}a_3}{-1-s_{22}} \quad (3.23)$$

in Figure 3.6 gate and source will be considered as input and output respectively. Then from (3.23) we have:

$$\begin{bmatrix} b_1 \\ b_3 \end{bmatrix} = \begin{bmatrix} s_{11} + \frac{s_{12}s_{21}}{-1-s_{22}} & s_{13} + \frac{s_{12}s_{23}}{-1-s_{22}} \\ s_{31} + \frac{s_{21}s_{32}}{-1-s_{22}} & s_{33} + \frac{s_{23}s_{32}}{-1-s_{22}} \end{bmatrix} \begin{bmatrix} a_1 \\ a_3 \end{bmatrix} \quad (3.24)$$

Now, we define the above S-matrix as S_d , that is

$$\begin{bmatrix} b_1 \\ b_3 \end{bmatrix} = \begin{bmatrix} s_{d11} & s_{d12} \\ s_{d21} & s_{d22} \end{bmatrix} \begin{bmatrix} a_1 \\ a_3 \end{bmatrix}$$

where

$$\begin{aligned} s_{d11} &= s_{11} + \frac{s_{12}s_{21}}{-1-s_{22}} \\ s_{d12} &= s_{13} + \frac{s_{12}s_{23}}{-1-s_{22}} \\ s_{d21} &= s_{31} + \frac{s_{21}s_{32}}{-1-s_{22}} \\ s_{d22} &= s_{33} + \frac{s_{23}s_{32}}{-1-s_{22}} \end{aligned} \quad (3.25)$$

Step 3: Obtaining chain scattering matrix for each FET.

For common source FET the chain scattering matrix is like as (3.11) and for common gate this matrix defines as:

$$\phi_d = \begin{bmatrix} s_{d21}^{-1} & -s_{d21}^{-1}s_{d22} \\ s_{d11}s_{d21}^{-1} & s_{d12}-s_{d11}s_{d21}^{-1}s_{d22} \end{bmatrix} \quad (3.26)$$

for configuration which has been shown in Fig. 3.5 chain scattering matrix can be obtained by multiplying the ϕ_d as the first stage by ϕ_s , as the second stage which in it port 2 is input and port 1 is output. We have

$$\begin{aligned} \phi_c' &= \phi_d \cdot \phi_s' \\ \text{or } \phi_c' &= \begin{bmatrix} s_{d21}^{-1} & -s_{d21}^{-1}s_{d22} \\ s_{d11}s_{d21}^{-1} & s_{d12}-s_{d11}s_{d21}^{-1}s_{d22} \end{bmatrix} \begin{bmatrix} s_{21}'^{-1} & -s_{21}'^{-1}s_{22}' \\ s_{11}'s_{21}'^{-1} & s_{12}'-s_{11}'s_{21}'^{-1}s_{22}' \end{bmatrix} \\ &= \begin{bmatrix} \phi_{c11} & \phi_{c12}' \\ \phi_{c21}' & \phi_{c22}' \end{bmatrix} \end{aligned} \quad (3.27)$$

where

$$\phi_{c11}' = s_{d21}^{-1}s_{21}'^{-1} + (-s_{d21}^{-1}s_{d22})(s_{11}'s_{21}'^{-1}) \quad (3.28.a)$$

$$\phi_{c12}' = s_{d21}^{-1}(-s_{21}'^{-1}s_{22}') + (-s_{d21}^{-1}s_{d22})(s_{12}'-s_{11}'s_{21}'^{-1}s_{22}') \quad (3.28.b)$$

$$\phi_{c21}' = (s_{d11}s_{d21}^{-1})(s_{21}'^{-1}) + (s_{d12}-s_{d11}s_{d21}^{-1}s_{d22})(s_{11}'s_{21}'^{-1}) \quad (3.28.c)$$

$$\phi_{c22}' = (s_{d11}s_{d21}^{-1})(-s_{21}'^{-1}s_{22}') + (s_{d12}-s_{d11}s_{d21}^{-1}s_{d22})(s_{12}'-s_{11}'s_{21}'^{-1}s_{22}') \quad (3.28.d)$$

Step 4: Obtaining scattering matrix for cascode circuit from ϕ_c' matrix in this case:

$$S_c' = \begin{bmatrix} \phi_{c21}'\phi_{c11}'^{-1} & \phi_{c22}'-\phi_{c21}'\phi_{c11}'^{-1}\phi_{c12}' \\ \phi_{c11}'^{-1} & -\phi_{c11}'^{-1}\phi_{c12}' \end{bmatrix} \quad (3.29)$$

$$= \begin{bmatrix} s'_{c11} & s'_{c12} \\ s'_{c21} & s'_{c22} \end{bmatrix}$$

If port 1 of cascode circuit (gate 1 in Fig. 3.5) terminated by an impedance (Z_1) with reflection coefficient Γ_1 which its magnitude is equal to 1 and its phase varies from zero to 360° by step 5° , then for reflection coefficient at port 1 (gate 2) we obtain:

$$s''_{c11} = s'_{c11} + \frac{s'_{c12}s'_{c21}\Gamma_1}{1-s'_{c22}\Gamma_1} \quad (3.30)$$

and stern stability factor (K) is:

$$K = \frac{1+|\Delta|^2 - |s'_{c11}|^2 - |s'_{c22}|^2}{2|s'_{c12}s'_{c21}|} \quad (3.31)$$

where

$$\Delta = s'_{c11}s'_{c22} - s'_{c12}s'_{c21}$$

for oscillation conditions at gate 2 of Fig. 3.5 with a variable impedance Z_1 at gate 1, there are two conditions which must be satisfied together. These conditions are:

$$|s''_{c11}| > 1 \quad (3.32)$$

and

$$K < 1 \quad (3.33)$$

It is written a program (cascode 2.for) and these conditions are investigated by changing the phase of Γ_1 from 0° to 360° .

The results of this program will be discussed in the next section.

3.3. Investigating Oscillation Conditions:

There are many ways to view an oscillator, ranging from positive feedback to negative resistance, and each will yield an oscillating circuit if applied correctly. Another way to view oscillator design is as a "reflection amplifier". This intuitive approach to oscillator design has been applied to yield consistent, repeatable results and provides insight as to why certain problems occur and how to avoid them. The reflection amplifier approach also provides a way to model and measure (using S-parameters) a circuit's potential as an oscillator and to predict its performance.

For simplicity, a one-port circuit with input S-parameter s_{11} and a resonant load with reflection coefficient Γ (Figure 3.7) is considered (both s_{11} and Γ are measured at the same reference plane). If a noise (signal) E is incident on the number 1-port, a portion will be reflected, given by $s_{11}^* E$. This signal will then be re-reflected by the load to give $s_{11}^* E^* \Gamma$. Which will again be incident on the input of the one-port.

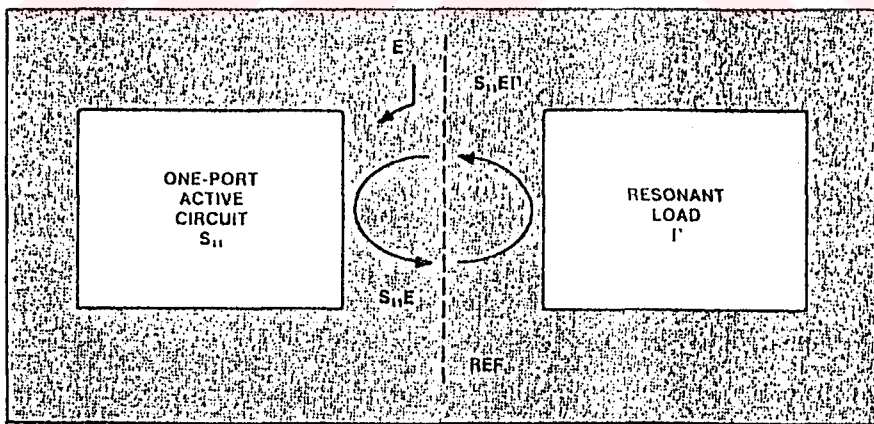


Fig. 3.7 Oscillator consisting of an active circuit with a resonant load.

These reflections add up to give an infinite series. Rather than including all of the terms, however, consider just $s_{11}^* E^* \Gamma$. For oscillation to occur, this

re-reflected signal must meet two requirements. First, it must be greater in magnitude, than the original signal E , second, it also must have the same phase as E . This gives two oscillation conditions:

$$|s_{11}^* E^* \Gamma| > |E| \quad \text{and} \quad (3.34)$$

$$\text{ang}(s_{11}) + \text{ang}(\Gamma) + \text{ang}(E) = \text{ang}(E) \quad (3.35)$$

or

$$|1/s_{11}| < |\Gamma| \quad (3.36)$$

$$\text{ang}(1/s_{11}) = \text{ang}(\Gamma) \quad (3.37)$$

Equations (3.36) and (3.37) lead to important observations. It is very helpful in oscillator design to think in terms of $1/s_{11}$.

This is in line with the "negative resistance" approach as well, for if $1/s_{11}$ is plotted on a smith chart, the values of R and X can be read and multiplied by -1 to obtain the correct values of the (negative) resistance and reactance.

3.3.1. Oscillator Stability Criterion:

In the range where oscillation criterion 1 (equation 3.36) is satisfied, there will be stable oscillation only when criterion (3.37) also is satisfied at only one frequency. Graphically this means that there will be stable oscillation only if the phases of $1/s_{11}$ and Γ are changing in apposite angular direction with changing frequency [16].

In other words $1/s_{11}$ must intersect the resonance loop, and the "arrows" indicating changes with frequency must point in apposite directions. As shown in Figure 3.8.

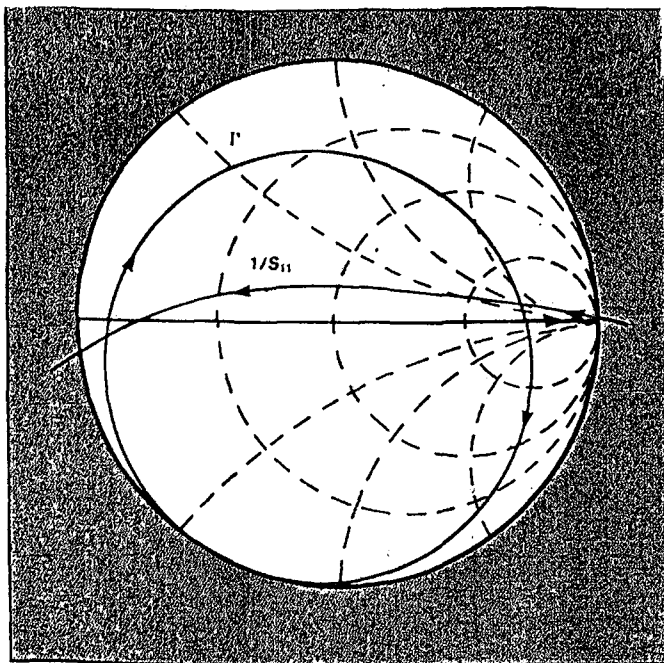


Fig. 3.8 Rotating $1/s_{11}$ to match the resonator Γ provides stable oscillation.

In this work for determining the direction of $1/s'_{11}$ for cascaded circuit, first of all a matching network for port 2 which will be terminated by RF signal at 12 GHz frequency, when port 1 is terminated by 50Ω (characteristic impedance of microstrip line) and drain is loaded by an open stub which its lengths is $\lambda/4$ and its admittance at any frequency is $Y=j\frac{1}{50} \tan \frac{\pi}{2} \cdot \frac{f}{11}$ (at 11 GHz behaves as a short circuit load), must be designed.

For designing the matching network at port two, we need to find the input impedance at port two when port 1 is terminated by 50Ω . The procedure for this work, as shown in Figure 3.9, is as follows:

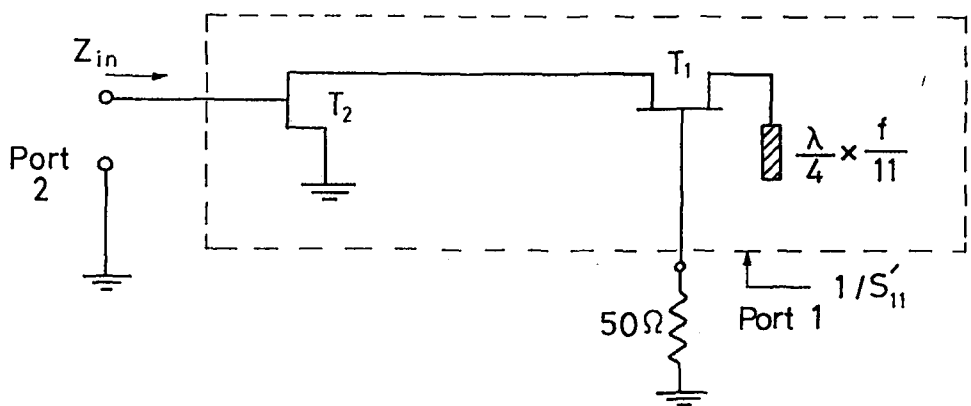
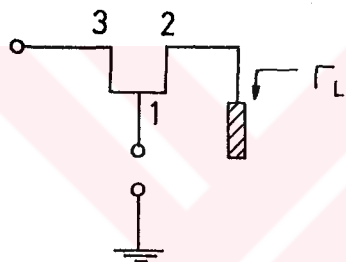


Fig. 3.9 Cascoded circuit of FET 1,2.

for FET 1 we have:



$$\frac{b_2}{a_2} = \Gamma_L \Rightarrow b_2 = \Gamma_L a_2 \quad (3.38)$$

Fig. 3.10 FET I

$$b_1 = s_{11}a_1 + s_{12}a_2 + s_{13}a_3$$

$$b_2 = s_{21}a_1 + s_{22}a_2 + s_{23}a_3 = \Gamma_L a_2$$

$$b_3 = s_{31}a_1 + s_{32}a_2 + s_{33}a_3$$

or

$$\begin{bmatrix} b_1 \\ b_3 \end{bmatrix} = \begin{bmatrix} s_{11} + \frac{s_{12}s_{21}}{\Gamma_L - s_{22}} & s_{13} - \frac{s_{12}s_{23}}{\Gamma_L - s_{22}} \\ s_{31} + \frac{s_{21}s_{32}}{\Gamma_L - s_{22}} & s_{33} - \frac{s_{23}s_{32}}{\Gamma_L - s_{22}} \end{bmatrix} \quad (3.39)$$

and for FET 2 we have:

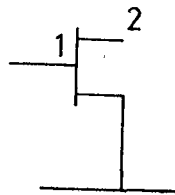


Fig. 3.11 FET 2

by chainging the input and output ports we will obtain

$$\begin{bmatrix} b_2 \\ b_1 \end{bmatrix} = \begin{bmatrix} s_{22} & s_{21} \\ s_{12} & s_{11} \end{bmatrix} \begin{bmatrix} a_2 \\ a_1 \end{bmatrix} \quad (3.40)$$

we can obtain ϕ matrix for any FET as mentioned before, and then we have:

$$\phi_{cc} = \phi_{T1} \cdot \phi_{T2} \quad (3.41)$$

and s_{cc} can be determined from s_{cs} (cc : refers to cascode) and

$$Z_{in} = Z_0 \cdot \frac{1+s_{cc11}}{1-s_{cc11}}$$

For a typical FET (Avantek 10650) at 12 GHz Z_{in} for cascaded circuit is equal to $0.28+j0.89$ (normalized impedance).

Note: For designing input matching network determining input impedance of cascode circuit (Mat. for) and (Imp. for) computer programs and smith chart are used.

Two type of matching network for this work are designed which for one of them Lumped element and for another type open stub are used. These circuits are shown as follows:

- a) Matching network by using lumped elements where it's input impedance is complex conjugate of the input

impedance of cascaded circuit.

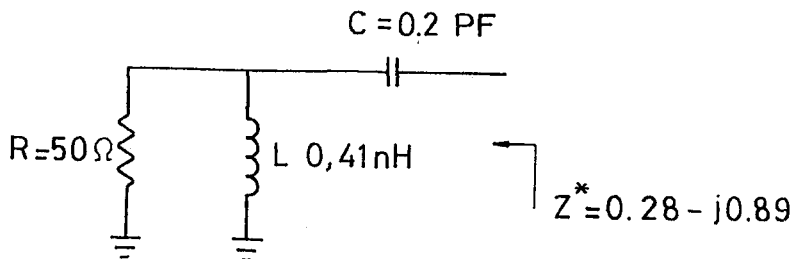


Fig. 3.12 Lumped elements circuit.

b) Matching network by using open stub.

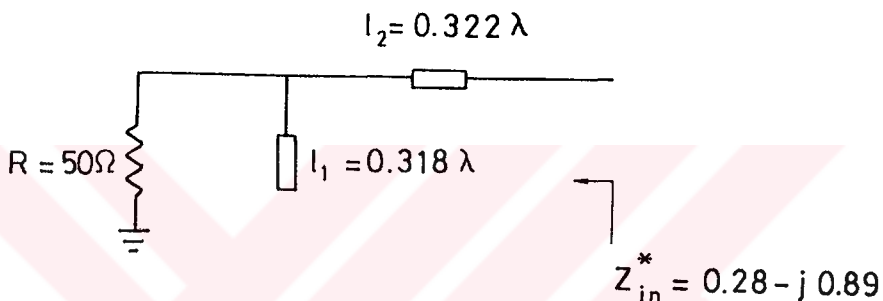


Fig. 3.13 Open stub network.

The input impedance of both matching circuit as shown above will be changed by changing frequency.

In this work for this type of FET only changing of impedance from 12 GHz to 11 GHz is determined. Then for open stub type by using smith chart we have:

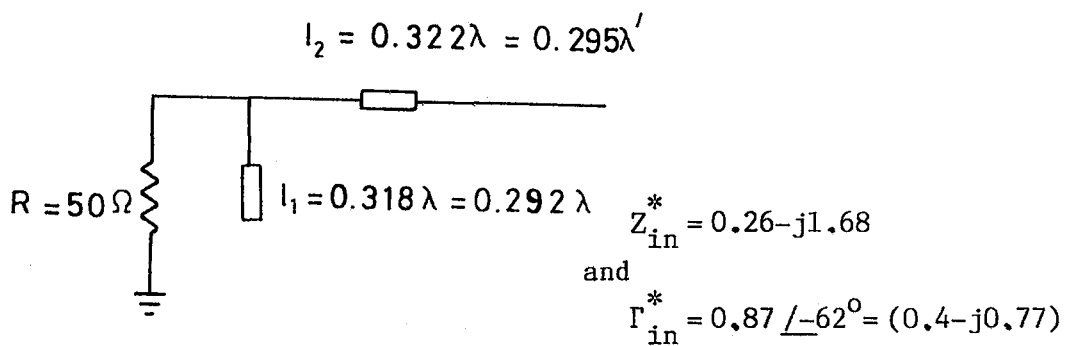


Fig. 3.14 Open stub network ($f=11$ GHz).

For both matching networks at 11 and 12 GHz, s'_{11} for cascode circuit is calculated from:

$$s'_{11} = s_{cc}(1,1) + \frac{s_{cc}(1,2) \cdot s_{cc}(2,1) \cdot \Gamma_{in}^*}{1 - s_{cc}(2,2) \cdot \Gamma_{in}^*}$$

where Γ_{in}^* refers to reflection coefficient from matching network at port 2 of circuit.

Figures 3.15 to 3.18 show this procedure. As shown in Figure 3.18 for lumped elements type and for open stub type at 11 and 12 GHz we have.

a) Lumped elements type:

$$\text{frequency: } 11 \text{ GHz, } 1/s'_{11} = 0.33/-99.7$$

$$\text{" : } 12 \text{ GHz, } 1/s'_{11} = 0.36/-78$$

b) Open stub type:

$$\text{frequency: } 11 \text{ GHz, } 1/s'_{11} = 0.36/-98$$

$$\text{" : } 12 \text{ GHz, } 1/s'_{11} = 0.36/-78$$

These results show $|1/s'_{11}| < |\Gamma|$ and the direction of $1/s'_{11}$ by increasing frequency is in opposite angular direction of reflection coefficient of load which has been obtained by experiment.

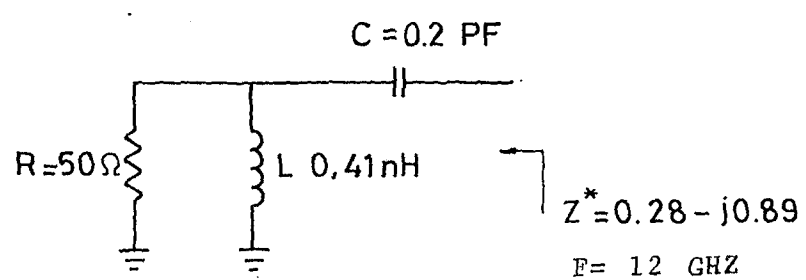
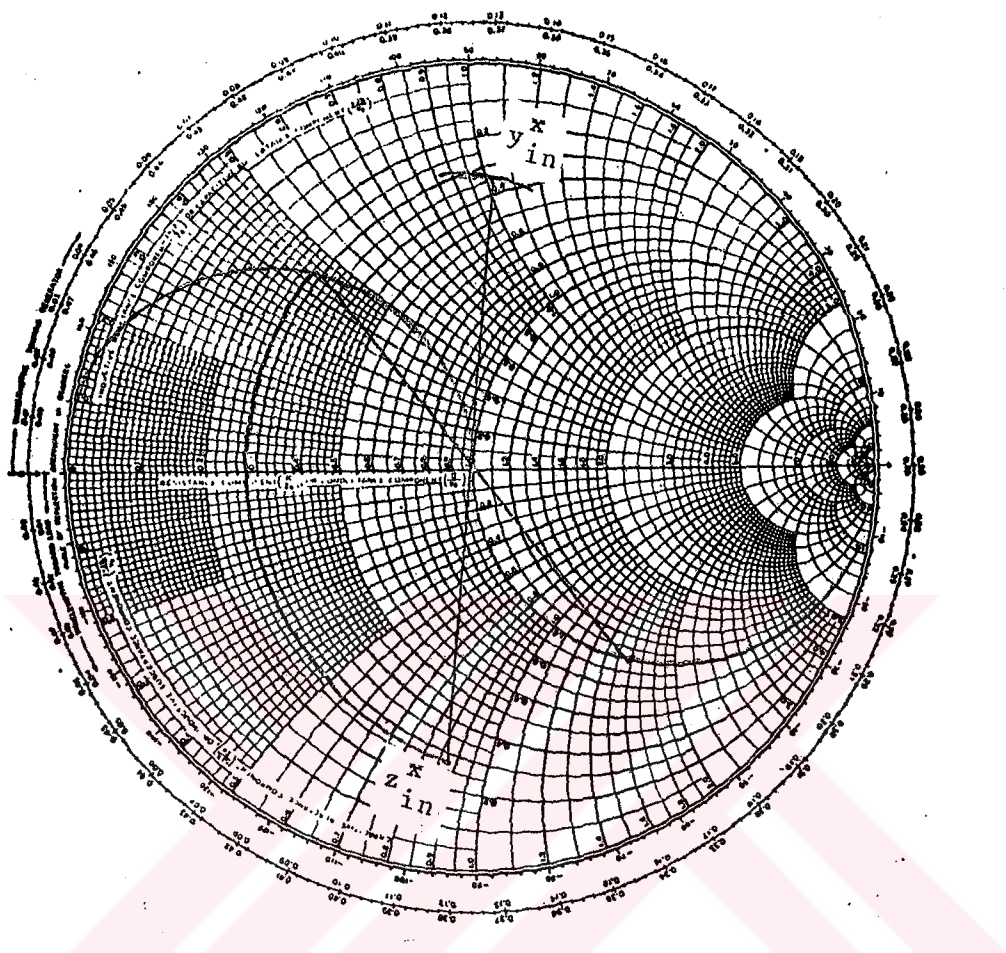
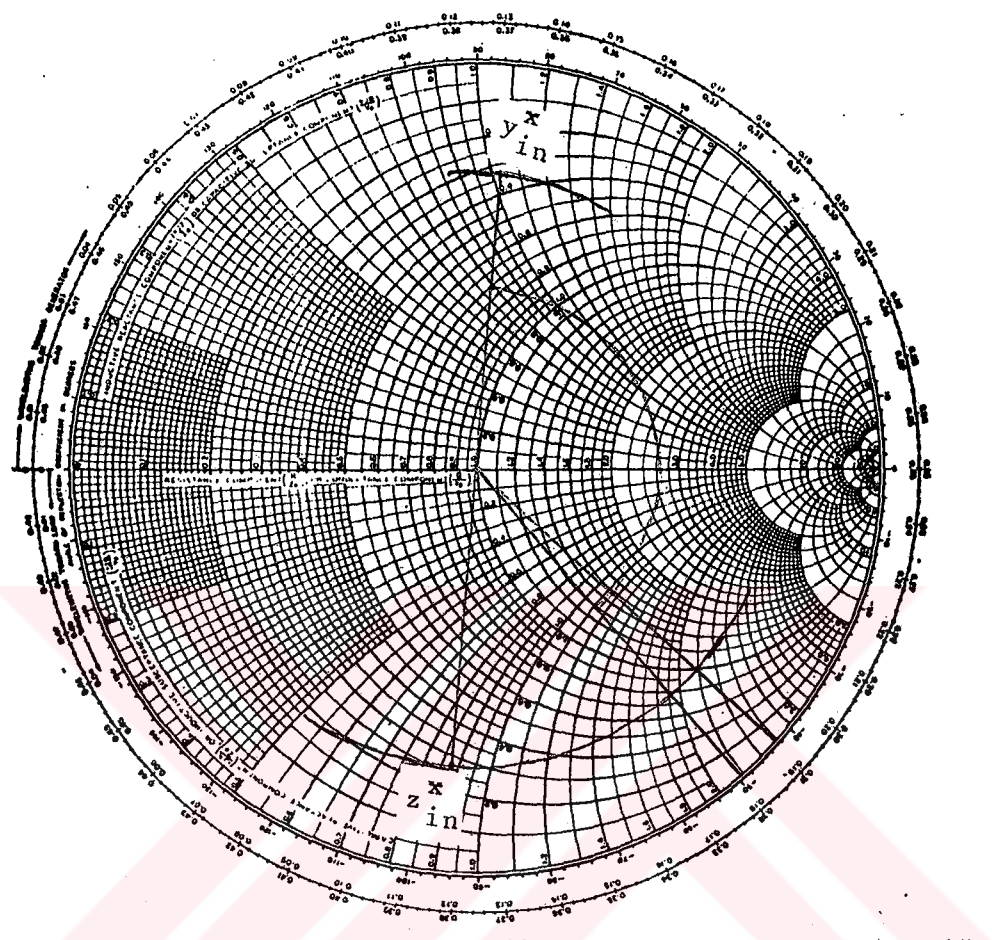
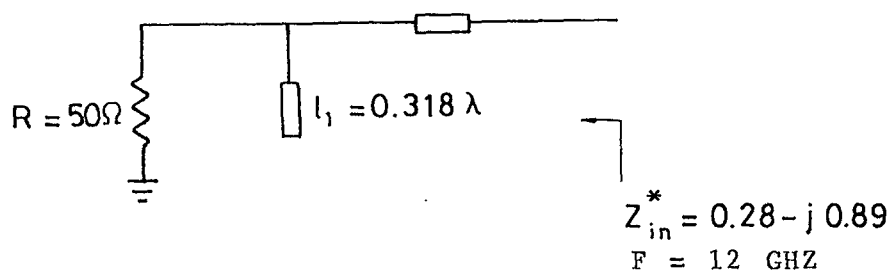


Fig. 3.15 Lumped elements for AVANTEK 10650-10650.



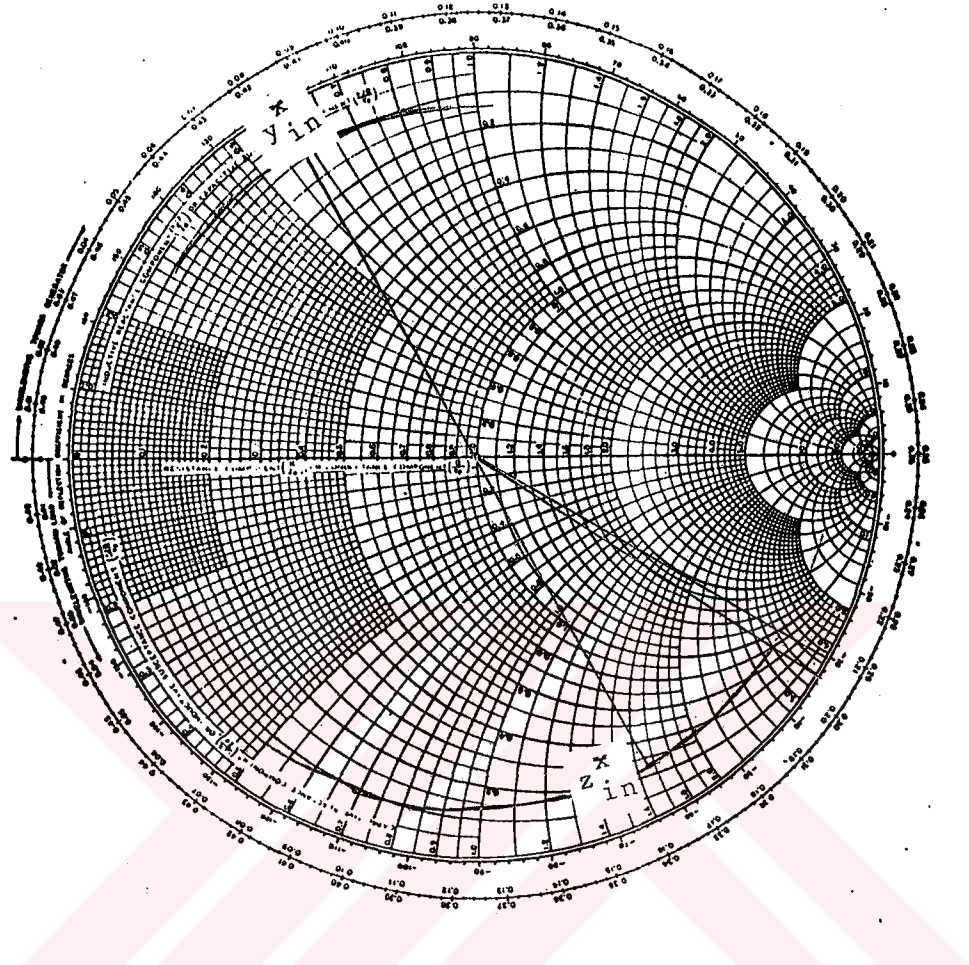
$$l_2 = 0.322 \lambda$$



$$Z_{in}^* = 0.28 - j 0.89$$

F = 12 GHZ

Fig. 3.16 Open stub for AVANTEK 10650-10650.



$$l_2 = 0.322\lambda = 0.295\lambda'$$

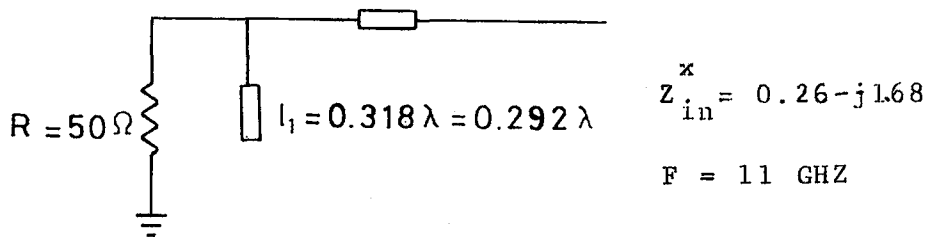


Fig. 3.17 Open stub for AVANTEK 10650-10650.

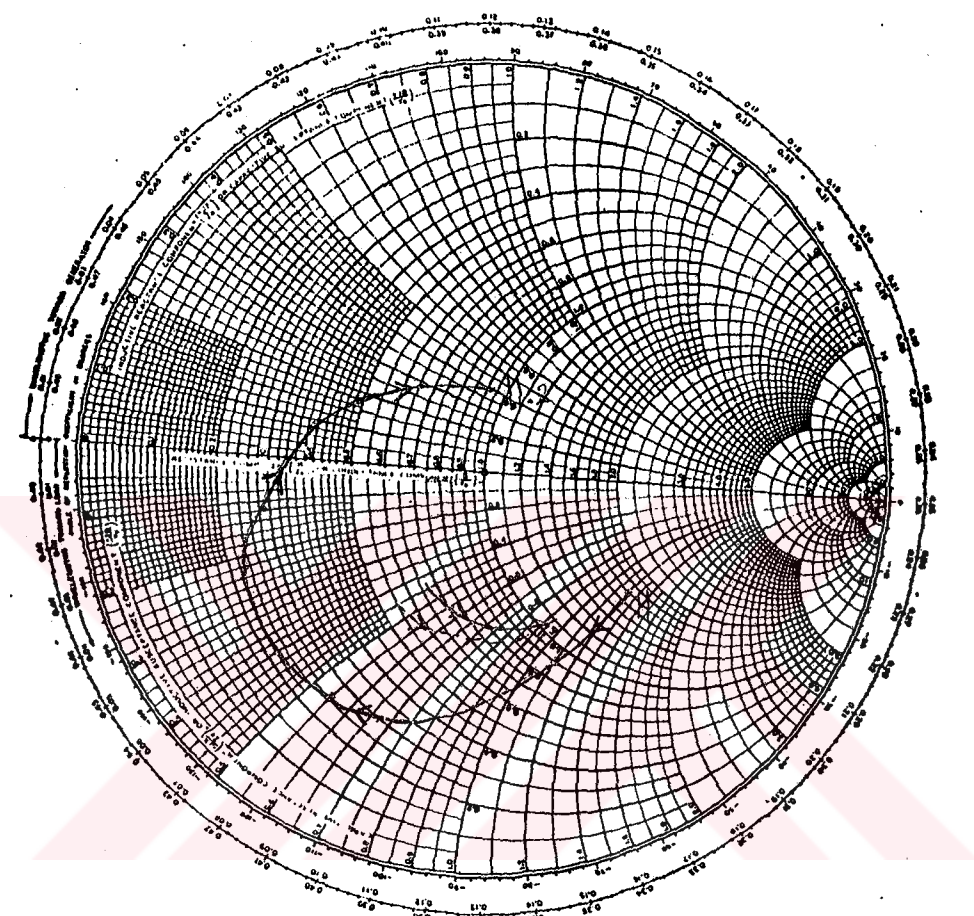


Fig. 3.18 By increasing frequency the direction of $1/s'_{11}$ is the opposite of the direction of Γ at port 1.

— Lumped elements
- - - Open stub

AVANTEK 10650-10650 ($f=11, 12$ GHz).

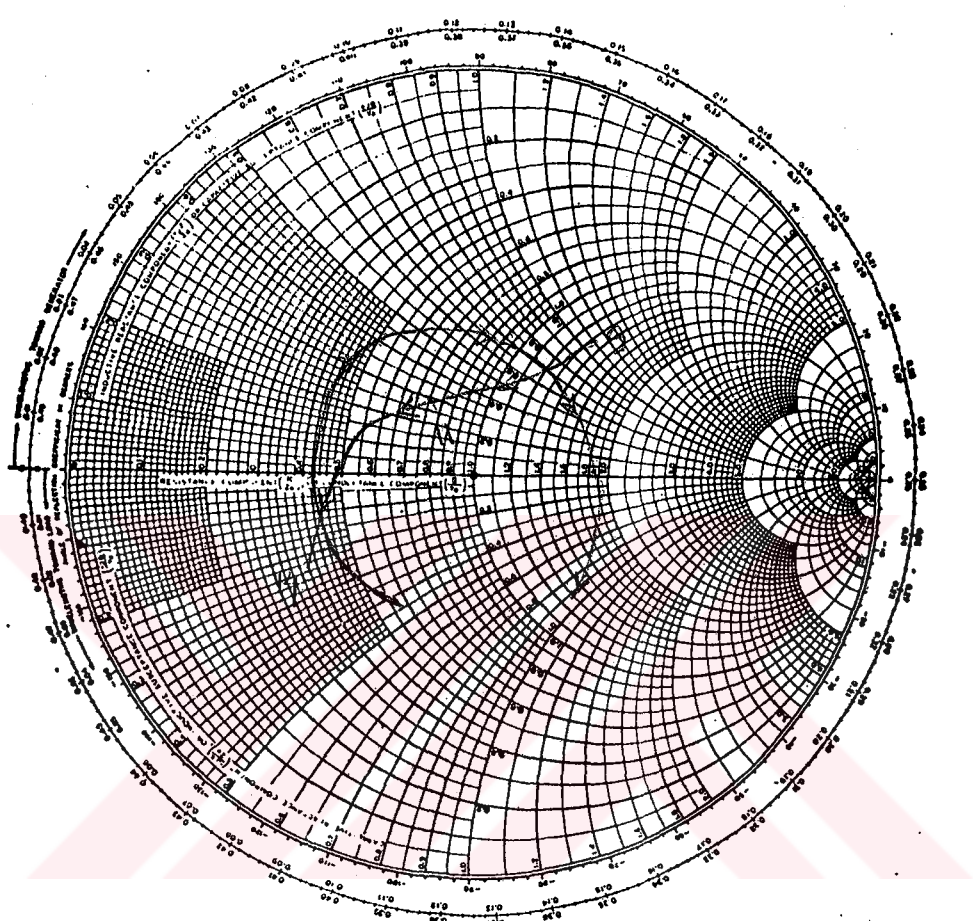


Fig. 3.19 this figure is related to the CFY18 GaAs FET. Where frequency changes between 9 to 14 GHz by step 0.2 GHz and reflection coefficient at port 2 is equal to $\Gamma=1/0-360^\circ$, output port (drain) is assumed as short circuit ($\lambda_{L0}/4$).

Here is another example for Avantek GaAs FET (11671). As shown in Fig. 3.23 the direction of $1/s'_{11}$ by increasing frequency is the same as reflection coefficient at port 1 (DR).

Figures 3.20 to 3.23 show the designing of matching network by using lumped elements and open stupa (port 2).

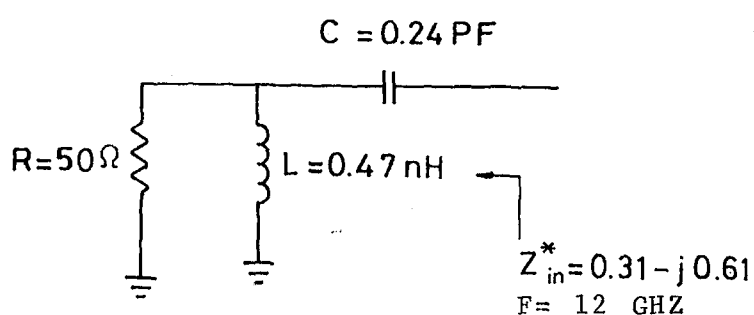
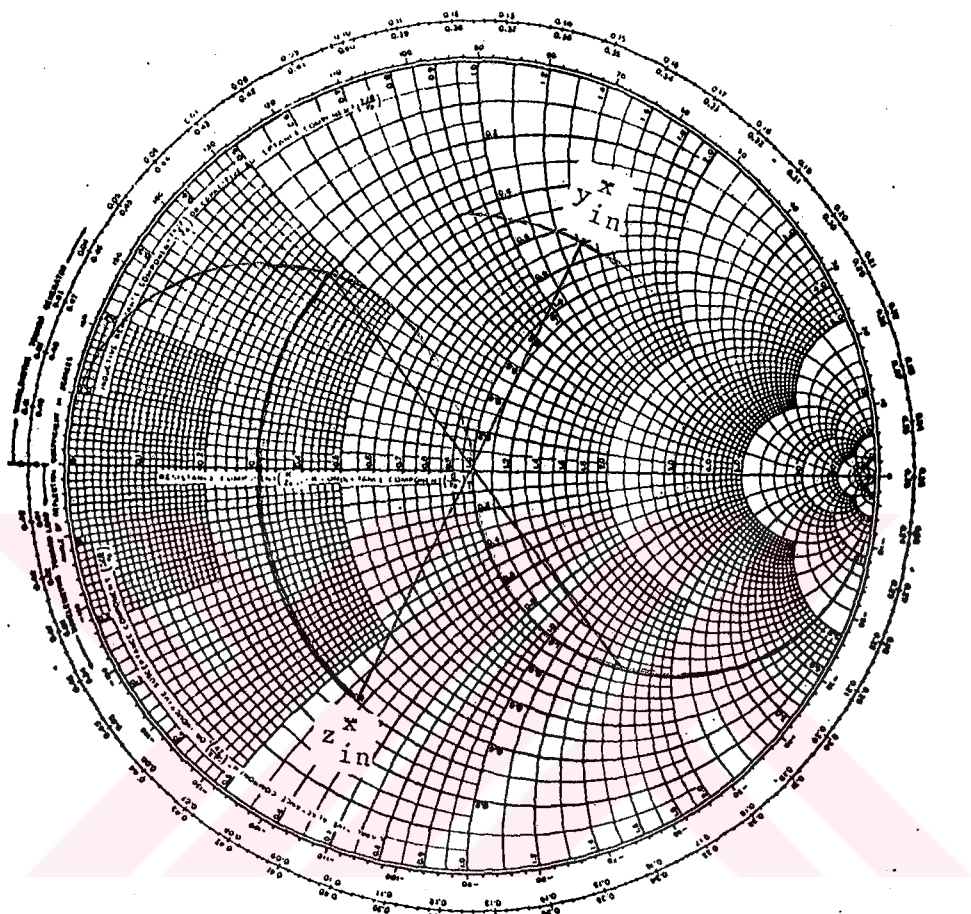


Fig. 3.20 Lumped elements for AVANTEK 11671-11671.

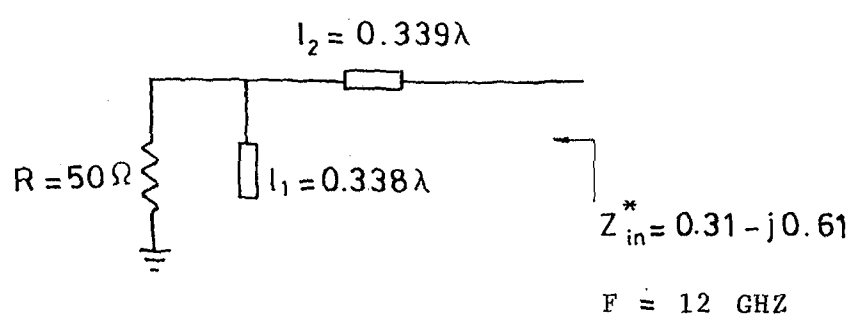
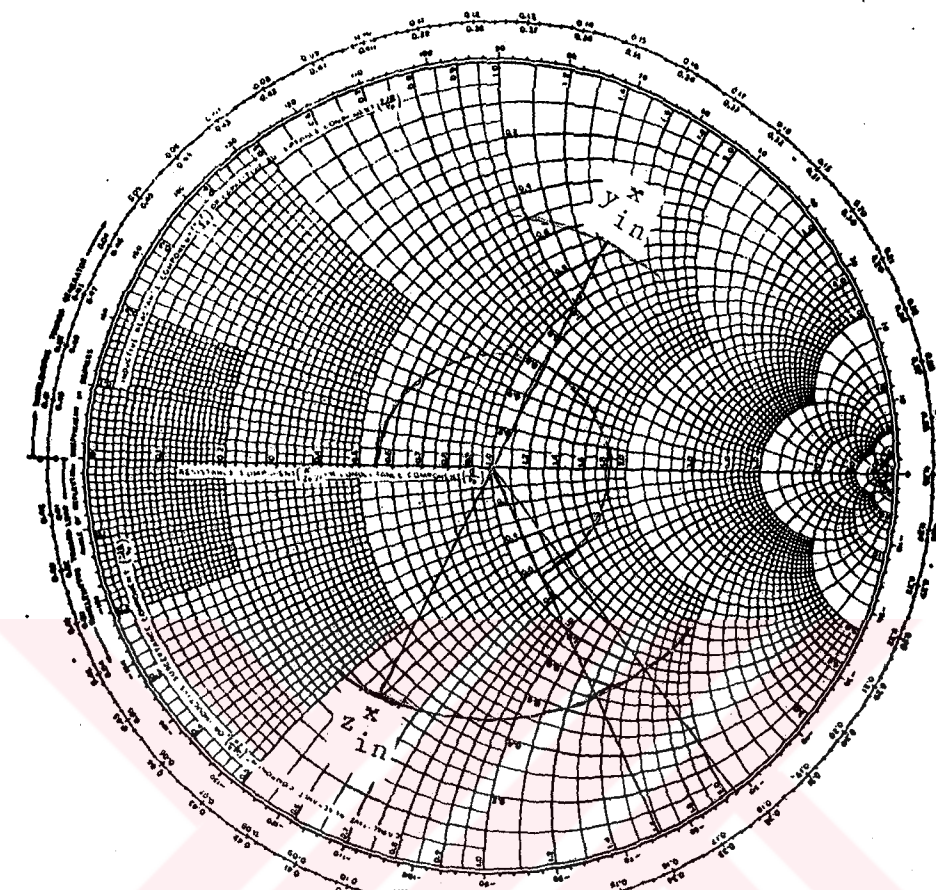


Fig. 3.21 Open stub for AVANTEK 11671-11671.

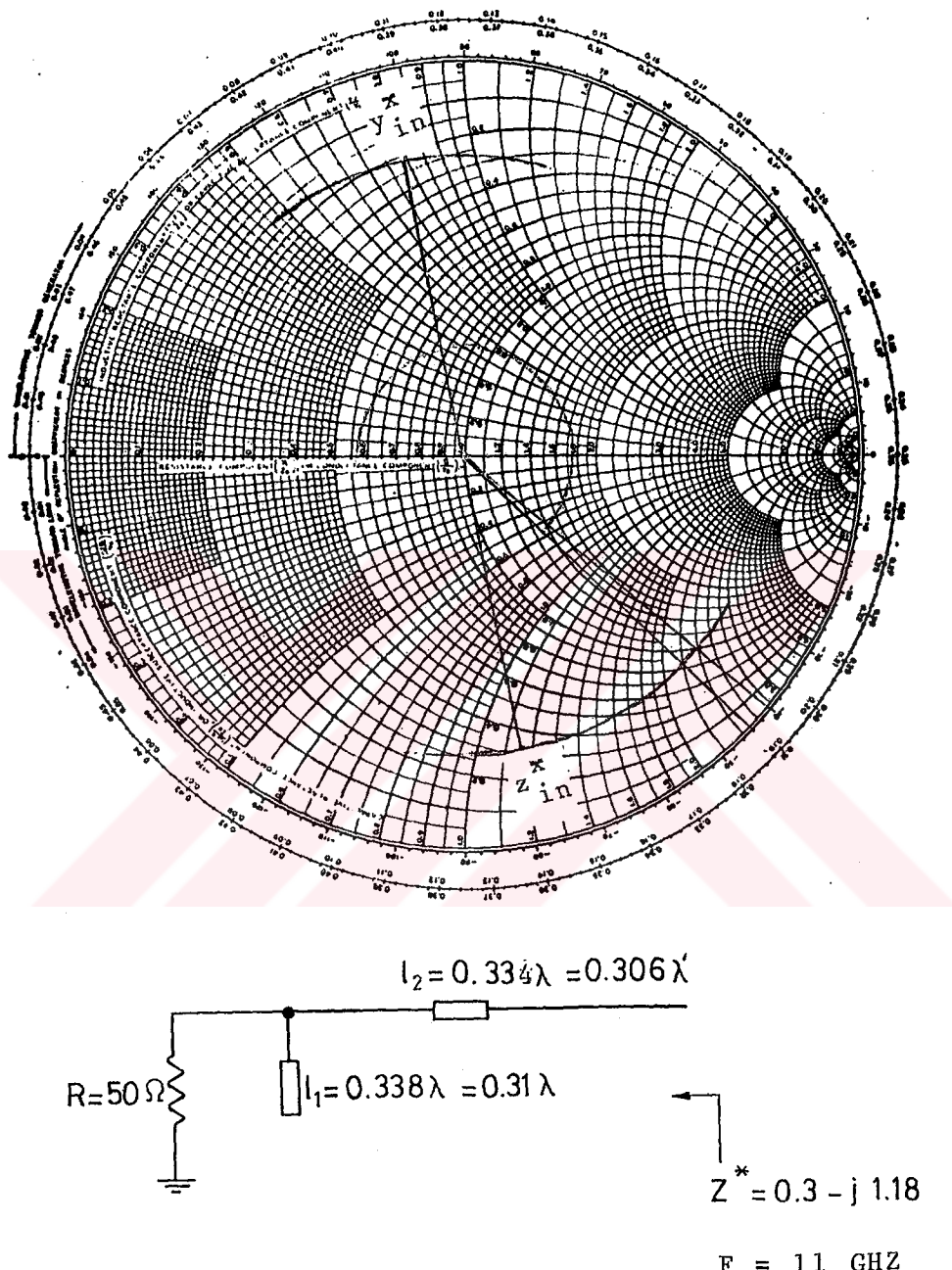


Fig. 3.22 Open stub for AVANTEK 11671-11671.

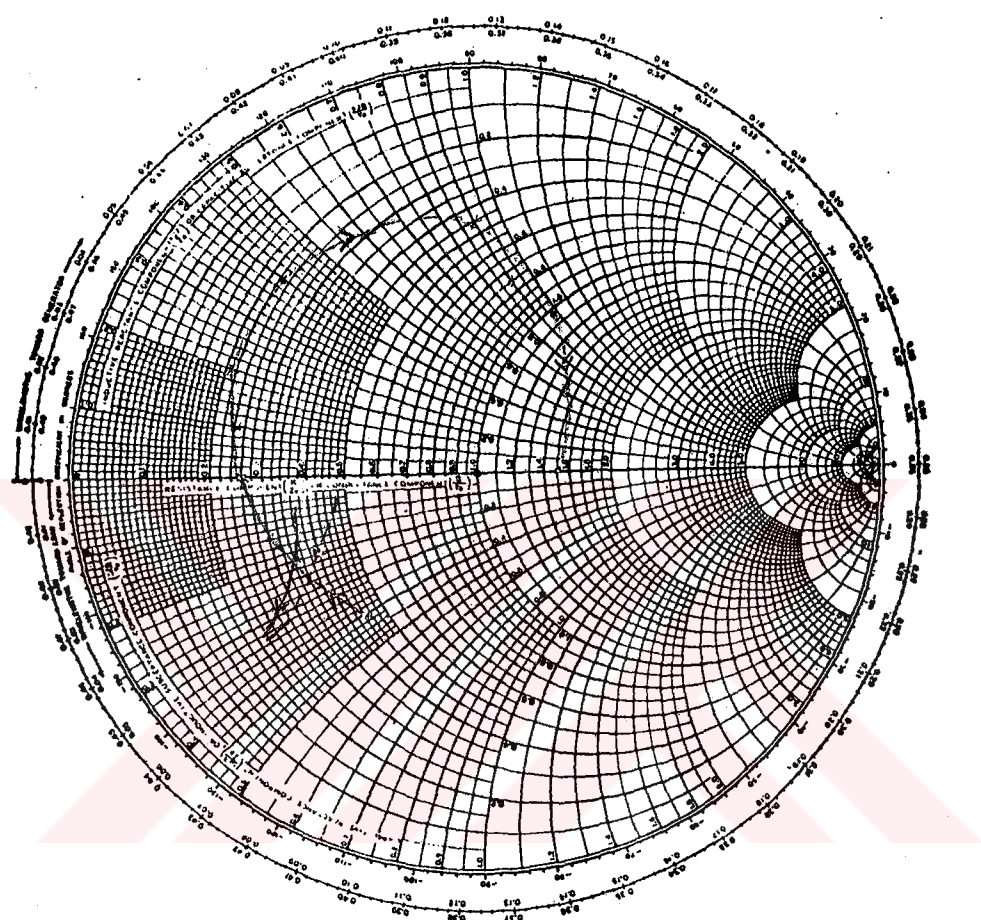
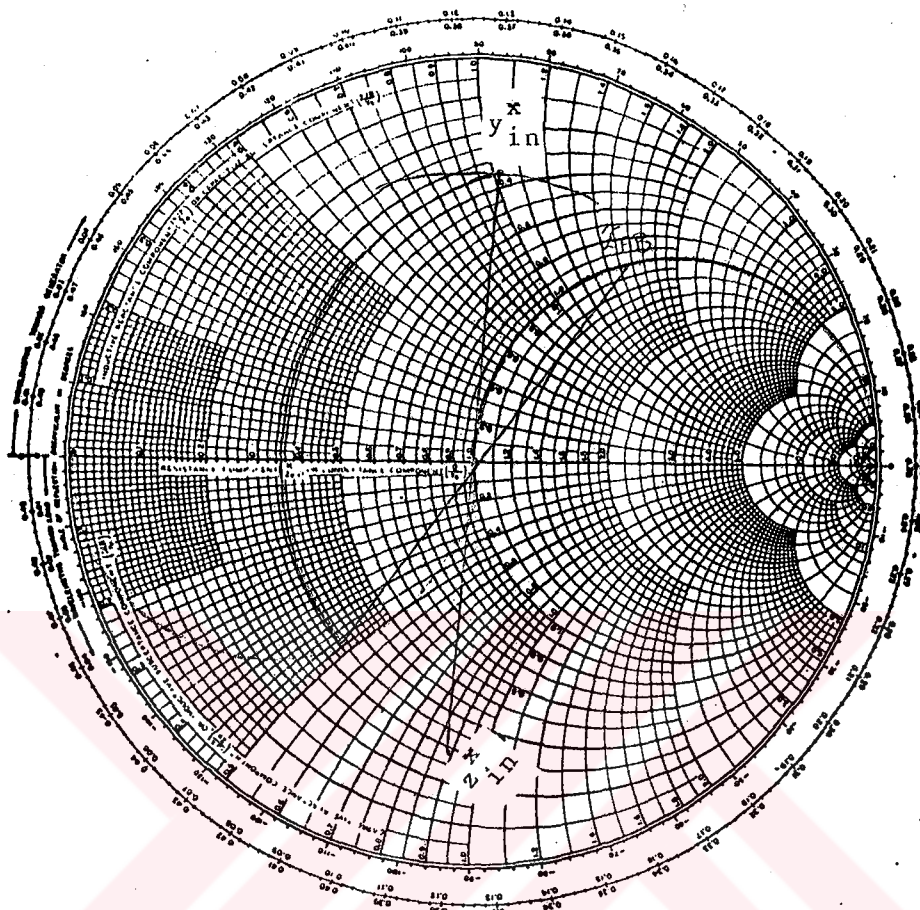


Fig. 3.23 By increasing frequency the direction of $1/s'_{11}$ is the same of the direction of Γ at port 1.

— Lumped elements
- - - Open stub

AVANTEK 11671-11671 ($f=11,12$ GHz).



$$L = \frac{Z_0 \cdot x_{ab}}{\omega} = \frac{50.1, 5}{2\pi \cdot 11 \cdot 10^9} = 1 \text{ nH}$$

$$C = (b_{in} - b_{ab}) / \omega \cdot Z_0 = \frac{(1+0.5)}{2\pi \cdot 11 \cdot 10^9 \cdot 50} = 0.43 \text{ pF}$$

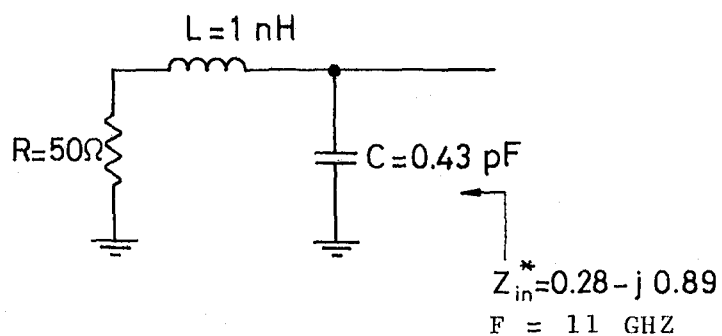


Fig. 3.24

Another type of L Section matching network.

CHAPTER 4

DUAL-GATE MESFET MIXERS

In modern microwave superhetrodyne receivers GaAs FET's are used as preamplifiers, local oscillators, and mixers in hybrid or monolithic versions. Both single gate FET's (SGFET's) and dual-gate FET's (DGFET's) are used as mixers, the second one had applications up to Ka band frequencies.

The advantages of employing DGFET'S as down converters instead of schottky diodes or SGFET's are, except for conversion gain and reasonable noise figure which are inherent also to SGFET mixers, the intrinsic separation of signal and local oscillator ports and, the possibility of separate matching and direct combination of the corresponding powers inside the device. This avoids cumbersome passive couplers and is an important requirement of monolithic circuit design.

In spite of the obvious importance of the mixer application of DGFET's the mixing mechanism of this device is not yet completely understood. This is due to the floating potential of the intergate channel region (D_1 in Fig. 4.1) strongly dependent on the two gates.

The bias and saturation conditions of both FET parts of the DGFET are consequently changing during L_0 voltage excursion and cause them to act as a mixer, or as RF respectively [11]. Fig. 4.1 illustrates the principle of DGFET mixer operation.

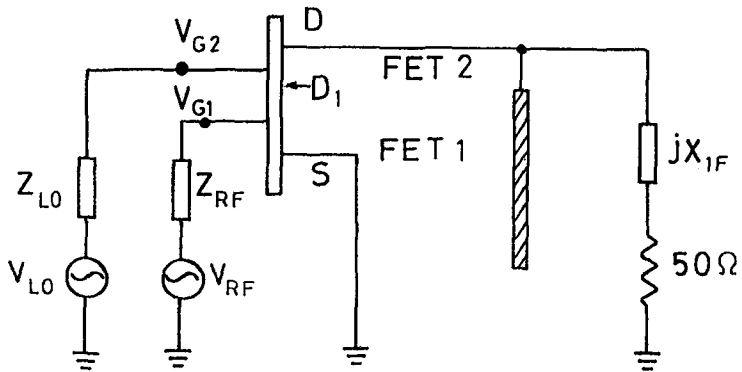


Fig. 4.1 Principle of DGFET mixer operation.

The signal and local oscillator power are injected into either one of the two gates. Usually, the local oscillator is connected with gate 2 and the signal is injected into gate 1.

In this way, a separation of signal and local oscillator power is assured so that well-known techniques for input power and noise matching of gate 1 can be applied.

The If signal is extracted from the drain and feed after reactive matching either to a 50Ω load or to the input port of a post amplifier.

The higher frequencies (f_{LO} , f_{RF}) are short circuited at the drain port using a $\lambda/4$ open microstrip-line at f_{LO} for the MIC design or a 1 PF interdigitated capacitor being in series resonance at 11 GHz.

The parameters to be adjusted for optimum bandwidth, conversion gain, and noise figure are:

- 1) The bias voltages V_{G1} and V_{G2} for a given V_{DS} ,
- 2) The impedance at all three ports at the main frequency components ω_{RF} , ω_{IF} , ω_{LO} , and the image frequency $\omega_{IM} = 2\omega_{LO} - \omega_{RF}$.
- 3) The level of the local oscillator power P_{LO} [11].

4.1. High-Frequency Model Of The Dual-Gate MESFET Mixer

The dc model is of course deficient in the reactive circuit elements that become important at microwave frequencies-in particular, the capacitances associated with the schottky barriers, which results in power being drown from the RF and L_0 sources. Inclusion of these in the model means that a new method of solution must be used. For which we proceed as follows.

In general, for a single-gate device,

$$I_{DS} \approx (1 - \frac{V_{GS}}{V_P})^2 (I_{DSS} + \frac{V_{DS}}{R_{DO}}) \quad (4.1)$$

or

$$I_{DS} = F(V_{GS}, V_{DS}) \quad (4.2)$$

where $F(V_{GS}, V_{DS})$ is a function of the gate-source and drain-source voltages. Differentiating gives

$$\delta I_{DS} = \left. \frac{\partial F}{\partial V_{GS}} \right|_{V_{DS}} \cdot \delta V_{GS} + \left. \frac{\partial F}{\partial V_{DS}} \right|_{V_{GS}} \cdot \delta V_{DS} \quad (4.3)$$

which can be written

$$\delta I_{DS} = G_M(V_{GS}, V_{DS}) \Delta V_{GS} + \frac{\Delta V_{DS}}{R_{DS}} (V_{GS}, V_{DS}) \quad (4.4)$$

where G_M and R_{DS} are the voltage-dependent, small signal, transconductance and source-drain resistance, respectively, and are given by

$$G_M = \left. \frac{\partial F}{\partial V_{GS}} \right|_{V_{DS}} \quad \text{and} \quad R_{DS} = 1 / \left. \frac{\partial F}{\partial V_{DS}} \right|_{V_{GS}} \quad (4.5)$$

The functional forms for G_M and R_{DS} can then be formed by differentiation of the $I_{DS}-V_{DS}$ expression which, for this model, gives

$$G_M = G_{M0} \left(1 - \frac{V_{GS}}{V_P} \right) \quad (4.6)$$

and

$$R_{DS} = \frac{R_{D0}}{\left(1 - \frac{V'_{GS}}{V_P}\right)^2} \quad (4.7)$$

where $G_{M0} = 48 \text{ mS}$ and $R_{D0} = 143 \Omega$.

In (4.7), V'_{GS} refers to the voltage across the input capacitors C_{GS1} and C_{GS2} as appropriate.

The high frequency model analyzed here is shown in Fig. 4.2, with the G_M and R_{DS} of each FET given by (4.6), (4.7), and the gate-source capacitances given by

$$C_{GS} = C_{GSO} \left(1 - \frac{V'_{GS}}{V_{bi}}\right)^{-1/2} \quad (4.8)$$

V_{bi} = Zero bias barrier height = 0.8 V, $C_{GSO} = 0.5 \text{ pF}$

Also

$$R_{GS1} \cdot C_{GS1} = R_{GS2} \cdot C_{GS2} = \tau \text{ where } \tau = 10^{-12} \text{ s} \quad (4.9)$$

Equation (4.8) and (4.9) with V'_{GS} replaced by V_{GD} , are also used to determine the gate-drain capacitances and resistances, which are calculated from the dc conditions and held at these values throughout [12].

4.2. The DC Analysis Of The Dual-Gate MESFET

The dc behavior of the dual-gate FET can be described as that of a cascode of two single gate FET's. From Figure 3.2 we deduce

$$I_D = I_{D1} = I_{DS} \quad (4.10.a)$$

$$V_{DS} = V_{DD1} + V_{D1S} \quad (4.10.b)$$

$$V_{G2D1} = V_{G2S} - V_{D1S} \quad (4.10.c)$$

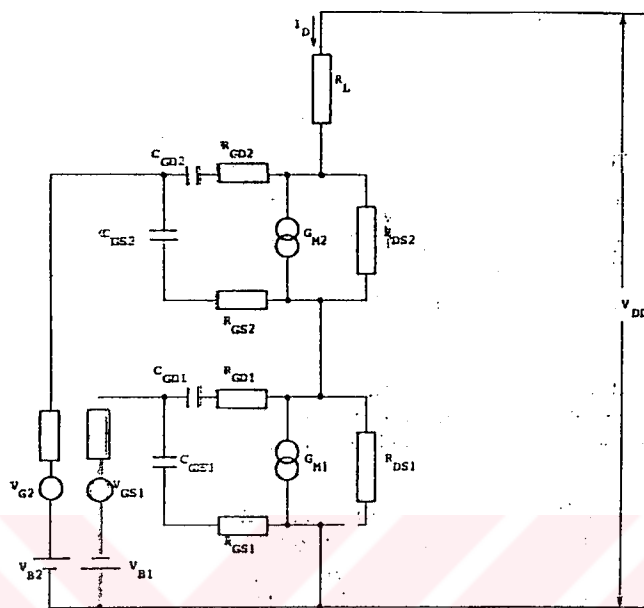


Fig. 4.2 Circuit used for high-frequency of the dual-gate MESFET mixer.

By using Equations (4.6) to (4.8) and Figure 4.2 we have:

$$V_{DS1} = (I_{DS} - G_{M1} V'_{g1}) R_{ds1} \quad (4.11)$$

where V'_{g1} is the voltage across C_{gs1} and

$$R_{ds1} = \frac{R_{d0}}{(1 - V'_{g1}/V_p)^2} \quad (4.12)$$

if we assume $(1 - \frac{V'_{g1}}{V_p}) = X$. Then we have

$$V'_{g1} = V_p - V_p X \quad (4.13)$$

and then

$$R_{ds1} = \frac{R_{d0}}{X^2} \quad (4.14)$$

$$G_{M1} = G_{M0} \left(1 - \frac{V'_{g1}}{V_p}\right) = G_{M0} X \quad (4.15)$$

$$I_{DS} = \left(1 - \frac{V'_{G1S}}{V_p}\right)^2 \left(I_{DSS} + \frac{V_{D1S}}{R_{d0}}\right) \quad (4.16)$$

From (4.11) we have

$$\begin{aligned} V_{D1S} &= I_{DS} - G_{M0} X (V_p - V_p X) - \frac{R_{d0}}{X^2} \\ \text{or } X^2 V_{D1S} &= I_{DS} R_{d0} - G_{M0} V_p R_{d0} X + G_{M0} V_p R_{d0} X^2 \\ \text{or } X^2 (V_{D1S} - G_{M0} V_p R_{d0}) &+ V_p \cdot G_{M0} R_{d0} X - I_{DS} R_{d0} = 0 \\ \text{and } X = &\frac{-V_p G_{M0} R_{d0} \pm \sqrt{(G_{M0} R_{d0} V_p)^2 + 4 \cdot I_{DS} R_{d0} (V_{D1S} - G_{M0} V_p R_{d0})}}{2(V_{D1S} - G_{M0} V_p R_{d0})} \end{aligned} \quad (4.17)$$

in equation (4.17) $X = (1 - \frac{V'_{g1}}{V_p})$ is a function of I_{D1S} and V_{D1S} and since I_{D1S} is a function of V_{G1S} and V_{D1S} is a function of V_{G2S} (eq. 4.1), this implies that the voltage across C_{gs1} is a function of V_{G1S} and V_{G2S} .

If V'_{g2} be the voltage across C_{gs2} we can also find this voltage as a function V_{G1S} and V_{G2S} as follows:

$$X' = 1 - \frac{V'_{g2}}{V_p} = \frac{-V_p G_{M0} R_{d0} \pm \sqrt{(R_{d0} V_p G_{M0})^2 + 4 I_{D1S} R_{d0} (V_{DS} - V_{D1S} - R_{d0} V_p G_{M0})}}{2(V_{DS} - V_{D1S} - R_{d0} V_p G_{M0})} \quad (4.18)$$

For $V_{DS} = \text{Constant}$ and changing V_{g1s} and V_{g2s} according to the DC characteristic of a dual-gate FET as shown in Figure 4.2 a (DC. For) computer program is written and Figures 4.3 - 4.8 show the variations of any element in the model by changing $-2 < V_{g2s} < 4$, $V_L = 3$ and $-1 < V_{g1s} < -2$ at $V_{DS} = 5$ Volt.

Note: For each value of V_{G1S} , V_{G2S} changes as follows:

$$V_{G2S} = V_{G2S0} + V_L \sin \omega_{L0} t$$

where V_{G2S0} is dc voltage, $V_L = 1, 2, 3$ and $\omega_{L0} t$ varies from 0° to 360° by step 10° .

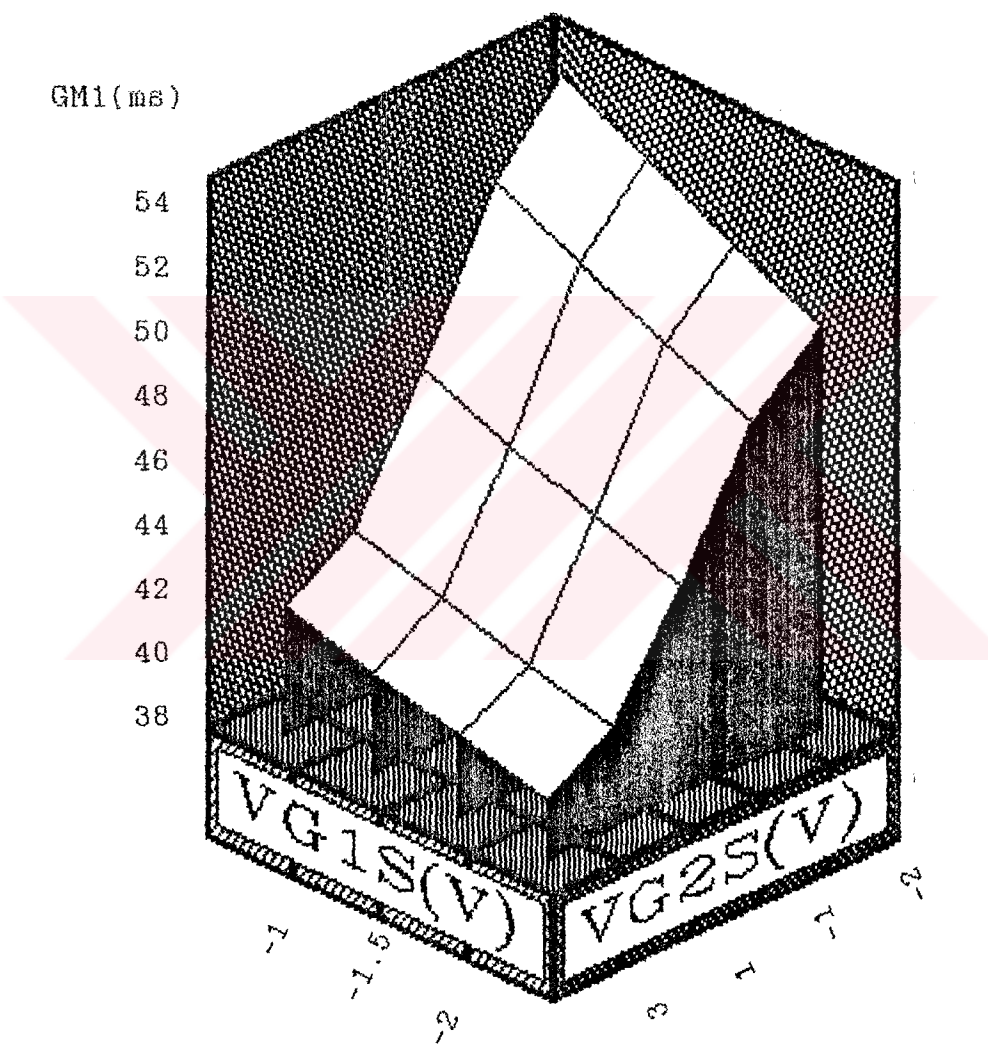


Fig. 4.3
 $G_{M1} = F(V_{G1S}, V_{G2S})$

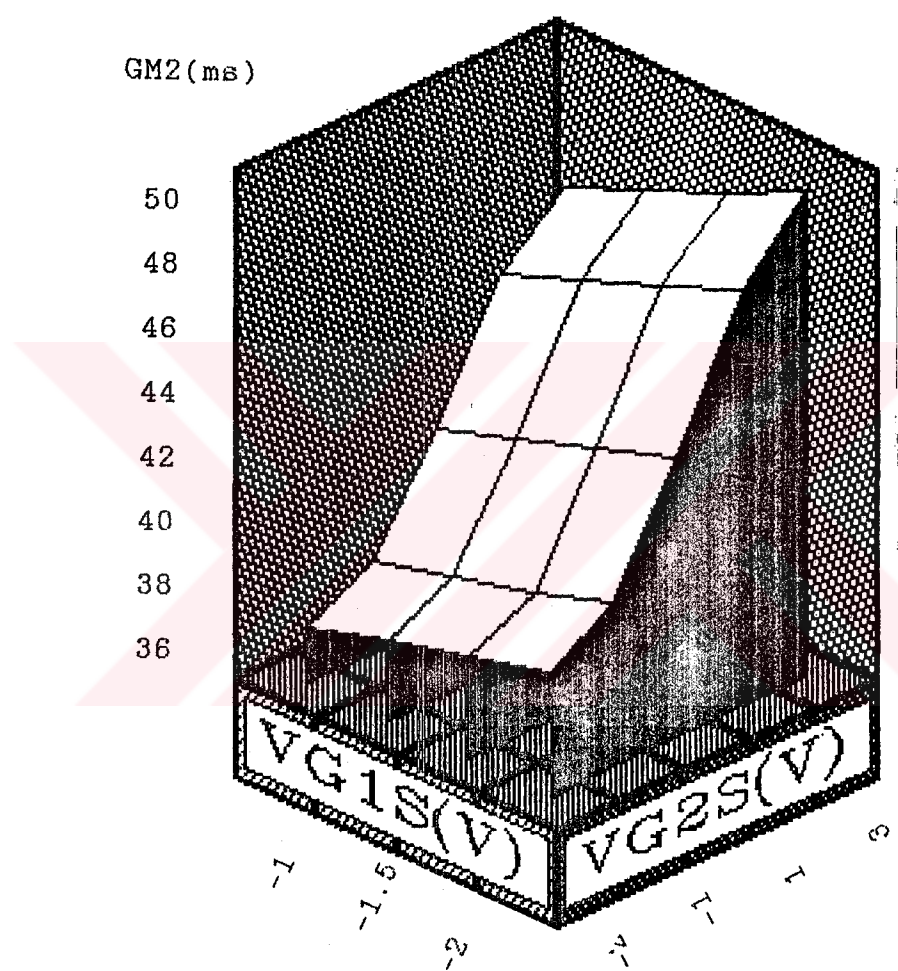


Fig. 4.4
 $G_{M2} = F(V_{G1S}, V_{G2S})$

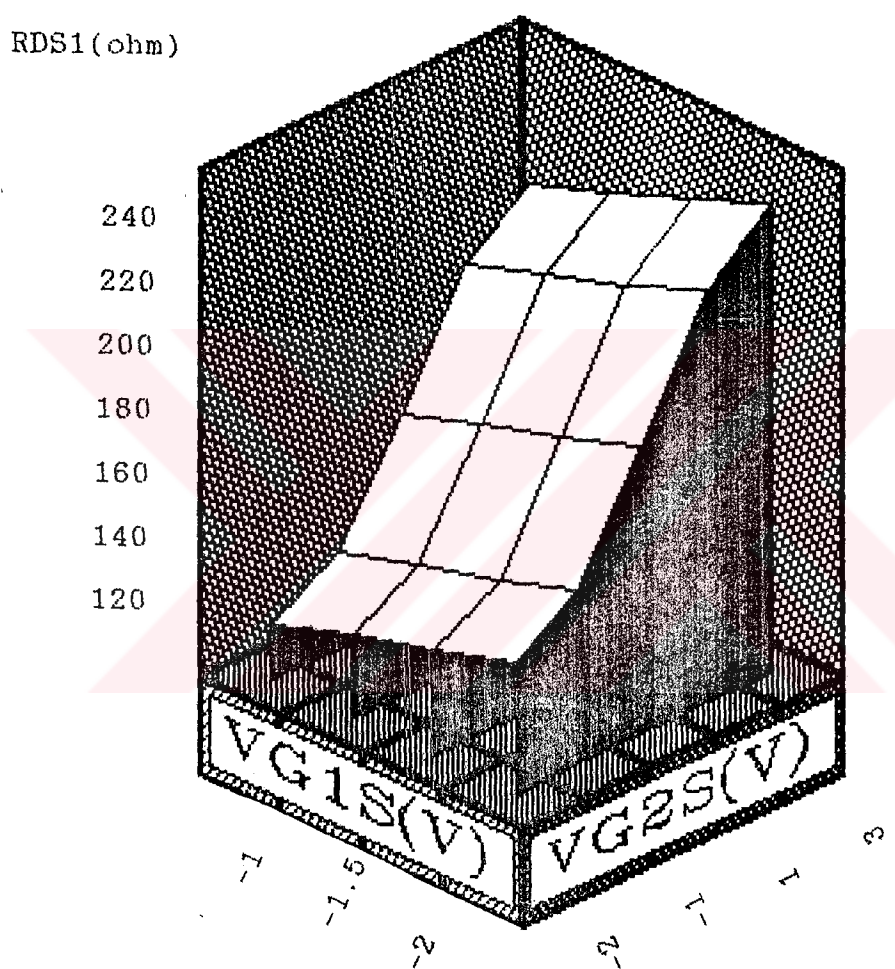


Fig. 4.5
 $R_{DS1} = F(V_{G1S}, V_{G2S})$

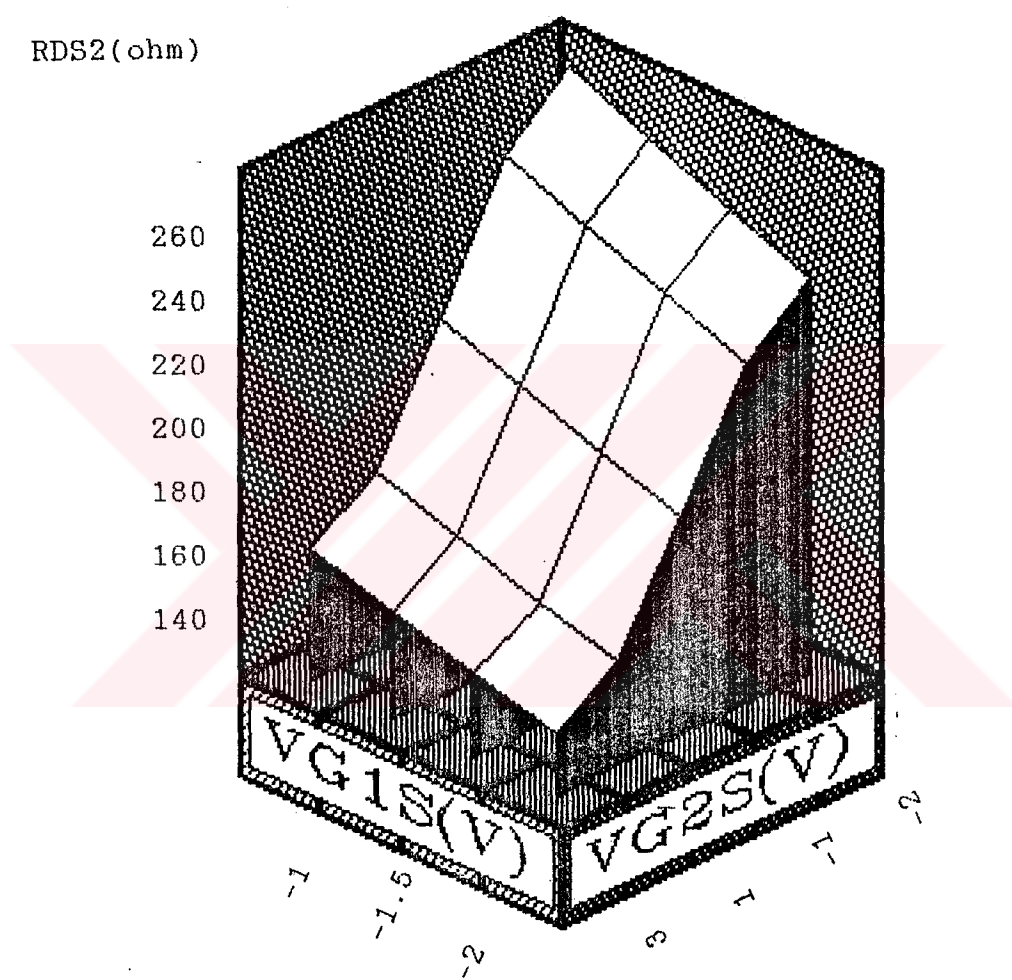


Fig. 4.6
 $R_{DS2} = F(V_{G1S}, V_{G2S})$

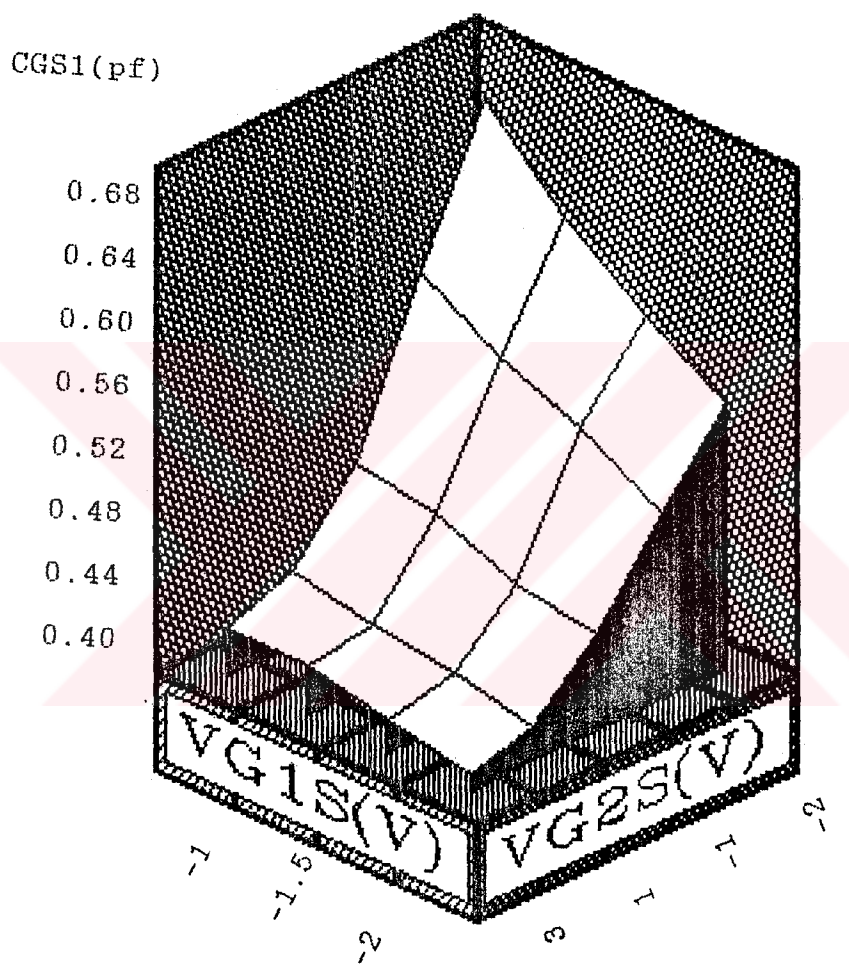


Fig. 4.7
 $c_{GS1} = F(V_{G1S}, V_{G2S})$

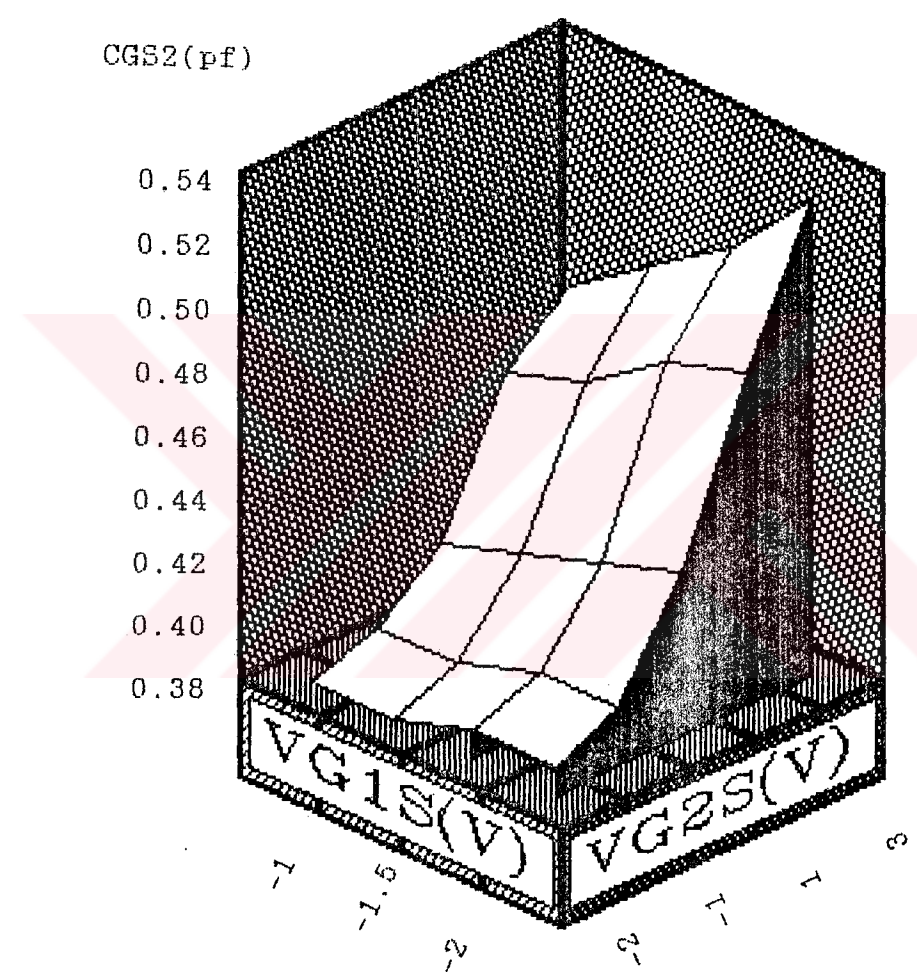


Fig. 4.8
 $C_{GS2} = F(V_{G1S}, V_{G2S})$

4.3. Numerical Analysis Of Nonlinear Model Of The Dual-Gate MESFET Mixer

The optimum design of microwave circuits containing nonlinear solid-state devices requires an accurate technique for predicting their nonlinear performance. The most common techniques are based on the analysis of a circuit-type model which simulates the nonlinear behavior of the device. Much work has been done on microwave solid-state device modeling and it is possible to find appropriate models for practically any device. However the high computational cost of the numerical methods used to analyze the interaction with the external circuit is the major drawback of these techniques.

Nonlinear microwave circuit have two important features:

- 1) The device-external circuit model usually includes many linear elements,
- 2) In most cases the excitation is periodic and only the steady-state response is required.

In order to reduce the number of unknown variables, separating the nonlinear network into linear and nonlinear subnetworks has been proposed. However, no general rules for optimum circuit partitioning have sofar been given.

After partitioning the frequency-domain and time-domain equations are written for the nonlinear and linear subnetworks, respectively. The response of the network is then described by a set of nonlinear equations whose unknowns are the harmonic components of the current and voltage magnitudes at the terminals.

Several numerical techniques like Newton-Raphson method have been employed to solve this nonlinear network in this work an analysis method is described which avoids the partitioning problem by introducing a criterion for

selecting the variables to be considered as unknowns and solving the resulting nonlinear system by a new and efficient algorithm. This method reduces time-domain analysis to the computation of currents and voltages at the nonlinear elements from the variable they depend on, and consequently takes full advantage of the linearities of the network.

4.3.1. Describing The Method:

Consider the situation represented in Fig. 4.9, where M-port is an arbitrary network, which contains both linear and nonlinear elements, is excited by M periodic sources (P-Voltage generators and Q-current generators, hence $M=P+Q$) all with the same period. It is assumed that a steady-state solution exists and the objective is to find it.

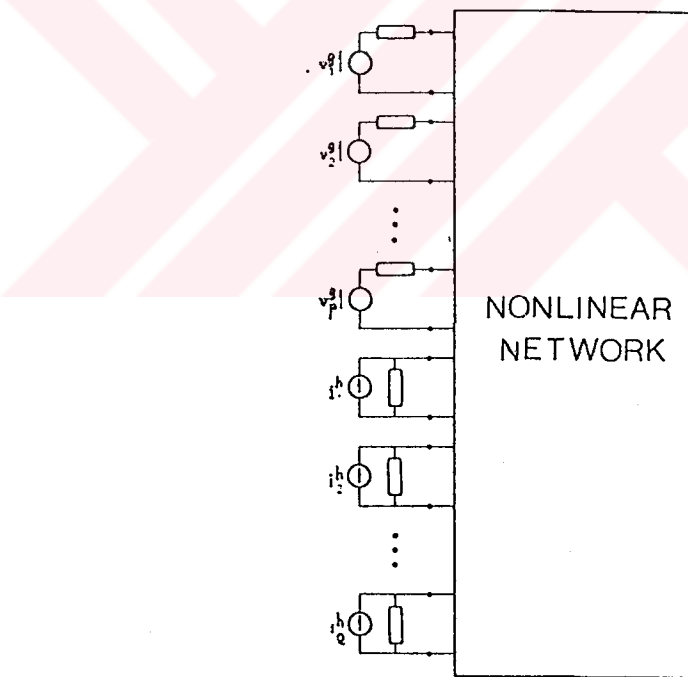


Fig. 4.9 The general nonlinear problem.

Every nonlinear element of the network can be considered either as a voltage generator or as a current generator controlled by other voltages and/or currents of the circuit.

Let $T+U$ be the number of nonlinear elements (T -voltage generator-type element and U -current generator-type elements) and let $v_1^x(t), v_2^x(t), \dots, v_R^x(t), i_1^y(t), i_2^y(t), \dots, i_s^y(t)$ be the voltages and currents controlling all the nonlinear elements. The aim of the method is to consider these voltages and currents as the unknown variables. Then, by this way, time domain analysis is reduced to the computation of the response (voltage or current) of every nonlinear element from the magnitudes it depends on and that the nonlinear problem is solved if these magnitudes are determined.

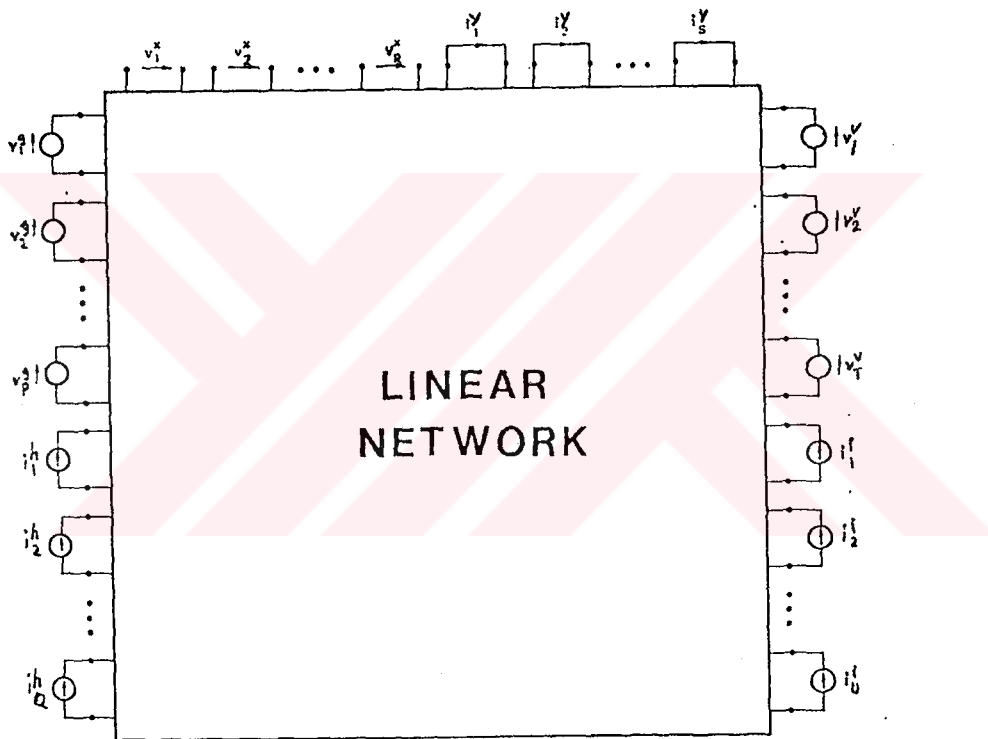


Fig. 4.10 The general nonlinear problem (rearranged).

The circuit in Fig. 4.9 can be rearranged in the way indicated in Fig. 4.10 where a $(M+R+S+T+U)$ port linear network, which includes all the linear elements of the primitive circuit, has M ports excited by independent sources, R ports open-circuited, S ports short-circuited, and each of the other $T+U$ ports loaded by one nonlinear element. The voltages and currents at the open circuited and short-circuited ports, respectively, are the variables controlling all the nonlinear elements. If these

magnitudes are known, voltages and currents at the non-linear elements can be calculated and, after that any electrical magnitude of the circuit can be obtained by linear transformations.

If the network is in the steady-state with periodic response of period T_0 , there will only be nf_0 (n -integer) frequency components in the circuit and every magnitude can be expressed by Fourier series

$$x(t) = \sum_{n=-\infty}^{\infty} X_n \exp(jn\omega_0 t) \quad (4.19)$$

with $\omega_0 = 2\pi/T_0 = 2\omega f_0$.

According to Fig. 4.10 it is possible to write for every frequency of interest:

$$\begin{bmatrix} V_{1,n}^x \\ V_{2,n}^x \\ \vdots \\ V_{R,n}^x \\ I_{1,n}^y \\ \vdots \\ I_{S,n}^y \end{bmatrix} = [A_n] \begin{bmatrix} V_{1,n}^v \\ \vdots \\ V_{T,n}^v \\ I_{1,n}^i \\ \vdots \\ I_{U,n}^i \\ v_{1,n}^g \\ \vdots \\ v_{p,n}^g \\ I_{1,n}^h \\ \vdots \\ I_{Q,n}^h \end{bmatrix} \quad (4.20)$$

where $V_{j,n}^x$, $I_{j,n}^y$, $V_{j,n}^v$, $I_{j,n}^i$, $v_{j,n}^g$ and $I_{j,n}^h$ are the Fourier

coefficients of the functions $v_j^x(t)$, $i_j^y(t)$, ... and $i_j^h(t)$ respectively, and $[A_n]$ is a matrix of $(R+S) \cdot (T+U+M)$ elements obtained by linear analysis of the network at the frequency nf_0 .

Since $v_{1,n}^v$, $v_{2,n}^v$, ..., $v_{T,n}^v$, $I_{1,n}^i$, $I_{2,n}^i$, ..., $I_{U,n}^i$ are nonlinear functions of $v_1^x(t)$, $v_2^x(t)$, ..., $v_R^x(t)$, $i_1^y(t)$, $i_2^y(t)$, ..., $i_s^y(t)$, the relation (4.20) is equivalent to an infinite system of nonlinear equations of the form

$$X_{i,n} = F_{i,n}(\bar{X}_1, \bar{X}_2, \dots, \bar{X}_{R+S}) \quad (4.21)$$

where

$$i = 1, 2, \dots, R+S$$

$$n = 0, 1, 2, \dots$$

$$\bar{X}_i (X_{i,1}, X_{i,2})$$

If only N harmonics are considered the problem is reduced to solving a system of $(N+1)(R+S)$ nonlinear equations. Its solution can be numerically found using the iteration technique defined by the expression

$$(X_{i,n})_{k+1} = (F_{i,n})_k + \frac{[(F_{i,n})_k - (F_{i,n})_{k-1}] \cdot [(X_{i,n})_k - (F_{i,n})_k]}{[(F_{i,n})_k - (X_{i,n})_k] - [(F_{i,n})_{k-1} - (X_{i,n})_{k-1}]} \quad (4.22)$$

Note that the proposed iteration technique is a direct iteration "corrected" to take into account the behaviour of the functions in the last two iterations and that it is only necessary compute the values of the functions $F_{i,n}$ at each step.

The iteration formula (4.22) fails if the denominator of the "correction factor" is equal to zero. In this case a direct iteration is used, i.e.

$$(X_{i,n})_{k+1} = (F_{i,n})_k \quad (4.23)$$

For the two first iterations the formula (4.22) is not defined and, consequently, it is necessary to assign appropriate initial values. A choice which has given excellent results is the following.

- 1) First Iteration: Assign to $x_{i,n}$ the values obtained when all voltage-generator type elements are short-circuited and all the current-generator type elements are open circuited, i.e setting

$$v_1^V(t) = v_2^V(t) = \dots = v_T^V(t) = i_1^I(t) = i_2^I(t) = \dots i_u^I(t) = 0$$

- 2) Second Iteration: Use a direct iteration i.e $(x_{i,n})_2 = (F_{i,n})_1$ [13].

4.3.2. Nonlinear Analysis Of Dual-Gate MESFET Mixer

Under Large Signal Excitation:

For dual-gate FET there is an equivalent circuit as shown as below Fig. 4.11. In mixer application the output is short circuited for the whole harmonic currents except the one at IF.

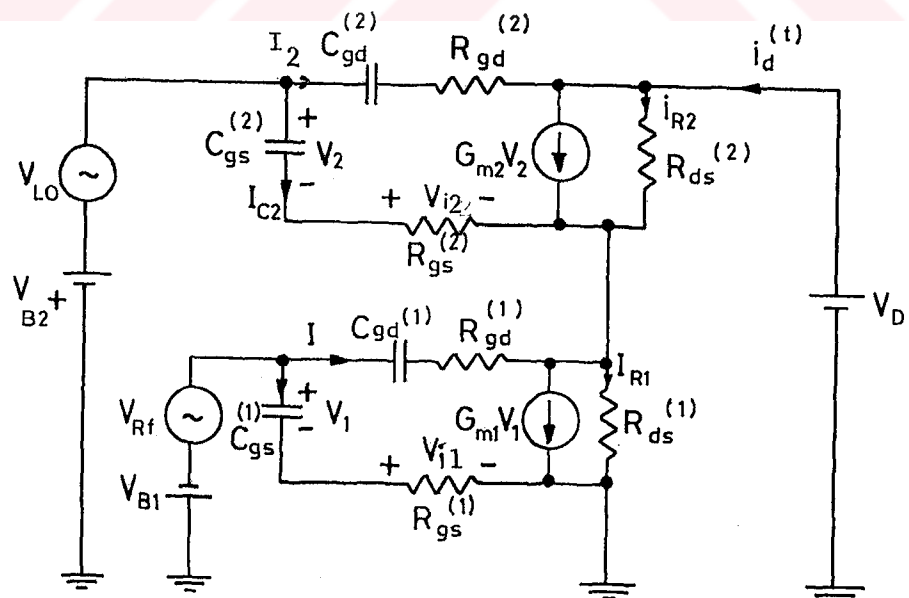


Fig. 4.11 Dual-gate FET.
(high frequency model)

It has been found in equivalent circuit that some of the elements in this circuit are so small that they can be ignored, for the sake of simplicity of nonlinear analysis, the equivalent circuit can be considered as in Fig. 4.12. (NOTE: In this Figure V_1, V_i, I_1, V_2 are not the same current or voltages as shown in Fig. 4.12).

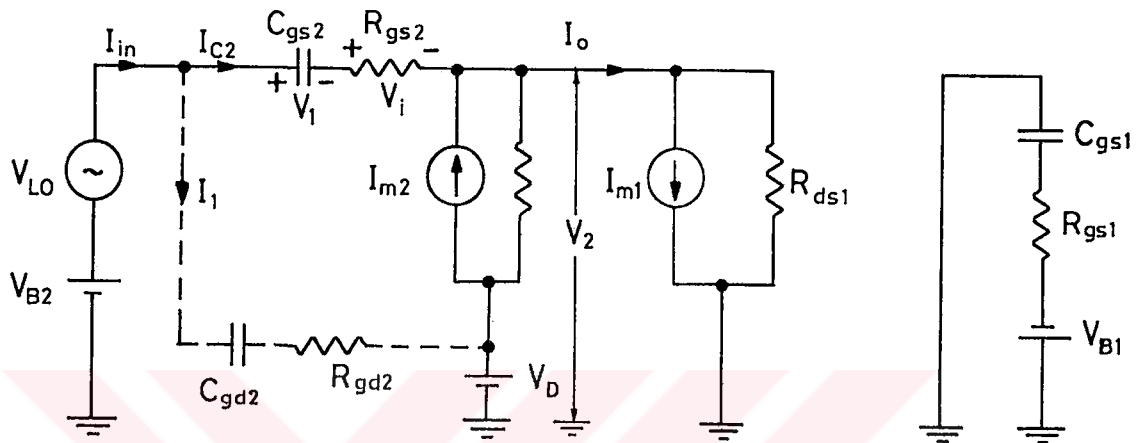


Fig. 4.12 Dual-gate FET (rearranged) model.

Since under large signal excitation $\bar{V}_{RF} \ll \bar{V}_{L0}$, V_{RF} can be neglected and also we assume that the effect of the branch $C_{gd1}-R_{gd1}$ is so small.

From the loop equation we have

$$V_{L0} = V_1 + V_i + V_2 \quad (4.24)$$

Since I_{m2} , R_{ds2} , R_{Gs2} and C_{gs2} are nonlinear and all of them dependent on the voltage across $C_{gs2}(V_1)$ then we have

$$\dot{v}_1(t) = \dot{v}_{L0}(t) - \dot{v}_i(t) - \dot{v}_2(t) \quad (4.25)$$

Because the nonlinear elements are periodic functions with period $T=2\pi/\omega_{L0}$, by harmonic analysis we have

$$V_{1n} = V_{L0n} - V_{in} - V_{2n} \quad (4.26)$$

where n is the n ,th harmonic. Since I_{m1} and R_{ds1} are dependent on the voltage across C_{gsl} and this voltage is equal to V_{B1} then I_{m1} and R_{ds1} can be assumed as linear elements.

By using kVL and kCL, For $v_2(t)$ we have

$$v_2(t) = \frac{R_{ds2}(t)[I_{m1} - i_{c2}(t) - i_{m2}(t)]R_{ds1} - R_{ds1}V_D}{-R_{ds2}(t) - R_{ds1}} \quad (4.27)$$

where

$$i_{c2}(t) = C_2(t) \frac{dv_1(t)}{dt} \quad (4.28)$$

and

$$v_1(t) = \sum_{\ell=-\infty}^{\infty} V_{1,\ell} e^{j\omega_0 \ell t} \quad (4.29)$$

$$C_2 = C_{20} \sqrt{1 - \frac{v_1(t)}{\phi}} \quad (4.30)$$

where ϕ is a constant, then we have

$$i_{c2}(t) = C_{20} \sqrt{1 - \frac{\sum_{\ell=-\infty}^{\infty} V_{1,\ell} e^{j\omega_0 \ell t}}{\phi}} \cdot \sum_{r=-\infty}^{\infty} V_{1,r} (j\omega_0 r) e^{j\omega_0 rt} \quad (4.31)$$

and Fourier coefficient of $i_{c2}(t)$ at any harmonic can be found by using DFT (Discrete Fourier Transform) techniques.

$$I_{c2,k} = \frac{1}{N} \sum_{n=0}^{N-1} i_{c2}(n\Delta t) e^{-j\omega_0 knT/N} \quad (4.32)$$

$$= \frac{1}{N} \sum_{n=0}^{N-1} \left[\frac{G_0}{\sqrt{1 - \frac{\sum_{r=-\infty}^{\infty} V_{1,r} e^{j2\pi rn/N}}{\phi}}} \sum_{\ell=-\infty}^{\infty} V_{1,\ell} e^{j2\pi n\ell/N} \cdot (j\omega_0 \ell) \right] e^{-j2\pi kn/N}$$

$$\begin{aligned}
 &= \frac{1}{N} \sum_{n=0}^{N-1} \sum_{\ell=-\infty}^{\infty} V_1 \ell(j\omega_o \ell) \frac{C_0}{\sqrt{1 - \frac{\sum_r V_{1,r} e^{j2\pi rn/N}}{r}}} e^{j2\pi n/N(\ell-k)} \\
 &= \sum_{\ell=-\infty}^{\infty} V_1 \ell(j\omega_o \ell) \cdot \frac{1}{N} \sum_{n=0}^{N-1} \frac{C_0}{\sqrt{1 - \frac{\sum_r V_{1,r} e^{j2\pi rn/N}}{r}}} e^{j2\pi n/N(\ell-k)} \\
 &= \sum_{\ell=-\infty}^{\infty} V_1 \ell(j\omega_o \ell) C_{\ell-k}
 \end{aligned} \tag{4.33}$$

For $i_{m2}(t)$ we can write

$$i_{m2}(t) = g_{m2} \cdot v_1(t) \tag{4.34}$$

$$= g_0 \left(1 - \frac{v_1(t)}{V_p} \text{constant}\right) v_1(t) \tag{4.35}$$

and

$$I_{m,k} = \frac{g_0}{N} \sum_{n=0}^{N-1} \left\{ \left[\left(1 - \frac{\sum_{r=-\infty}^{\infty} V_{1,r} e^{j2\pi rn/N}}{V_p} \right) \right] \sum_{\ell=-\infty}^{\infty} V_1 \ell e^{j2\pi \ell n/N} \right\} e^{-j2\pi kn/N} \tag{4.36}$$

For $R_{ds2}(t)$ we have

$$R_{ds2}(t) = \frac{R_0}{\left(1 - \frac{v_1(t)}{V_p}\right)^2} \tag{4.37}$$

Then the Fourier coefficients of this resistance can be written as:

$$R_{ds2,k} = \frac{1}{N} \sum_{n=0}^{N-1} \left[\frac{R_0}{\left(1 - \frac{\sum_m V_{1,m} e^{j2\pi mn/N}}{V_p}\right)^2} \right] e^{j2\pi nk/N} \tag{4.38}$$

For $v_i(t)$ we have,

$$v_i(t) = I_{c2}(t)R_{ds2}(t) = C_2(t) \frac{dv_1(t)}{dt} \cdot R_{ds2}(t) = C_2(t)R_{ds2}(t) \frac{dv_1(t)}{dt}$$

$$= \tau_i \frac{dv_1(t)}{dt} \quad (4.39)$$

Therefore

$$v_i(t) = \sum_{k=-\infty}^{\infty} v_{i,k} e^{j\omega_0 kt} = \tau_i \sum_{r=-\infty}^{\infty} (j\omega_0 r) e^{j\omega_0 rt} \quad (4.40)$$

Then $v_{i,r} = \tau_i (j\omega_0 r) = j(\omega_0 r \tau_i)$ where $r = -N, \dots, N$. For N harmonic, we also have,

$$v_{2,k} = \frac{1}{N} \sum_{n=0}^{N-1} v_2(n\Delta t) e^{-jkn2\pi/N} \quad (4.41)$$

Since all these equations are dependent on $v_1(t)$,

they can be written as $X=F(X)$ and the solution of this equation is $\hat{X}=F(\hat{X})$ where \hat{X} is found by using a computer program (DC. for program). \hat{X} is found after 8 iteration until,

$$|\hat{X} - F(\hat{X})| < 0.04 \quad (4.42)$$

is satisfied.

In Fig. 4.11 if we assume, the branches between (G_1, D_1) and (G_2, D_2) can not be neglected and also the impedance matching network from small signal analysis in Chapter 3 added between G_1 and source (source is grounded) from loop equation we have:

$$[V_n] = [A_n] [X_n] \quad (4.43)$$

where $[V_n] = (v_{1,n}, v_{2,n})^T$

and $[A_n] = (A_{n,1}, A_{n,2})$

where $A_{n,1} = \left[\begin{array}{c} \frac{Z^2(R_1+R_2)}{D} - Z, \frac{ZR_1R_2}{D}, \frac{-ZR_1R_2}{D}, \frac{ZR_1R_2}{D}, \\ -1, 0, 1 - \frac{Z(R_1+R_2)}{D}, \frac{ZR_1}{D}, 0 \end{array} \right]$ (4.44)

and $A_{n,2} = \left[\begin{array}{c} \frac{(Z+Z_{g1})(R_1+R_2)}{D} + Z, \frac{(Z_1+Z_{g1})(-R_1R_2)}{D}, \\ \frac{(Z+Z_{g1})(R_1R_2)}{D}, \frac{(Z+Z_{g1})(-R_1R_2)}{D}, 0, -1, \frac{(R_1+R_2)(Z+Z_{g1})}{D}, \\ \frac{(-R_1)(Z+Z_{g1})}{D}, 1 \end{array} \right]$ (4.45)

and

$$X_n = (I_{c1,n}, I_{c2,n}, I_{m1,n}, I_{m2,n}, V_{i1,n}, V_{i2,n}, V_{B1}, V_{B2}, V_{L0,n})^T$$
 (4.46)

where Z can be calculated from Fig. 4.13.

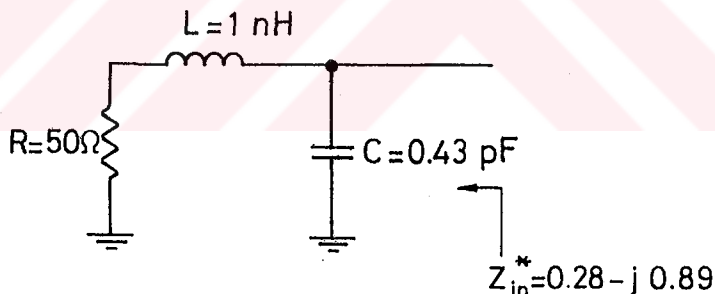


Fig. 4.13 Impedance matching network.

and R_1, R_2 refer to R_{ds1}, R_{ds2}

$$I_{m1} = G_{M1}V_1$$
 (4.47)

$$I_{m2} = G_{M2}V_2$$
 (4.48)

$$Z_g = (R_{gd} - \frac{j}{C_{gd} \cdot 2\pi n f_0})$$
 (4.49)

$$D = R_2 R_1 + (R_2 + R_1)(Z + Z_{g1})$$
 (4.50)

In DC case for determining V_1 Fig. 4.14 can be used.

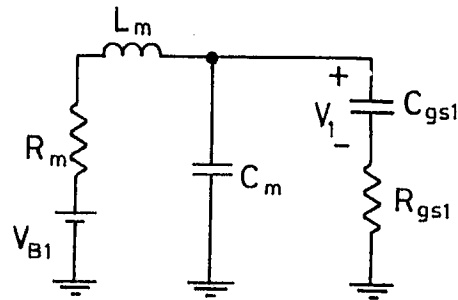


Fig. 4.14 Determining of V_1 (DC case)

From Fig. 4.14 we can write,

$$V_1 = V_{B1} \quad (\text{for steady state case}) \quad (4.51)$$

and for V_2 from loop equation we have:

$$V_2 = \frac{R_1 R_2}{R_1 + R_2} \cdot I_{m1} - \frac{R_1 R_2}{R_1 + R_2} I_{im2} - \frac{R_1}{R_1 + R_2} V_D + V_{B2} \quad (4.52)$$

From the method as described in section (4.3.1) and using another computer program (NL. for) V_1 and V_2 obtained after 11 iteration.

4.4. Small Signal Analysis Of The Mixer

Under RF small signal conditions, the frequencies being present in the mixer are given by

$$f_{k,s} = kf_0 + sf_s \quad (4.53)$$

with $-\infty \leq k \leq +\infty$ and $s=0$ and ± 1 , f_0 and f_s are the L_0 and RF frequency respectively.

According to this, all the magnitudes in the circuit have the form

$$\begin{aligned} x(t) &= \sum_{k=-\infty}^{\infty} \sum_{s=0, \pm 1} X_{k,s} \exp[j(k\omega_0 + s\omega_s)t] \\ &= x_{L0}(t) + x_{MX}(t) \end{aligned} \quad (4.54)$$

where

$$x_{L0}(t) = \sum_{k=-\infty}^{\infty} x_{k,0} \exp(jk\omega_0 t) \quad (4.55)$$

$$x_{MX}(t) = \sum_{k=-\infty}^{\infty} \sum_{s=\pm 1}^{\infty} x_{k,s} \exp[j(k\omega_0 + s\omega_s)t] \quad (4.56)$$

Obviously $x_{L0}(t)$ is the local oscillator component of $x(t)$, while $x_{MX}(t)$ denotes the small-signal mixing products. Since all the magnitudes involved are real, then

$$x_{k,s} = (x_{-k,-s})^* \quad (4.57)$$

It is only necessary to take into consideration one of the two values for s ($s=1$, for instance).

These coefficients are more conveniently represented in matrix form as follows:

$$X = (X_{-N}, X_{-N+1}, \dots, X_0, \dots, X_{N-1}, X_N)^T \quad (4.58)$$

where the second subscript has been omitted for the sake of simplicity, and it has been assumed that a finite number of components are considered.

It can be shown that the relationship between the mixing products of the voltage and the current across C_{gs} can be expressed by

$$I_C = j\Omega CV \quad (4.59)$$

with

$$I_C = (I_{C,-N}, I_{C,-N+1}, \dots, I_{C,0}, \dots, I_{C,N-1}, I_{C,N})^T \quad (4.60)$$

$$V = (V_{-N}, V_{-N+1}, \dots, V_0, \dots, V_{N-1}, V_{1N})^T \quad (4.61)$$

$$\Omega = \begin{bmatrix} \omega_s - N\omega_o & 0 & 0 \\ 0 & \omega_s - \omega_o & 0 \\ 0 & 0 & \omega_s + N\omega_o \end{bmatrix} \quad (4.62)$$

$$C = \begin{bmatrix} c_0 & \cdot & \cdot & \cdot & \cdot \\ \cdot & c_0 & c_1^* & c_2^* & \cdot \\ \cdot & c_1 & c_0 & c_1^* & \cdot \\ \cdot & c_2 & c_1 & c_0 & \cdot \\ \cdot & \cdot & \cdot & \cdot & c_0 \end{bmatrix} \quad (4.63)$$

For the resistance $R_{GS}(V)$, the relation ship is given by

$$V_{ik} = j\tau_i \Omega V_k \quad \text{for } k=1, 2 \quad (4.64)$$

with

$$V_i = (V_{i,-N}, V_{i,-N+1}, \dots, V_{i,0}, \dots, V_{i,N-1}, V_{i,N})^T \quad (4.65)$$

while that for the current generator $i_m(v)$ has the following form

$$I_{mj} = G_{mj} V_j \quad j=1, 2 \quad (4.66)$$

$$I_m = (I_{m,-N}, I_{m,-N+1}, \dots, I_{m,0}, \dots, I_{m,N-1}, I_{m,N})^T \quad [14]$$

$$G_m = \begin{bmatrix} G_{m0} & & & & \\ & G_{m0} & G_{m1}^* & G_{m2}^* & \\ & G_{m1} & G_{m0} & G_{m1}^* & \\ & G_{m2} & G_{m1} & G_{m0} & \\ & & & & G_{m0} \end{bmatrix} \quad (4.67)$$

once vector V_1 and V_2 are determined, terminal current (Fig. 4.10) I_d can be easily computed by the formula

$$I_d = G_{M2} V_2 + I_{R2} - I_2 \quad (4.68)$$

where I_{R2} and I_2 are the current, that flow in R_{ds2} and the branch between G_2 and D respectively.

By using "H" character for showing the elements in $A_{n,1}$, $A_{n,2}$ vectors in (4.44) and (4.45) section 4.2 we have

$$A_{n,1} = (H_1, H_2, -H_2, H_2, -1, 0, H_3, H_4, 0) \quad (4.69.a)$$

$$A_{n,2} = (H_5, H_6, -H_6, H_6, 0, -1, H_7, H_8, 1) \quad (4.69.b)$$

Then for V_1 and V_2 the voltages across the C_{gs1} , C_{gs2} we have

$$V_1 = H_1 I_{c1} + H_2 I_{c2} - H_2 I_{m1} + H_2 I_{m2} - V_{in} + H_3 V'_{g1} + H_4 V_{LO} \quad (4.70.a)$$

$$V_2 = H_5 I_{c1} + H_6 I_{c2} - H_6 I_{m1} + H_6 I_{m2} - V_{in} + H_7 V'_{g1} + H_8 V_D + V_{LO} \quad (4.70.b)$$

where I_{cn} , I_{mn} V_{in} (for $n=1, 2$) can be obtained from (4.59), (4.60) and (4.61). Then we have

$$V_1 = H_1 (j\Omega C_1 V_1) + H_2 (j\Omega C_2 V_2) - H_2 (G_{m1} V_1) + H_2 (G_{m2} V_2) - j\tau_i \Omega V_1 + H_3 V'_{g1} + H_4 V_{LO} \quad (4.71.a)$$

$$V_2 = H_5 (j\Omega C_1 V_1) + H_6 (j\Omega C_2 V_2) - H_6 G_{m1} V_1 + H_6 G_{m2} V_2 - j\tau_i \Omega V_2 + H_7 V'_{g1} + H_8 V_D + V_{LO} \quad (4.71.b)$$

or

$$A_{11} V_1 + A_{12} V_2 = E'_1 \quad (4.72.a)$$

$$A_{21} V_1 + A_{22} V_2 = E'_2 \quad (4.72.b)$$

where

$$A_{11} = I - jH_1 \Omega C_1 + H_2 G_{m1} + j\tau_i \Omega \quad (4.73.a)$$

$$A_{12} = -(jH_2 \Omega C_2 + H_2 G_{m2}) \quad (4.73.b)$$

$$A_{21} = -jH_5 \Omega C_1 + H_6 G_{m1} \quad (4.73.c)$$

$$A_{22} = I - jH_6 \Omega C_2 - H_6 G_{m2} + j\tau_i \Omega \quad (4.73.d)$$

where I is a unit matrix and $\tau=2,5$ PS and

$$E'_1 = -H_3 V'_{g1} - H_4 V_{L0} \quad (4.74.a)$$

$$E'_2 = -H_7 V'_{g1} - H_8 V_D - V_{L0} \quad (4.74.b)$$

where

$$V'_{g1} = V_{g1} (-j/C_m \omega) / \left[R + j(\omega L_m - \frac{1}{\omega L_m}) \right] \quad (4.75.a)$$

where

$$V_{g1} = V_{B1} + \bar{V}_{Rf} \cos \omega_{Rf} t \quad (4.75.b)$$

$$V_{L0} = V_{B2} + \bar{V}_{L0} \cos \omega_{L0} t \quad (4.75.c)$$

and

$$H_j = \begin{bmatrix} H_j(\omega_s - \omega_o) & 0 \\ 0 & H_j(\omega_s) \\ 0 & H_j(\omega_s + \omega_o) \end{bmatrix} \text{ for } j=1,2,\dots,8 \text{ and } s=1 \quad (4.76)$$

with

$$E'_m = [E'_m(\omega_s - \omega_o), E'_m(\omega_s), E'_m(\omega_s + \omega_o)]^T \text{ for } m=1,2$$

and $\omega_{Rf} \triangleq \omega_s, \omega_{L0} \triangleq \omega_o$

By using SMS-FOR computer program H_j and then whole the elements in A_{ij} ($i,j=1,2$) matrices are found, so we have

$$\begin{bmatrix} V_1 \\ V_2 \end{bmatrix} = \begin{bmatrix} A_{11} & A_{12} \\ A_{21} & A_{22} \end{bmatrix}^{-1} \begin{bmatrix} E'_1 \\ E'_2 \end{bmatrix} \quad (4.77)$$

where $A_{11}, A_{12}, A_{21}, A_{22}$ are 3×3 matrices in this work.

By using another computer program (Root. for) V_1 and V_2 for four different values of V_{g1}, V_{g2}, V_{L0} are found.

Now we can determine the output current $i_d(t)$ for the large signal case ($s=0$) and small signal case ($s=1$) that is

$$i_d(t) = I_{d(-1)} e^{-j\omega_{L0}t} + I_{d(0)} + I_{d(+1)} e^{j\omega_{L0}t} + I_{d(1,-1)} e^{j(\omega_s - \omega_{L0})t} + \\ I_{d(1,0)} e^{j\omega_s t} + I_{d(1,1)} e^{j(\omega_s + \omega_{L0})t} \quad (4.78)$$

from loop equation for large signal case we have

$$I_{dn} = \frac{V_{2n} + V_{i2n} + V_{L0n}}{R_{d2}} + G_{m2n} V_{2n} - \frac{(V_{L0n} - V_D)}{Z_{g2n}} \quad (4.79)$$

where n refers to n'th harmonic, Z_{g2n} is equal to Z_{g1n} and must be calculated at any harmonic of frequency and $V_{i2n} = j\tau_n V_{2n}$. For small signal case we have

$$I_d = (y_2 + j\Omega\tau y_2 + G_{m2}) V_2 \quad (4.80)$$

or

$$\begin{bmatrix} I_{d(-)} \\ I_{d(0)} \\ I_{d(+)} \end{bmatrix} = \left(\begin{bmatrix} y_2 & 0 & 0 \\ 0 & y_2 & 0 \\ 0 & 0 & y_2 \end{bmatrix} + j\tau y_2 \begin{bmatrix} \omega_s - \omega_o & 0 \\ 0 & \omega_s \\ 0 & \omega_s + \omega_o \end{bmatrix} + \begin{bmatrix} G_{m20} & G_{m21}^* & 0 \\ G_{m21} & G_{m20} & G_{m21}^* \\ 0 & G_{m21} & G_{m20} \end{bmatrix} \right) \begin{bmatrix} V_{2(-)} \\ V_{2(0)} \\ V_{2(+)} \end{bmatrix}$$

where $y_2 = 1/R_{d2}$ and $I_{d(-)}$, $I_{d(0)}$, $I_{d(+)}$ are the Fourier coefficients of $(\omega_s - \omega_{L0})$, (ω_s) , $(\omega_s + \omega_o)$ respectively, and they are found by sms. for computer program.

CHAPTER 5

RESULTS AND CONCLUSION

Instead of using dual gate MESFET, two identical FETs, are used for describing self oscillating microwave mixer.

By using the small signal scattering parameters oscillation conditions are investigated. For this investigation three different computer programs (cascade. for, math. for, imp. for) are used. Using those programs, S-parameters for two port cascode configuration, input impedance, matching network are calculated.

In this work S-parameters of two types of FETs (AVANTEK 10650 and AVANTEK 11671) are considered, but only for the first one, as shown in Chapter 3 oscillation conditions are provided.

Since the amplitude of the voltage of local oscillator is much greater than the RF signal in mixer application, FETs has been modeled under large signal excitation. In this model, the magnitudes of the nonlinear elements are controlled by the voltages across C_{gs1} and C_{gs2} (As shown in Chapter 4). A new method for nonlinear analysis has been described. The reduction in time-domain calculations obtained by systematic selection of the unknown variables (The voltages across the capacitances), and the convergence characteristics shown by the proposed algorithm [13].

Using the NL-FOR program those voltages (V_1, V_2) and also Fourier coefficients of $G_{M1}, G_{M2}, C_{gs1}, C_{gs2}$ are obtained. For small signal analysis those Fourier coefficients are used as the input of SMS-FOR program for determining the output current.

Different values for bias conditions and amplitude of local oscillator with $V_{DS} = \text{const.}$ are choosen in these programs.

In the case of:

$V_m = +1$ V, $V_{G1S} = -2$ V and $V_{G2S} = -1$ V (V_m refers to the amplitude of V_{LO}), the term:

$$\left| \frac{I_d(\text{If})}{V_S(\text{Rf})} \right|$$

by comparing with the other cases has a maximum value. The Fourier coefficients of nonlinear elements and $i_d(t)$ under this condition are also shown in the attached figures.

Fourier coefficients for $i_d(t)$, C_{GS1} , C_{GS2} , G_{M2} and G_{M1} .

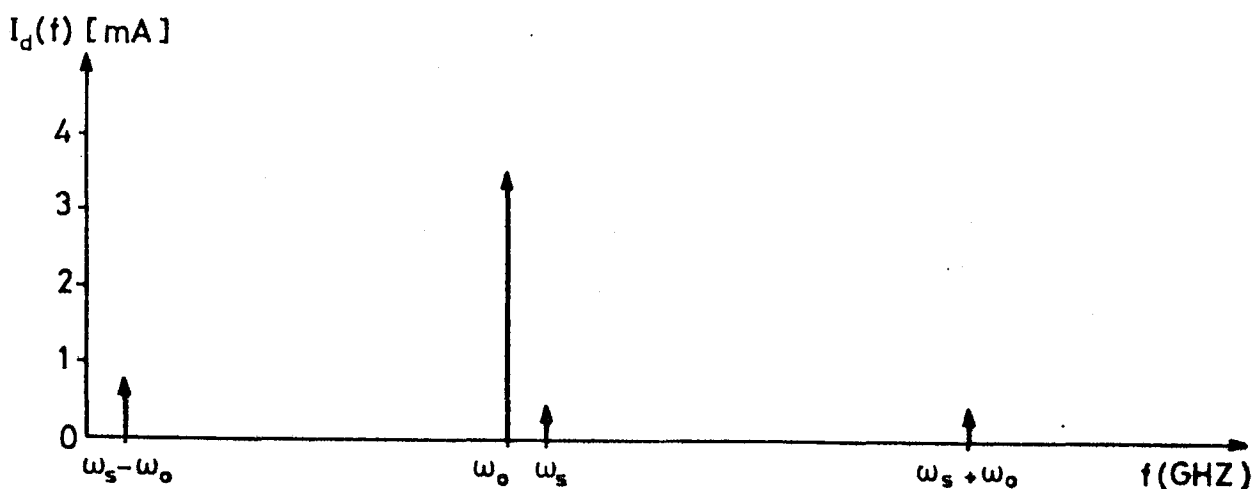


Fig. 5.1 $\bar{V}_{LO} = 0.8$, $V_{B1} = -3$, $V_{B2} = -1.5$

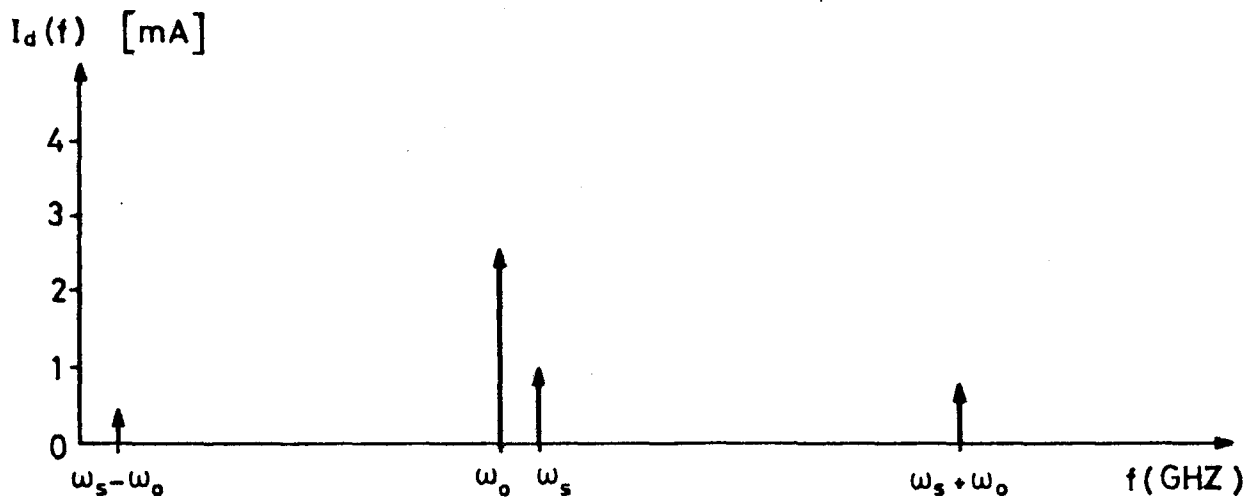


Fig. 5.2 $\bar{V}_{L0} = 1.2$ V, $V_{B1} = -4$ V, $V_{B2} = -2.5$ V

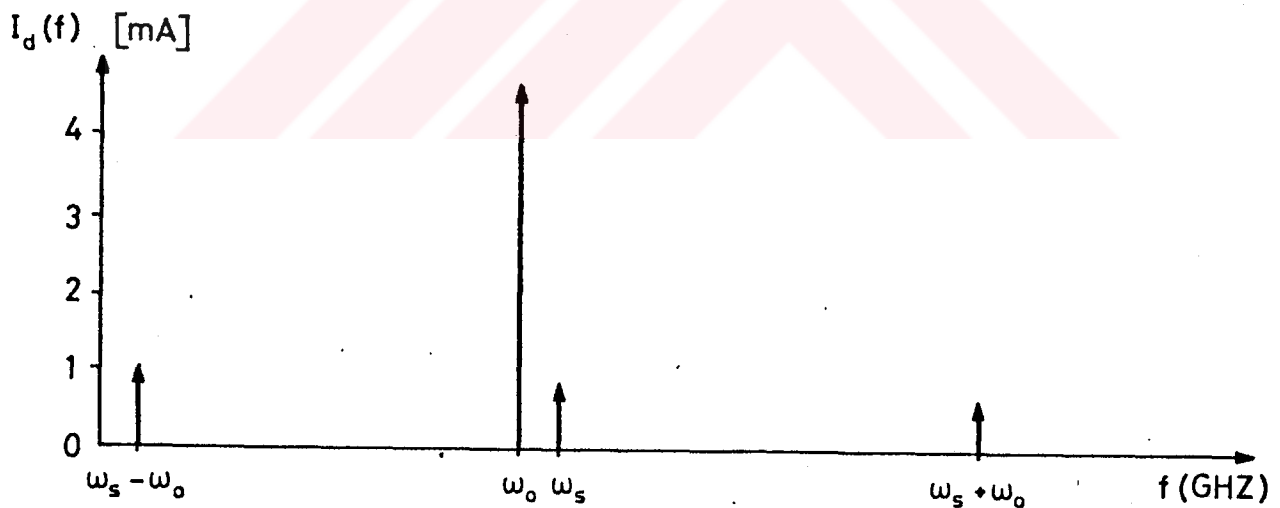


Fig. 5.3 $\bar{V}_{L0} = +1$, $V_{B1} = -2$ V, $V_{B2} = -1$ V

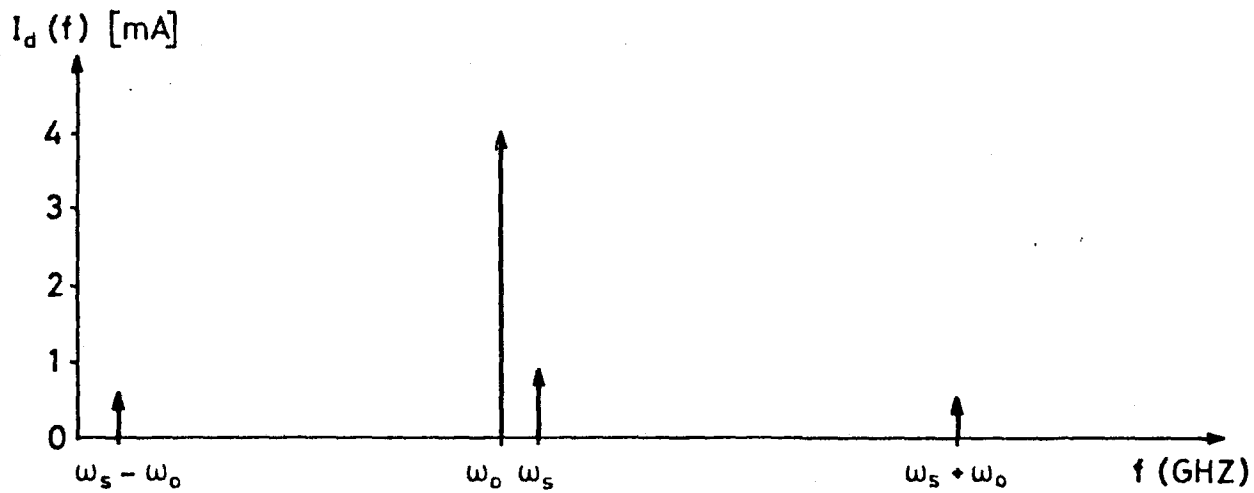


Fig. 5.4 $V_{B2} = -1$, $V_{B1} = -3$, $\bar{V}_{LO} = 0.6$

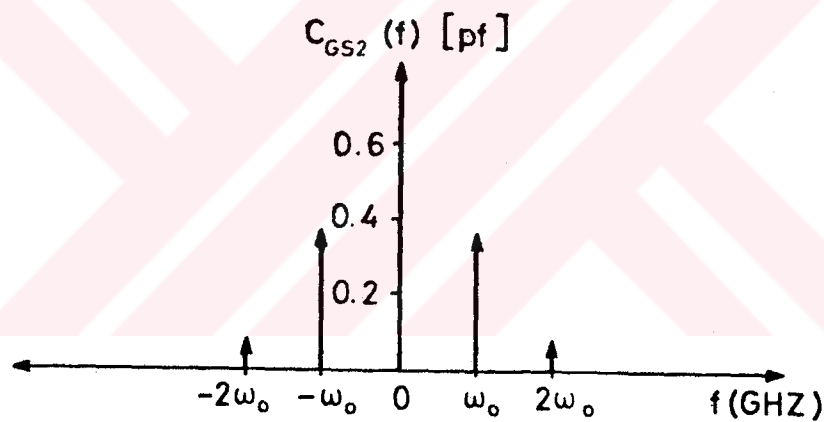


Fig. 5.5 Fourier coefficients of C_{gs2} .

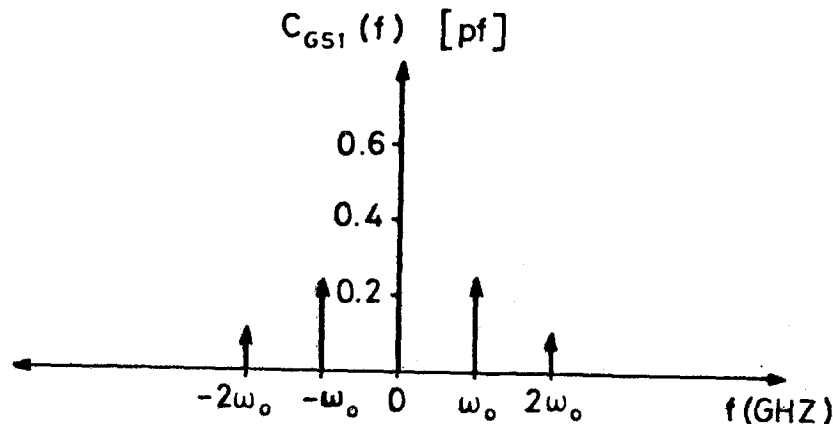


Fig. 5.6 Fourier coefficients of C_{gs1} .

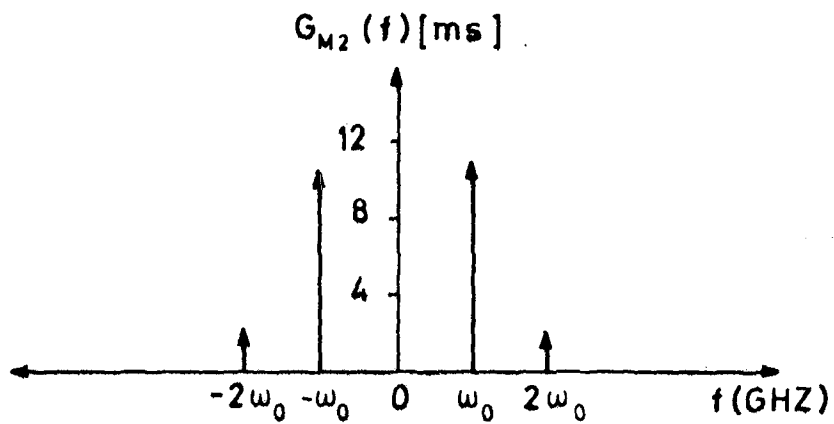


Fig. 5.7 Fourier coefficients of G_{M2} .

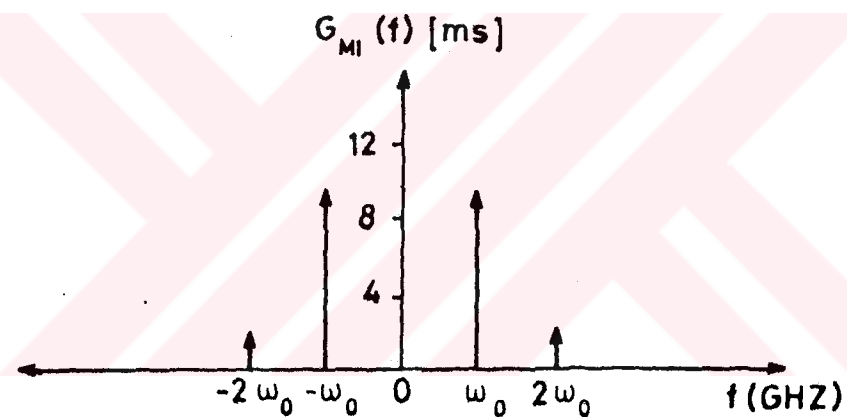


Fig. 5.8 Fourier coefficients of G_{M1} .

REFERENCES

- [1] ISHIHARA, O., MORTI, T., SAWANO, H., "A Highly Stabilized GaAs FET Oscillator Using a Dielectric Resonator Feedback Circuit in 9-14 GHz", IEEE Transactions on Microwave Theory and Tech., Vol.MTT-28, No.8, pp. 817-823, August 1980.
- [2] PURNELL, M., "The Dielectric Resonator Oscillator. A New Class of Microwave Signal Source", Microwave Journal, Vol.24, pp. 103-107, November 1981.
- [3] SOARES, R., GRAFFEUIL, J., OBREGON, J., "Application of GaAs MESFETs", Artech House Inc., pp. 243-284, 1983.
- [4] TRI T. HA, "Solid-State Microwave Amplifier Design", By John Wiley & Sons Inc., New York, pp. 63-70, 1981.
- [5] RAYMOND, S., PENGELLY, "Microwave Field-Effect Transistors Theory, Design and Applications", By John Wiley & Sons Ltd., London, pp. 44-48, 1982.
- [6] TSIRONIS, C., MEIERER, R., "Equivalent Circuit of GaAs Dual Gate MESFETs", Electronics Letters, Vol.17, No.13, pp. 477-478, June 1981.
- [7] MIZUMURA, M., WADA, K., HAGA, I., "Oscillators Stabilized With a Dielectric Resonator in Microwave Communication Systems", NEC Res., Develop., No.70, pp. 112-119, July 1983.
- [8] KHANNA, A., GARAUIT, Y., "Determination of Loaded, Unloaded, and External Quality Factors of a Dielectric Resonator Coupled to a Microstrip Line", IEEE Transactions on Microwave Theory and Tech., Vol.MTT-31, No.3, pp. 261-264, March 1983.
- [9] KAJFEZ, D., GUILLOU, P., "Dielectric Resonator", Artech House Inc., 1986.

- [10] TSIRONIS, C., "12 GHz Receiver With Self-Oscillating Dual-Gate MESFET Mixer", Electronics Letter, Vol.17, No.17, pp. 617-618, August 1981.
- [11] TSIRONIS, C., MEIERER, R., STAHLMANN, R., "Dual-Gate MESFET Mixers", IEEE Transactions on Microwave Theory and Tech., Vol.MTT-32, No.3, pp. 248-255, March 1984.
- [12] MILES, E.R., HOWES, J.M., "Large-Signal Equivalent Circuit Model of a GaAs Dual-Gate MESFET Mixer", IEEE Transactions on Microwave Theory and Tech., Vol.MTT-33, No.5, pp. 433-436, May 1985.
- [13] CAMACHO-PENALOSA, C., "Numerical Steady-State Analysis of Nonlinear Microwave Circuits With Periodic Excitation", IEEE Transactions on Microwave Theory and Tech., Vol.MTT-31, No.9, pp. 724-730, September 1983.
- [14] CAMACHO-PENALOSA, C., S. AITCHISON, C., "Analysis and Design of MESFET GATE Mixers", IEEE Transactions on Microwave Theory and Tech., Vol.MTT-35, No.7, pp. 643-652, July 1987.
- [15] LIECHTI, A.C., "Performance of Dual-Gate GaAs MESFET's as Gain Controlled Low-Noise Amplifiers and High-Speed Modulators", Reprinted From IEEE Trans. Microwave Theory and Tech., Vol.MTT-23, pp. 461-469, June 1975.
- [16] BOYLES, W.J., "The Oscillator as a Reflection Amplifier: An Intuitive Approach to Oscillator Design", Microwave Journal, pp. 82-94, June 1986.

APPENDIX-A: PROGRAMS

```
**** cascoda1.forg program *****
complex s(2,2),ts,tg,fi21,fi21p,fi21pp
complex cx,sum,gl,tf,fi22,fi22p,fi22pp
complex d(3,3),de,sg(2,2),sc(2,2)
complex fi11,fi12,fi12p,fi12pp,sc11p
complex delta,b,sf,cf1,sf2,sf3
dimension ph(2,2)
fm(cx)=cabs(cx)
fa(cx)=180./p*atan2(aimag(cx),real(cx))
p=3.1415926
read(6,*) s(1,1),s(1,2),s(2,1),s(2,2)
read(6,*) ph(1,1),ph(1,2),ph(2,1),ph(2,2)
do 10 i=1,2
do 10 j=1,2
10  write(7,*) s(i,j),ph(i,j)
do 15 i=1,2
do 15 j=1,2
ph(i,j)=ph(i,j)*p/180.
sr=real(s(i,j))*cos(ph(i,j))
si=real(s(i,j))*sin(ph(i,j))
s(i,j)=cmplx(sr,si)
15  write(7,*) s(i,j)
sum=cmplx(0.,0.)
do 20 i=1,2
do 20 j=1,2
20  sum=sum+s(i,j)
b=4.-sum
write(7,*) sum,b
d(3,3)=sum/b
d(3,2)=(1.+d(3,3))*(1.-s(1,2)-s(2,2))/2.
d(2,3)=(1.+d(3,3))*(1.-s(2,1)-s(2,2))/2.
d(2,2)=s(2,2)+d(2,3)*d(3,2)/(1.+d(3,3))
d(3,1)=1.-d(3,3)-d(3,2)
d(1,3)=1.-d(2,3)-d(3,3)
d(1,2)=1.-d(2,2)-d(3,3)
d(2,1)=1.-d(2,2)-d(2,3)
d(1,1)=1.-d(2,1)-d(3,1)
do 50 i=1,3
do 50 j=1,3
50  write(7,*) d(i,j)
f=126.
r=f*p/180.
gr=0.59*cos(r)
gi=0.59*sin(r)
gl=cmplx(gr,gi)
de=gl-d(1,1)
sg(1,1)=d(3,3)+d(3,1)*d(1,3)/de
sg(1,2)=d(3,2)+d(3,1)*d(1,2)/de
sg(2,1)=d(2,3)+d(2,1)*d(1,3)/de
sg(2,2)=d(2,2)+d(2,1)*d(1,2)/de
ts=1./s(2,1)
tg=1./sg(2,1)
fi11=ts*tg+sg(1,1)*tg*(-1.*ts*s(2,2))
tf=1./fi11
fi12p=-1.*ts*tg*sg(2,2)
sf=sg(1,1)*tg*sg(2,2)
fi12pp=-1.*ts*s(2,2)*(sg(1,2)-sf)
fi12=fi12p+fi12pp
fi21p=s(1,1)*ts*tg
sf1=ts*s(2,2)
fi21pp=sg(1,1)*tg*(s(1,2)-s(1,1)*sf1)
```

```
fi21=fi21p+fi21pp
fi22p=s(1,1)*tg*(-1.*tg*sg(2,2))
sf2=(s(1,2)-s(1,1)*te*s(2,2))
fi22pp=(sg(1,2)-sg(1,1)*tg*sg(2,2))*sf2
fi22=fi22p+fi22pp
sc(1,1)=fi21*tf
sc(1,2)=fi22-fi21*tf*fi12
sc(2,1)=tf
sc(2,2)=-1.*tf*fi12
sc11p=sc(1,1)-sc(1,2)*sc(2,1)/(1.+sc(2,2))
sim=fm(sc11p)
s1a=fa(sc11p)
ri=1./sim
delta=sc(1,1)*sc(2,2)-sc(1,2)*sc(2,1)
sf3=cabs(sc(2,2))
so=1.+cabs(delta)**2-cabs(sc(1,1))**2-sf3)**2
cm=2.*cabs(sc(1,2)*sc(2,1))
sk=so/cm
s2a=-1*s1a
write(7,8) f,sim,s1a
8 format(5x,'fi(dg)=',f6.2,3x,'|s`11|=',e12.6)
write(7,3) ri,s2a,sk
3 format(5x,'|1/s`11|=',e12.6,3x,'<1/s`11=',f8.2)
stop
end
```

```
c ****cascode2.for program****
complex s(2,2),d(3,3)
complex cx,sum,b,sd(2,2),sc(2,2)
complex de,fid(2,2),td,ts
complex fis(2,2),fic(2,2)
complex tf,delta,glp,sc11p
complex zc,zl,zrl,zgp,zgpn
dimension ph(2,2)
fm(cx)=cabs(cx)
fa(cx)=180./p*atan2(aimag(cx),real(cx))
p=3.1415926
f=9.
fz=9.*10**(+9.)
c=0.402*10**(-12.)
r=50.
rl=0.37*10**(-9.)
do 110 k=1,26
read(6,*) s(1,1),s(1,2),s(2,1),s(2,2)
read(6,*) ph(1,1),ph(1,2),ph(2,1),ph(2,2)
do 10 i=1,2
do 10 j=1,2
10 write(7,*) s(i,j),ph(i,j)
do 15 i=1,2
do 15 j=1,2
ph(i,j)=ph(i,j)*p/180.
sr=real(s(i,j))*cos(ph(i,j))
si=real(s(i,j))*sin(ph(i,j))
15 s(i,j)=cmplx(sr,si)
sum=cmplx(0.,0.)
do 20 i=1,2
do 20 j=1,2
20 sum=sum+s(i,j)
b=4.-sum
d(3,3)=sum/b
d(3,2)=(1.+d(3,3))*(1.-s(1,2)-s(2,2))/2.
d(2,3)=(1.+d(3,3))*(1.-s(2,1)-s(2,2))/2.
d(2,2)=s(2,2)+d(2,3)*d(3,2)/(1.+d(3,3))
d(3,1)=1.-d(3,3)-d(3,2)
d(1,3)=1.-d(2,3)-d(3,3)
d(1,2)=1.-d(2,2)-d(3,3)
d(2,1)=1.-d(2,2)-d(2,3)
d(1,1)=1.-d(2,1)-d(3,1)
de=-1.-d(2,2)
sd(1,1)=d(1,1)+d(1,2)*d(2,1)/de
sd(1,2)=d(1,3)+d(2,3)*d(1,2)/de
sd(2,1)=d(3,1)+d(3,2)*d(2,1)/de
sd(2,2)=d(3,3)+d(3,2)*d(2,3)/de
td=1./sd(2,1)
fid(1,1)=td
fid(1,2)=-1.*td*sd(2,2)
fid(2,1)=sd(1,1)*td
fid(2,2)=sd(1,2)-sd(1,1)*td*sd(2,2)
ts=1./s(1,2)
fis(1,1)=ts
fis(1,2)=-1.*ts*s(1,1)
fis(2,1)=s(2,2)*ts
fis(2,2)=s(2,1)-s(2,2)*ts*s(1,1)
fic(1,1)=fid(1,1)*fis(1,1)+fid(1,2)*fis(2,1)
fic(1,2)=fid(1,1)*fis(1,2)+fid(1,2)*fis(2,2)
fic(2,1)=fid(2,1)*fis(1,1)+fid(2,2)*fis(2,1)
fic(2,2)=fid(2,1)*fis(1,2)+fid(2,2)*fis(2,2)
```

```
tf=1./fic(1,1)
sc(1,1)=fic(2,1)*tf
sc(1,2)=fic(2,2)-fic(2,1)*tf*fic(1,2)
sc(2,1)=tf
sc(2,2)=-1.*tf*fic(1,2)
delta=sc(1,1)*sc(2,2)-sc(1,2)*sc(2,1)
sr1=cabs(sc(2,2))**2
so=1.+cabs(delta)**2-cabs(sc(1,1))**2-sr1
cm=2.*cabs(sc(1,2)*sc(2,1))
sk=so/cm
do 100 i=1,2
do 100 j=1,2
100 write(7,*) sc(i,j)
write(7,8) sk
8   format(5x,'k=',e12.6)
xc=1./(2.*p*fz*c)
x1=2*p*fz*rl
z1=cmplx(0.,1.*x1)
zc=cmplx(0.,-1.*xc)
zrl=(r*z1)/(r+z1)
zgp=zrl+zc
zgpn=zgp/r
glp=(zgpn-1.)/(zgpn+1.)
gpm=fm(glp)
gpa=fa(glpm)
sr2=1.-sc(2,2)*glp
sc11p=sc(1,1)+sc(1,2)*sc(2,1)*glp/sr2
s1m=fm(sc11p)
s1a=fa(sc11p)
s2a=-1.*s1a
ri=1./s1m
write(7,32) f,zgpn
32  format(5x,'f(GHZ)=',f5.2,3x,'zg=',2e12.6)
write(7,34) glp
34  format(5x,'gamlp=',2e12.6)
write(7,33) gpm,gpa
33  format(5x,'|gamlp|=',f9.4,5x,f8.2)
write(7,9) s1m,s1a
9   format(5x,'|s`11|=',e12.6,3x,f8.2)
f=f+0.2
fz=fz+(0.2*10**(+9.))
110 write(7,31) ri,s2a
31  format(20x,'|1/s`11|=',e12.6,3x,f8.2)
stop
end
```

```
****match.for program****
complex s(2,2),zl,zc,zgp
complex zgpn,sp,cx,glp,zrl
fm(cx)=cabs(cx)
fa(cx)=180./p*atan2(aimag(cx),real(cx))
p=3.1415926
fz=11.*10**(+9.)
read(8,*) s(1,1),s(1,2),s(2,1),s(2,2)
c=0.245*10**(-12.)
r=50.
rl=0.29*10**(-9.)
xc=1./(2.*p*fz*c)
xl=2.*p*fz*rl
zl=cmplx(0.,1.*xl)
zc=cmplx(0.,-1.*xc)
zrl=(r*zl)/(r+zl)
zgp=zrl+zc
zgpn=zgp/r
glp=(zgpn-1.)/(zgpn+1.)
zd=1.s(2,2)*glp
sp=s(1,1)+s(1,2)*s(2,1)*glp/zd
s1m=fm(sp)
s1a=fa(sp)
s2a=-1.*s1a
ri=1./s1m
write(9,10)glp
10 format(5x,'glp=',2e12.6)
write(9,11)ri,s2a
11 format(5x,'1/s^11=' ,e12.6,3x,f8.2)
stop
end

complex gama,s(2,2),cx,sp
fm(cx)=cabs(cx)
fa(cx)=180./p*atan2(aimag(cx),real(cx))
p=3.1415926
read(8,*) s(1,1),s(1,2),s(2,1),s(2,2)
gama=cmplx(0.4,-0.77)
dd=1.-s(2,2)*gama
sp=s(1,1)+s(1,2)*s(2,1)*gama/dd
s1m=fm(sp)
s1a=fa(sp)
s2a=-1.*s1a
ri=1./s1m
do 11 i=1,2
do 11 j=1,2
11 write(3,*) s(i,j)
write(3,12) ri,s2a
12 format(5x,'1/s^11=' ,e12.6,5x,f8.2)
stop
end
```

```
***imp.for program***  
complex de,zi,zr  
complex zf,zo,zout  
complex s11,s12,s21,s22  
s11=cmplx(-3.154,-1.96)  
s12=cmplx(3.24,0.233)  
s21=cmplx(-0.075,-0.206)  
s22=cmplx(-0.57,0.29)  
de=(1.-s11)*(1.-s22)-s12*s21  
zi=50.*((1.+s11)*(1.-s22)+s12*s21)/de  
zr=50.*2.*s12/de  
zf=100.*s21/de  
zo=50.*((1.-s11)*(1.+s22)+s12*s21)/de  
zout=zo-(zr*zf)/(zi+50.)  
write(*,*) 'de=',de,'      ', 'zi=',zi  
write(*,*) 'zf=',zf,'      ', 'zo=',zo  
stop  
end
```

```
*****DC.FOR PROGRAM ****
dimension vg2d1(4),vg1s(4),vl(3)
data vl(1),vl(2),vl(3)/1.,2.,3/
data vg2d1(1),vg2d1(2),vg2d1(3)/0.,-0.5/
data vg2d1(3),vg2d1(4)/-1.,-1.5/
data cgso,vg2so,gmo/0.5,1.,0.048/
data vbi,vp,rdo/0.8,-3.,143./
vds=5.
idss=0.054
do 20 j=1,4
20   vg1s(j)=vg2d1(j)
      do 15 n=1,3
      do 30 k=1,4
      do 40 m=1,361,45
         fm=m-1
         d=fm
         x=(3.14*d)/180.
         vg2s=vg2so+vl(n)*sin(x)
         vd1s=vg2s-vg2d1(k)
         vg1d1=vg1s(k)-vd1s
         if(vg1d1.gt.0.7) go to 21
         cgd1=cgso*(1.-vg1d1/vbi)**(-1./2.)
21    vg2d2=vg2s-vds
         cgd2=cgso*(1.-vg2d2/vbi)**(-1./2.)
         id1s=(1-vg1s(k)/vp)**2*(idss+vd1s/rdo)
         dz=vd1s-gmo*vp*rdo
         delta1=(gmo*rdo*vp)**2+4.*id1s*rdo*dz
         de1=2.*(vd1s-gmo*vp*rdo)
         x1=(-1.*gmo*rdo*vp+sqrt(delta1))/de1
         x2=(-1.*gmo*rdo*vp-sqrt(delta1))/de1
         vpg1=vp-vp*x2
         dz2=vds-vd1s-rdo*vp*gmo
         delta2=(rdo*vp*gmo)**2+4.*id1s*rdo*dz2
         de2=2.*(vds-vd1s-rdo*vp*gmo)
         y1=(-1.*rdo*vp*gmo+sqrt(delta2))/de2
         y2=(-1.*rdo*vp*gmo-sqrt(delta2))/de2
         vpg2=vp-vp*y2
         a=1.-vpg1/vp
         b=1.-vpg2/vp
         c=1.-vpg1/vbi
         h=1.-vpg2/vbi
         if(a.eq.0.) go to 31
         gm1=gmo*(1.-vpg1/vp)
         rds1=rdo*(1.-vpg1/vp)**(-2)
31    if(c.eq.0.) go to 32
         cgs1=cgso*(1.-vpg1/vbi)**(-1./2.)
32    if(b.eq.0.) go to 33
         gm2=gmo*(1.-vpg2/vp)
         rds2=rdo*(1.-vpg2/vp)**(-2)
33    if(h.eq.0.) go to 34
         cgs2=cgso*(1.-vpg2/vbi)**(-1./2.)
34    write(7,9)n,k,m,gm1
9     format(5x,'n=',i3,2x,'k=',i3,2x,'m=',i4)
      write(7,11)gm2,rds1,rds2
11   format(5x,'gm2='f7.4,2x,'rds1='f6.2)
      write(7,8)vpg1,vpg2,cgs1
8     format(5x,'vpg1='f6.2,2x,'vpg2='f6.2)
      write(7,19)vg1d1,vg2d2,cgd2,cgd1
19   format(5x,'vg1d1='f6.2,2x,'vg2d2='f6.2)
40    write(7,12)cgs2,vg2d1(k),vl(n)
12    format(5x,'cgs2='f6.2,2x,'vg2d1(k)='f6.2)
30    continue 15 Continue end
```

```
c ****nl.for program*****
complex cx,a,v1(11,21),vlo(11),h1,h2
complex sumo,v11(11,21),fui(25,25)
complex c1(21),sums,sumz1,topz,etz,dep2
complex ez,z1,eb,sumi,zi ,ch,topb,gm3
complex cr,sol,de1,zr,etb,fu2(25,25)
complex chc,ric1(11),sim1,sim2,eb1,zg3
complex zg4,so2,de2,c21,sumv1,v22(25,25)
complex eg,pt1,za2,za1,vi1(25),rim2(11)
complex v2(11,21),sumv2,sumic2,sumim2
complex et,eb2,pay,sumkz,sumkk,vx(11)
complex zg1(11),sim1p,za1p,za2p,svx,gm3p
complex svi2,sv2,sic,svlo,zm(11),zg(11)
complex vi2(11),ri1(11),h3,h4,h5,h6,h7
complex sv1,svi1,si1,a5,si1p,si11,zg2
complex h8,h9,h10,chcp,ric2(11),a2(11)
complex sumsp,sumz1p,c2(21),sumip,chp
complex rim1(11),gm2(11),gm1(11),sim2p
complex h22,hp5,hp7,hp9,sop1,dep1,sop2
real n,nh4,nsp1,iz,nh8,110,mh10,ms1,im
real nsp2,nh10,ni12,nh12,nh14,isp,nhip
real lm,im7,im8,nio5,jh
data rg,rm/40.,50/
data vm,n,vb,vp/+0.8,10.,0.9,-3./
data vd,ro,r1,r2/5.0,143.,427.,427./
m=1
cg=0.05
s4=-1.5
vg1=-3.
cm=0.4
lm=1.1
p=3.141593
f=11.
to=2.5*10**(-12)
c2o=0.5
gmo=0.05
a=cmplx(0.,0.)
do 1 i1=1,4
1 v2(i1,m)=a
v2(5,m)=cmplx(vm/2.,0.)
v2(6,m)=cmplx(-r1/(r1+r2)*vd+s4,0.)
v2(7,m)=cmplx(vm/2.,0.)
do 2 i2=1,4
2 i2=i2+7
2 v2(i2,m)=a
do 21 i21=1,5
21 vlo(i21)=v2(i21,m)
vlo(6)=cmplx(s4,0.)
do 221 k4=1,5
k41=k4+6
221 vlo(k41)=v2(k41,m)
do 22 l22=1,11
22 v22(l22,m)=v2(l22,m)
do 61 n2=1,5
61 v1(n2,m)=a
v1(6,m)=cmplx(vg1,0.)
do 62 n3=1,5
n4=n3+6
62 v1(n4,m)=a
do 63 n5=1,11
63 v11(n5,m)=v1(n5,m)
```

```
      do 3 i3=1,11
3       write(7,*) 'v2(i3,m)=',v2(i3,m)
      do 64 n6=1,11
64     write(7,*) 'v1(n6,m)=',v1(n6,m)
      do 100 k=1,12
         if(k.eq.1)go to 44
      do 66 l16=1,11
66     v1(l16,k)=v11(l16,k)
      do 67 n7=1,11
67     v2(n7,k)=v22(n7,k)
44     n41=1
      do 4 i4=1,21
         nh4=i4-11
         sums=a
         sumsp=a
      do 5 ns1=1,20
         nsp1=ns1-1
         sumz1=a
         sumz1p=a
      do 6 iz6=1,11
         iz=iz6-6
         y1=sin(iz*2.*p*nsp1/20.)
         ez=cmplx(cos(iz*2.*p*nsp1/20.),y1)
         sumz1=sumz1+v2(iz6,k)*ez
6        sumz1p=sumz1p+v1(iz6,k)*ez
         s2=sumz1
         s2p=sumz1p
         sumz=1.-s2/vb
         sumzp=1.-s2p/vb
         rb=sqrt(sumz)
         rbp=sqrt(sumzp)
         tz1=1./rb
         tz1p=1./rbp
         y2=-1.*sin(2.*p*nh4*nsp1/20.)
         eb=cmplx(cos(2.*p*nh4*nsp1/20.),y2)
         sums=sums+eb*tz1
5        sumsp=sumsp+eb*tz1p
         c2(i4)=c2o/20.*sums
         c1(i4)=c2o/20.*sumsp
4        continue
150    as1=1.
      do 8 i8=1,11
         sumi=a
         sumip=a
      do 9 i9=1,11
         i9=i9-1
         i10=i9-6
         zi=cmplx(0.,0.069*i10)
         ch=c2(i8+10-i9)*v2(i9,k)
         chp=c1(i8+10-i9)*v1(i9,k)
         chc=zi*ch
         chcp=zi*chp
         sumip=sumip+chcp
9        sumi=sumi+chc
         ric2(i8)=sumi
         ric1(i8)=sumip
8        continue
151    as2=2.
      do 27 m7=1,11
         im7=m7-6
27     vi1(m7)=cmplx(0.,0.172*im7)*v1(m7,k)
```

```
do 28 m8=1,11
im8=m8-6
28 v12(m8)=cmplx(0.,0.172*im8)*v2(m8,K)
do 10 i10=1,11
sim2=a
sim2p=a
nh10=i10-6
gm3=a
gm3p=a
do 11 ns2=1,10
nsp2=ns2-1
sim1=a
sim1p=a
do 12 i12=1,11
ni12=i12-6
y3=sin(2.*p*ni12*nsp2/n)
eg= cmplx(cos(2.*p*ni12*nsp2/n),y3)
za1=eg*v2(i12,k)
za1p=eg*v1(i12,k)
sim1=sim1+za1
12 sim1p=sim1p+za1p
pt1=1.-sim1/vp
pt1p=1.-sim1p/vp
za2=pt1*sim1
za2p=pt1p*sim1p
y4=-1.*sin(2.*p*nh10*nsp2/n)
eb1=cmplx(cos(2.*p*nh10*nsp2/n),y4)
gm3=gm3+pt1*eb1
gm3p=gm3p+pt1p*eb1
sim2=sim2+za2*eb1
11 sim2p=sim2p+za2p*eb1
rim2(i10)=gmo/n*sim2
rim1(i10)=gmo/n*sim2p
gm2(i10)=gm3*gmo/n
gm1(i10)=gm3p*gmo/n
10 continue
do 335 j36=1,11
jh=j36-6
if(jh.eq.0.) go to 337
d2=(2.0*p*f*jh)**4*lm**2*cm**2
d3=(2.0*p*f*jh)**2*cm**2*rm**2
dp1=-2.*(2.*p*f*jh)**2*lm*cm/1000.
d1=(d2+d3)/1000000.+1.+dp1
a1=rm/d1
bp1=(2.*p*f*jh)*cm*rm**2
bp2=(2.*p*f*jh)**3*lm**2*cm
b1=(bp2+bp1)/1000.*(-1.)
b2=(2.*p*f*jh)*lm
b3=b1+b2
b4=b3/d1
zm(j36)=cmplx(a1,-b4)
zg1(j36)=cmplx(rg,-1000./(2.*p*f*jh*cg))
a2(j36)=r2*r1+(r2+r1)*(zm(j36)+zg1(j36))
337 zm(6)=cmplx(0.,0.)
a2(6)=cmplx(0.,0.)
335 zg1(6)=cmplx(0.,0.)
do 13 nc=1,11
if(nc.eq.6) go to 131
h1=(zm(nc)**2*(r1+r2)/a2(nc)-zm(nc))
h1=h1*ric1(nc)
h22=(zm(nc)*r1*r2/a2(nc))*rim1(nc)
```

```
h2=(zm(nc)*r1*r2/a2(nc))*ric2(nc)-h22
h3=(zm(nc)*r1*r2/a2(nc))*rim2(nc)-vi1(nc)
v11(nc,k+1)=h1+h2+h3
go to 132
131 cp=c1(11)
v11(nc,k+1)=vg1
h13=r1*r2/(r1+r2)
h10=r1*r2/(r1+r2)*rim1(6)-h13*rim2(6)
v22(nc,k+1)=h10-r1/(r1+r2)*vd+vlo(6)
go to 13
132 hp5=(zm(nc)+zg1(nc))*(r1+r2)*(-1.*zm(nc))
h5=hp5/a2(nc)+zm(nc)
h6=h5*ric1(nc)
hp7=((zm(nc)+zg1(nc))*(-1.*r1*r2)/a2(nc))
h7=hp7*ric2(nc)
h8=((zm(nc)+zg1(nc))*r1*r2/a2(nc))*rim1(nc)
hp9=(zm(nc)+zg1(nc))*(-r1*r2)/a2(nc)
h9=hp9*rim2(nc)-vi2(nc)+vlo(nc)
v22(nc,k+1)=h6+h7+h8+h9
13 write(7,*)'v11(nc,k+1)=',v11(nc,k+1)
do 29 nc2=1,11
29 write(7,*)'v22(nc2,k+1)=',v22(nc2,k+1)
if(k.gt.1)go to 88
do 15 i15=1,11
fu1(i15,k)=v11(i15,k+1)
fu2(i15,k)=v22(i15,k+1)
15 write(7,*)'fu1(i15,k)=',fu1(i15,k)
go to 100
88 n81=1
do 17 l17=1,11
fu1(l17,k)=v11(l17,k+1)
sop1=fu1(l17,k)-fu1(l17,k-1)
so1=sop1*(v11(l17,k)-fu1(l17,k))
dep1=fu1(l17,k)-v11(l17,k)
de1=dep1-(fu1(l17,k-1)-v11((l17,k-1)))
if(de1.eq.a)go to 83
v11(l17,k+1)=fu1(l17,k)+so1/de1
go to 171
83 v11(l17,k+1)=fu1(l17,k)
171 fu2(l17,k)=v22(l17,k+1)
sop2=fu2(l17,k)-fu2(l17,k-1)
so2=sop2*(v22(l17,k)-fu2(l17,k))
dep2=fu2(l17,k)-v22(l17,k)
de2=dep2-(fu2((l17,k-1))-v22(l17,k-1))
if(de2.eq.a)go to 31
v22(l17,k+1)=fu2(l17,k)+so2/de2
go to 17
31 v22(l17,k+1)=fu2(l17,k)
17 write(7,*)'v11(l17,k+1)=',v11(l17,k+1)
do 172 km=1,11
172 write(7,*)'v22(km,k+1)=',v22(km,k+1)
100 continue
end
```

```
*****ELT.FOR PROGRAM*****
complex v1(11),v2(11),c2(21),gm1(11)
complex gm2(11),rim2(11),sim1,ez,eg
complex rim1(11),sums,sumz1,sum2,zai
complex pt1,sumv1,et,eb2,zg(11)
complex sumi,ch,che,sr2,sr1,sumv2
complex sim2p,gm3p,sim1p,zai1p,za2p
complex eb1,eb,ric2(11),ri2(11),sr(11)
complex r2(11),r1(11),a,zi,gm3,za2
real nh3,nsp1,iz,n,nh10,nsp2,l10
real mh10,ms1,im,j5p,ni12
data p,c2o,n,ro/3.1415,0.5,10.,143./
data cg,f,gmo,vb/0.15,11.,0.05,0.9/
data rg,vp/50.,-3./
do 1 i1=1,3
i11=i1+4
1   read(8,*) v1(i11)
do 2 i2=1,3
i21=i2+4
2   read(8,*) v2(i21)
do 24 m4=1,11
write(9,*)"v1(m4)=",v1(m4)
do 25 m5=1,11
write(9,*)"v2(m5)=",v2(m5)
a=complx(0.,0.)
do 3 i3=1,21
nh3=i3-11
sums=a
sr11=a
do 4 ns1=1,20
nsp1=ns1-1
sumz1=a
do 5 iz5=1,11
iz=iz5-6
e1=sin(iz*2.*p*nsp1/20.)
ez=complx(cos(iz*2.*p*nsp1/20.),e1)
sumz1=sumz1+v2(iz5)*ez
s2=sumz1
sumz=1.-1.*(s2/vb)
su=sumz
rb=sqrt(su)
tz1=1./rb
e2=-1.*sin(2.*p*nh3*nsp1/20.)
eb=complx(cos(2.*p*nh3*nsp1/20.),e2)
sums=sums+eb*tz1
sr11=sr11+eb*tz1
5   continue
c2(i3)=c2o/20.*sums
ri2(i3)=2.5/(c2o*n)*sr11
3   write(9,*)"c2(i3)=",c2(i3)
do 8 i8=1,11
sumi=a
do 9 i9=1,11
i9=i9-1
l10=i9-6
zi=complx(0.,0.069*l10)
ch=c2(i8+10-i9)*v2(i9)
che=zi*ch
9   sumi=sumi+che
ric2(i8)=sumi
8   write(9,*)"ic2(i8)=",ric2(i8)
```

```
do 10 i10=1,11
sim2=a
sim2p=a
nh10=i10-6
gm3=a
gm3p=a
do 11 ns2=1,10
nsp2=ns2-1
sim1=a
sim1p=a
do 12 i12=1,11
ni12=i12-6
e3=sin(2.*p*ni12*nsp2/n)
eg=cmplx(cos(2.*p*ni12*nsp2/n),e3)
zal=eg*v2(i12)
za1p=eg*v1(i12)
sim1=sim1+zal
12 sim1p=sim1p+za1p
pt1=1.-sim1/vp
pt1p=1.-sim1p/vp
za2=pt1*sim1
za2p=pt1p*sim1p
e4=-1.*sin(2.*p*nh10*nsp2/n)
eb1=cmplx(cos(2.*p*nh10*nsp2/n),e4)
gm3=gm3+pt1*eb1
gm3p=gm3p+pt1p*eb1
sim2=sim2+za2*eb1
sim2p=sim2p+za2p*eb1
11 continue
rim2(i10)=gmo/n*sim2
rim1(i10)=gmo/n*sim2p
gm2(i10)=gm3*gmo/n
gm1(i10)=gm3p*gmo/n
10 write(9,*)'im2(i10)=',rim2(i10)
do 42 ki=1,11
42 write(9,*)'GM2(ki)=',gm2(ki)
do 38 l2=1,11
38 write(9,*)'IM1=',rim1(l2)
do 37 l3=1,11
37 write(9,*)'GM1=',gm1(l3)
do 110 m10=1,11
mh10=m10-6
sr2=a
sri=a
do 111 ms=1,10
ms1=ms-1
sumv2=a
sumv1=a
do 112 m12=1,11
im=m12-6
e5=sin(im*2.*p*ms1/n)
et=cmplx(cos(im*2.*p*ms1/n),e5)
sumv2=sumv2+v2(m12)*et
sumv1=sumv1+v1(m12)*et
112 x1p=sumv1
x2p=sumv2
sumkz1=(1.-x1p/vp)**2
sumkz2=(1.-x2p/vp)**2
e6=-1.*sin(2.*p*mh10*ms1/n)
eb2=cmplx(cos(2.*p*mh10*ms1/n),e6)
sri=sri+sumkz1*eb2
```

```
111 sr2=sr2+sumkz2*eb2
110 r2(m10)=ro/n*sr2
      r1(m10)=ro/n*sr1
      do 50 j5=1,11
      j5p=j5-6
      if(j5p.eq.0.) go to 50
      zg(j5)=cmplx(rg,-1000./(2.*p*f*j5p*cg))
50    write(9,*) 'ZG(J5)=' ,zg(j5), 'j5=' ,j5
      end
```

```
c ****SMS FOR PROGRAM*****
complex zn,zz,zp,zgn,zgz,zgp,s3
complex w(9),hn(8),hz(8),hp(8),s1
complex x(9),den,dez,dep,gm1n,gm1z
complex y(9),u1,u2,u3,to,v2(3),gm1p
complex rid(3),v2l(3),vlo(3),ridl(3)
complex z(9),gm2n,gm2z,gm2p,t,zg(3),q3
complex c2n,c2z,c2p,c1n,c1z,c1p,q1,q2
real lm
data wn,wz,wp,p/6.283,75.4,144.5,3.1415/
data lm,cm,rm,rg,cg/1.1,0.4,50.,40.,0.05/
data r1,r2/427.,427./
u=1000.
zg(1)=cmplx(rg,-1000./(2.*p*11.*cg*(-1.)))
zg(2)=cmplx(0.,0.)
zg(3)=cmplx(rg,-1000./(2.*p*11.*cg))
y2=1./r2
to=cmplx(0.,2.5*y2/1000.)
do 21 i=1,3
21  read(8,*)v2(i)
do 31 j=1,3
31  read(8,*)v2l(j)
do 41 k=1,3
41  read(8,*)vlo(k)
do 51 i1=1,3
51  write(7,*)"v2s(i1)=",v2(i1),'i1=',i1
do 61 j1=1,3
61  write(7,*)"v2l(j1)=",v2l(j1),'j1=',j1
do 71 k1=1,3
71  write(7,*)"vlo(k1)=",vlo(k1),'k1=',k1
u1=cmplx(0.,2.5*wn/u)
u2=cmplx(0.,2.5*wz/u)
u3=cmplx(0.,2.5*wp/u)
c1n=cmplx(-0.21,0.12)
c1z=cmplx(0.48,0.)
c1p=cmplx(-0.21,-0.12)
c2n=cmplx(-0.054,0.246)
c2z=cmplx(0.49,0.)
c2p=cmplx(-0.054,-0.246)
gm1n=cmplx(-0.0053,0.0031)
gm1z=cmplx(0.000016,0.)
gm1p=cmplx(-0.0053,-0.0031)
gm2n=cmplx(-0.00133,0.00603)
gm2z=cmplx(0.003315,0.)
gm2p=cmplx(-0.00133,-0.00603)
t=cmplx(0.,1.)
dn2=1.-2.*wn**2*lm*cm/1000.
dz2=1.-2.*wz**2*lm*cm/1000.
dp2=1.-2.*wp**2*lm*cm/1000.
dnp=wn**4*lm**2*cm**2+wn**2*cm**2*rm**2
dn=dnp/1000000.+dn2
dzp=wz**4*lm**2*cm**2+wz**2*cm**2*rm**2
dz=dzp/1000000.+dz2
dpp=wp**4*lm**2*cm**2+wp**2*cm**2*rm**2
dp=dpp/1000000.+dp2
an=rm/dn
az=rm/dz
ap=rm/dp
bin=-(wn**3*lm**2*cm+wn*cm*rm**2)/1000.
biz=-(wz**3*lm**2*cm+wz*cm*rm**2)/1000.
bip=-(wp**3*lm**2*cm+wp*cm*rm**2)/1000.
```

```
b2n=wn*lm
b2z=wz*lm
b2p=wp*lm
b3n=(b1n+b2n)/dn
b3z=(b1z+b2z)/dz
b3p=(b1p+b2p)/dp
zn=cmplx(an,-b3n)
zz=cmplx(az,-b3z)
zp=cmplx(ap,-b3P)
zgn=cmplx(rg,-1000./wn*cg)
zgz=cmplx(rg,-1000./wz*cg)
zgp=cmplx(rg,-1000./wp*cg)
den=r2*r1+(r2+r1)*(zn+zgn)
dez=r2*r1+(r2+r1)*(zz+zgz)
dep=r2*r1+(r2+r1)*(zp+zgp)
hn(1)=zn**2*(r1+r2)/den-zn
hz(1)=zz**2*(r1+r2)/dez-zz
hp(1)=zp**2*(r1+r2)/dep-zp
hn(2)=zn*r1*r2/den
hz(2)=zz*r1*r2/dez
hp(2)=zp*r1*r2/dep
hn(3)=1.-zn*(r1+r2)/den
hz(3)=1.-zz*(r1+r2)/dez
hp(3)=1.-zp*(r1+r2)/dep
hn(4)=zn*r1/den
hz(4)=zz*r1/dez
hp(4)=zp*r1/dep
hn(5)=(zn+zgn)*(r1+r2)*(-1.*zn)/den+zn
hz(5)=(zz+zgz)*(r1+r2)*(-1.*zz)/dez+zz
hp(5)=(zp+zgp)*(r1+r2)*(-1.*zp)/dep+zp
hn(6)=-1.*(zn+zgn)*r1*r2/den
hz(6)=-1.*(zz+zgz)*r1*r2/dez
hp(6)=-1.*(zp+zgp)*r1*r2/dep
hn(7)=(r1+r2)*(zn+zgn)/den-1.
hz(7)=(r1+r2)*(zz+zgz)/dez-1.
hp(7)=(r1+r2)*(zp+zgp)/dep-1.
hn(8)=-1.*r1*(zn+zgn)/den
hz(8)=-1.*r1*(zz+zgz)/dez
hp(8)=-1.*r1*(zp+zgp)/dep
do 1 i=1,8
1   write(7,*) 'hn(i)=',hn(i), 'i=',i
do 2 j=1,8
2   write(7,*) 'hz(j)=',hz(j), 'j=',j
do 3 k=1,8
3   write(7,*) 'hp(k)=',hp(k), 'k=',k
w(1)=1.-t*hn(1)*wn*c1z/u+hn(2)*gm1z+u1
w(2)=-t*hn(1)*wn*c1n/u+hn(2)*gm1n
w(3)=-t*hz(1)*wz*c1p/u+hz(2)*gm1p
w(4)=1.-t*hz(1)*wz*c1z/u+hz(2)*gm1z+u2
w(5)=-t*hz(1)*wz*c1n/u+hz(2)*gm1n
w(6)=-t*hp(1)*wp*c1p/u+hp(2)+gm1p
w(7)=1.-t*hp(1)*wp*c1z/u+hp(2)+gm1z+u3
x(1)=-t*hn(2)*wn*c2z/u-hn(2)*gm2z
x(2)=-t*hn(2)*wn*c2n/u-hn(2)*gm2n
x(3)=-t*hz(2)*wz*c2p/u-hz(2)*gm2p
x(4)=-t*hz(2)*wz*c2z/u-hz(2)*gm2z
x(5)=-t*hz(2)*wz*c2n/u-hz(2)*gm2n
x(6)=-t*hp(2)*wp*c2p/u-hp(2)*gm2p
x(7)=-t*hp(2)*wp*c2z/u-hp(2)*gm2z
y(1)=-t*hn(5)*wn*c1z/u+hn(6)*gm1z
y(2)=-t*hn(5)*wn*c1n/u+hn(6)*gm1n
```

```
y(3)=-t*hz(5)*wz*c1p/u+hz(6)*gm1p
y(4)=-t*hz(5)*wz*c1z/u+hz(6)*gm1z
y(5)=-t*hz(5)*wz*c1n/u+hz(6)*gm1n
y(6)=-t*hp(5)*wp*c1p/u+hp(6)*gm1p
y(7)=-t*hp(5)*wp*c1z/u+hp(6)*gm1z
z(1)=1.-t*hn(6)*wn*c2z/u-hn(6)*gm2z+u1
z(2)=-t*hn(6)*wn*c2n/u-hn(6)*gm2n
z(3)=-t*hz(6)*wz*c2p/u-hz(6)*gm2p
z(4)=1.-t*hz(6)*wz*c2z/u-hz(6)*gm2z+u2
z(5)=-t*hz(6)*wz*c2n/u-hz(6)*gm2n
z(6)=-t*hp(6)*wp*c2p/u-hp(6)*gm2p
z(7)=1.-t*hp(6)*wp*c2z/u-hp(6)*gm2z+u3
do 4 i4=1,7
 4  write(7,*)'w(i4)=',w(i4), 'i4=',i4
  do 5 i5=1,7
  5  write(7,*)'x(i5)=',x(i5), 'i5=',i5
  do 6 i6=1,7
  6  write(7,*)'y(i6)=',y(i6), 'i6=',i6
  do 7 i7=1,7
  7  write(7,*)'z(i7)=',z(i7), 'i7=',i7
  s1=cmplx(0.,-1.*2.5*2.*3.1415*11./1000.)
  s3=cmplx(0.,2.*2.5*3.1415*11./1000.)
  rid(1)=(y2+wn*to+gm2z)*v2(1)+gm2n*v2(2)
  q1=gm2n*v2(3)
  rid(2)=gm2p*v2(1)+(y2+to*wz+gm2z)*v2(2)+q1
  rid(3)=gm2p*v2(2)+(gm2z+y2+to*wp)*v2(3)
  q2=gm2n*v2(1)-vlo(1)/zg(1)
  ridl(1)=(v2l(1)+s1*v2l(1)-vlo(1))/r2+q2
  ridl(2)=(v2l(2)-vlo(2))/r2+gm2z*v2(2)
  q3=gm2p*v2(3)-vlo(3)/zg(3)
  ridl(3)=(v2l(3)+s3*v2l(3)-vlo(3))/r2+q3
  do 100 m2=1,3
100   write(7,*)'rid(m2)=',rid(m2)
  do 101 m3=1,3
101   write(7,*)'ridl(m3)=',ridl(m3)
  end
```

```
*****ROOTS.FOR PROGRAM*****  
COMPLEX*16 Q(64,64),A(64),B(64)  
READ(*,*) N  
DO 10 I=1,N  
DO 10 J=1,N  
READ(1,*) X,Y  
10 Q(I,J)=CMPLX(X,Y)  
DO 20 I=1,N  
READ(1,*) X,Y  
20 A(I)=CMPLX(X,Y)  
CALL GAUSS(N,Q,B,A)  
DO 30 I=1,N  
30 WRITE(2,*) REAL(B(I)),AIMAG(B(I))  
STOP  
END  
  
C  
SUBROUTINE GAUSS(N,CMN,EN,EM)  
COMPLEX*16 CMN(64,64),EN(64),EM(64),D2,T,DA  
DO 30 K=1,N-1  
D=0.0  
DO 40 I=K,N  
C=CABS(CMN(I,K))  
IF(D.GE.C) GOTO 40  
D=C  
LL=I  
40 CONTINUE  
L1=LL  
IF(L1.EQ.K) GOTO 50  
DO 60 J=K,N  
DA=CMN(K,J)  
CMN(K,J)=CMN(L1,J)  
60 CMN(L1,J)=DA  
D2=EM(K)  
EM(K)=EM(L1)  
EM(L1)=D2  
50 DO 70 I=K+1,N  
T=-CMN(I,K)/CMN(K,K)  
CMN(I,K)=T  
DO 80 J=K+1,N  
80 CMN(I,J)=CMN(I,J)+T*CMN(K,J)  
70 EM(I)=EM(I)+T*EM(K)  
30 CONTINUE  
EN(N)=EM(N)/CMN(N,N)  
DO 90 I=N-1,1,-1  
DA=EM(I)  
DO 100 J=I+1,N  
100 DA=DA-CMN(I,J)*EN(J)  
90 EN(I)=DA/CMN(I,I)  
RETURN  
END
```

APPENDIX-B: OUTPUTS FOR PROGRAMS

the output of cascod2.for program
S-Parameter for two port common source FET

(6.400000E-001,.0000000) 128.0000000
(1.020000E-001,.0000000) 11.0000000
(1.130000,.0000000) -17.0000000
(6.000000E-001,.0000000) -142.0000000

S-Parameter for cascade circuit which the gate of common drain FET is as input and the gate of common source FET is as output ports.

(-2.0094320,3.172233E-001)
(2.889619E-001,-1.1003920)
(-9.022266E-002,-6.028760E-002)
(-3.909151E-001,4.505720E-001)
k=-.696277E+01
f(GHZ)=11.00 zo= .150672E+02 .210778E+02
zin= .150672E+02-.210778E+02
zinn=0.301 -0.4215
gainn=-.390915E+00-.450572E+00
|gainn|= .5965 <gainn= -130.94
|s`11|= .192497E+01 <s`11= 170.06
|1/s`11|= .519488E+00 <1/s`11= -170.06

S-Parameter for two port common source FET

(6.700000E-001,.0000000) 108.0000000
(1.100000E-001,.0000000) -1.0000000
(1.0500000,.0000000) -33.0000000
(6.100000E-001,.0000000) -145.0000000

S-Parameter for cascade circuit which the gate of common drain FET is as input and the gate of common source FET is as output ports.

(-1.5667360,9.345811E-001)
(-3.497517E-001,-1.0632280)
(-9.924534E-002,3.392251E-003)
(-2.488641E-001,5.797699E-001)
k=-.512511E+01
f(GHZ)=12.00 zo= .158755E+02 .305819E+02
zin= .158755E+02-.305819E+02
zinn=0.317 -0.611
gainn=-.248864E+00-.579770E+00
|gainn|= .6309 <gainn= -113.23
|s`11|= .171079E+01 <s`11= 150.03
|1/s`11|= .584524E+00 <1/s`11= -150.03

S-Parameter for two port common source FET

(6.800000E-001,.0000000) 117.0000000
(1.290000E-001,.0000000) -88.0000000
(1.580000,.0000000) -47.0000000
(4.700000E-001,.0000000) 157.0000000

S-Parameter for cascade circuit which the gate of common drain FET is as input and the gate of common source FET is as output ports.

(-1.683214E-001,2.7989190)
(-7.239437E-001,-6.048806E-001)
(2.389210E-001,-5.357925E-003)
(-3.020495E-001,7.263950E-001)

k=-.784043E+01
f(GHZ)=11.00 zo= .857218E+01 .326766E+02
zin= .857218E+01-.326766E+02
zinn=0.1714 -0.6535
gainn=-.302050E+00-.726395E+00
|gainn|= .7867 <gainn= -112.58
|s'11|= .325976E+01 <s'11= 95.22
|1/s'11|= .306771E+00 <1/s'11= -95.22

S-Parameter for two port common source FET

(6.700000E-001,.0000000) 103.0000000
(1.300000E-001,.0000000) -100.0000000
(1.450000,.0000000) -64.0000000
(5.000000E-001,.0000000) 142.0000000

S-Parameter for cascade circuit which the gate
of common drain FET is as input and the gate of
common source FET is as output ports.

(6.284419E-001,2.0115230)
(-4.191723E-001,-1.684499E-002)
(1.395013E-001,-1.228903E-001)
(-6.371017E-002,6.979936E-001)
k=-.125013E+02
f(GHZ)=12.00 zo= .157149E+02 .431213E+02
zin= .157149E+02-.431213E+02
zinn=0.314 -0.8624
gainn=-.637102E-01-.697994E+00
|gainn|= .7009 <gainn= -95.22
|s'11|= .220373E+01 <s'11= 71.38
|1/s'11|= .453776E+00 <1/s'11= -71.38

S-Parameter for two port common source FET

(6.800000E-001,.0000000) 117.0000000
(1.290000E-001,.0000000) -88.0000000
(1.580000,.0000000) -47.0000000
(4.700000E-001,.0000000) 157.0000000

S-Parameter for cascade circuit which the gate
of common drain FET is as input and the gate of
common source FET is as output ports.

(-1.683214E-001,2.7989190)
(-7.239437E-001,-6.048806E-001)
(2.389210E-001,-5.357925E-003)
(-3.020495E-001,7.263950E-001)
k=-.784043E+01
f(GHZ)= 9.00 zg= .149015E+00-.523692E+00
gamlp= .340000E+00-.770000E+00
|gamlp|= .8417 <gamlp= -66.18
|s'11|= .276867E+01 <s'11= 98.78
|1/s'11|= .361184E+00 <1/s'11= -98.78

S-Parameter for two port common source FET

(6.700000E-001,.0000000) 103.0000000
(1.300000E-001,.0000000) -100.0000000
(1.450000,.0000000) -64.0000000
(5.000000E-001,.0000000) 142.0000000

S-Parameter for cascade circuit which the gate
of common drain FET is as input and the gate of
common source FET is as output ports.

```
-----  
(6.284419E-001,2.0115230)  
(-4.191723E-001,-1.684499E-002)  
(1.395013E-001,-1.228903E-001)  
(-6.371017E-002,6.979936E-001)  
k=-.125013E+02  
f(GHZ)= 9.20 zg= .154676E+00-.499074E+00  
gamlp= .340000E+00-.770000E+00  
|gamlp|= .8417 <gamlp= -66.18  
|s`11|= .220651E+01 <s`11= 74.29  
|1/s`11|= .453205E+00 <1/s`11= -74.29
```

S-Parameter for two port common source FET

```
-----  
(6.400000E-001,.0000000) 128.0000000  
(1.020000E-001,.0000000) 11.0000000  
(1.130000,.0000000) -17.0000000  
(6.000000E-001,.0000000) -142.0000000
```

S-Parameter for cascade circuit which the gate of common drain FET is as input and the gate of common source FET is as output ports.

```
-----  
(-2.0094320,3.172233E-001)  
(2.889619E-001,-1.1003920)  
(-9.022266E-002,-6.028760E-002)  
(-3.909151E-001,4.505720E-001)  
k=-.696277E+01  
f(GHZ)= 9.00 zg= .149015E+00-.523692E+00  
gamlp= .160000E+00-.760000E+00  
|gamlp|= .7767 <gamlp= -78.11  
|s`11|= .205105E+01 <s`11= 167.74  
|1/s`11|= .487556E+00 <1/s`11= -167.74
```

S-Parameter for two port common source FET

```
-----  
(6.700000E-001,.0000000) 108.0000000  
(1.100000E-001,.0000000) -1.0000000  
(1.050000,.0000000) -33.0000000  
(6.100000E-001,.0000000) -145.0000000
```

S-Parameter for cascade circuit which the gate of common drain FET is as input and the gate of common source FET is as output ports.

```
-----  
(-1.5667360,9.345811E-001)  
(-3.497517E-001,-1.0632280)  
(-9.924534E-002,3.392251E-003)  
(-2.488641E-001,5.797699E-001)  
k=-.512511E+01  
f(GHZ)= 9.20 zg= .154676E+00-.499074E+00  
gamlp= .160000E+00-.760000E+00  
|gamlp|= .7767 <gamlp= -78.11  
|s`11|= .173931E+01 <s`11= 146.00  
|1/s`11|= .574941E+00 <1/s`11= -146.00
```

the output of math.for program
glp=-.141569E+00-.838036E+00
|1/s`11|= .448223E+00 <1/s`11= 156.27

glp=.368887E-01-.788628E+00
|1/s`11|= .339307E+00 <1/s`11= -99.74

(-1.700000E-001,2.7989000)
(-7.230000E-001,-6.000000E-001)
(2.380000E-001,-5.000000E-003)
(-3.000000E-001,7.260000E-001)
|1/s`11|= .363928E+00 <1/s`11= -98.58

(-2.500000,-3.140000E-001)
(-4.990000E-001,-2.100000)
(-8.000000E-002,1.650000E-001)
(-4.100000E-001,6.770000E-001)
|1/s`11|= .482594E+00 <1/s`11= 167.61

THE OUTPUT OF DC, FOR PROGRAM
n= 1 k= 1 m= 1 gm1=.0458
gm2=.0402 rds1=157.23 rds2=203.95
vpg1=-.14 vpg2=-.49 cgs1=.46
vg1d1=-1.00 vg2d2=-4.00 cgd2=.20 .33
cgs2=.39 vg2d1(k)=.00 vl(n)=1.00
n= 1 k= 1 m= 46 gm1=.0443
gm2=.0414 rds1=167.69 rds2=192.40
vpg1=-.23 vpg2=-.41 cgs1=.44
vg1d1=-1.71 vg2d2=-3.29 cgd2=.22 .28
cgs2=.41 vg2d1(k)=.00 vl(n)=1.00
n= 1 k= 1 m= 91 gm1=.0438
gm2=.0419 rds1=172.13 rds2=187.70
vpg1=-.27 vpg2=-.38 cgs1=.43
vg1d1=-2.00 vg2d2=-3.00 cgd2=.23 .27
cgs2=.41 vg2d1(k)=.00 vl(n)=1.00
n= 1 k= 1 m= 136 gm1=.0443
gm2=.0414 rds1=167.71 rds2=192.38
vpg1=-.23 vpg2=-.41 cgs1=.44
vg1d1=-1.71 vg2d2=-3.29 cgd2=.22 .28
cgs2=.41 vg2d1(k)=.00 vl(n)=1.00
n= 1 k= 1 m= 181 gm1=.0458
gm2=.0402 rds1=157.25 rds2=203.92
vpg1=-.14 vpg2=-.49 cgs1=.46
vg1d1=-1.00 vg2d2=-4.00 cgd2=.20 .33
cgs2=.39 vg2d1(k)=.00 vl(n)=1.00
n= 1 k= 1 m= 226 gm1=.0473
gm2=.0391 rds1=147.12 rds2=215.82
vpg1=-.04 vpg2=-.56 cgs1=.49
vg1d1=-.29 vg2d2=-4.71 cgd2=.19 .43
cgs2=.38 vg2d1(k)=.00 vl(n)=1.00
n= 1 k= 1 m= 271 gm1=.0480
gm2=.0386 rds1=143.00 rds2=220.88
vpg1=.00 vpg2=-.59 cgs1=.50
vg1d1=.00 vg2d2=-5.00 cgd2=.19 .50
cgs2=.38 vg2d1(k)=.00 vl(n)=1.00
n= 1 k= 1 m= 316 gm1=.0473
gm2=.0391 rds1=147.07 rds2=215.88
vpg1=-.04 vpg2=-.56 cgs1=.49
vg1d1=-.29 vg2d2=-4.71 cgd2=.19 .43
cgs2=.38 vg2d1(k)=.00 vl(n)=1.00
n= 1 k= 1 m= 361 gm1=.0458
gm2=.0402 rds1=157.18 rds2=204.00
vpg1=-.14 vpg2=-.49 cgs1=.46
vg1d1=-1.00 vg2d2=-4.00 cgd2=.20 .33
cgs2=.39 vg2d1(k)=.00 vl(n)=1.00
n= 1 k= 2 m= 1 gm1=.0447
gm2=.0410 rds1=164.59 rds2=195.74
vpg1=-.20 vpg2=-.44 cgs1=.45
vg1d1=-2.00 vg2d2=-4.00 cgd2=.20 .27
cgs2=.40 vg2d1(k)=-.50 vl(n)=1.00
n= 1 k= 2 m= 46 gm1=.0434
gm2=.0423 rds1=175.29 rds2=184.43
vpg1=-.29 vpg2=-.36 cgs1=.43
vg1d1=-2.71 vg2d2=-3.29 cgd2=.22 .24
cgs2=.42 vg2d1(k)=-.50 vl(n)=1.00
n= 1 k= 2 m= 91 gm1=.0428
gm2=.0428 rds1=179.83 rds2=179.83
vpg1=-.32 vpg2=-.32 cgs1=.42
vg1d1=-3.00 vg2d2=-3.00 cgd2=.23 .23
cgs2=.42 vg2d1(k)=-.50 vl(n)=1.00

n= 1 k= 2 m= 136 gm1= .0434
gm2= .0423 rds1=175.31 rds2=184.41
vpg1= -.29 vpg2= -.36 cgs1= .43
vg1d1= -2.71 vg2d2= -3.29 cgd2= .22 .24
cgs2= .42 vg2d1(k)= -.50 vl(n)= 1.00
n= 1 k= 2 m= 181 gm1= .0447
gm2= .0410 rds1=164.62 rds2=195.72
vpg1= -.20 vpg2= -.44 cgs1= .45
vg1d1= -2.00 vg2d2= -4.00 cgd2= .20 .27
cgs2= .40 vg2d1(k)= -.50 vl(n)= 1.00
n= 1 k= 2 m= 226 gm1= .0462
gm2= .0399 rds1=154.24 rds2=207.38
vpg1= -.11 vpg2= -.51 cgs1= .47
vg1d1= -1.29 vg2d2= -4.71 cgd2= .19 .31
cgs2= .39 vg2d1(k)= -.50 vl(n)= 1.00
n= 1 k= 2 m= 271 gm1= .0469
gm2= .0394 rds1=150.03 rds2=212.33
vpg1= -.07 vpg2= -.54 cgs1= .48
vg1d1= -1.00 vg2d2= -5.00 cgd2= .19 .33
cgs2= .39 vg2d1(k)= -.50 vl(n)= 1.00
n= 1 k= 2 m= 316 gm1= .0462
gm2= .0399 rds1=154.20 rds2=207.43
vpg1= -.11 vpg2= -.51 cgs1= .47
vg1d1= -1.29 vg2d2= -4.71 cgd2= .19 .31
cgs2= .39 vg2d1(k)= -.50 vl(n)= 1.00
n= 1 k= 2 m= 361 gm1= .0447
gm2= .0410 rds1=164.54 rds2=195.79
vpg1= -.20 vpg2= -.44 cgs1= .45
vg1d1= -2.00 vg2d2= -4.00 cgd2= .20 .27
cgs2= .40 vg2d1(k)= -.50 vl(n)= 1.00
n= 1 k= 3 m= 1 gm1= .0438
gm2= .0419 rds1=172.13 rds2=187.70
vpg1= -.27 vpg2= -.38 cgs1= .43
vg1d1= -3.00 vg2d2= -4.00 cgd2= .20 .23
cgs2= .41 vg2d1(k)= -1.00 vl(n)= 1.00
n= 1 k= 3 m= 46 gm1= .0424
gm2= .0432 rds1=183.07 rds2=176.62
vpg1= -.35 vpg2= -.30 cgs1= .42
vg1d1= -3.71 vg2d2= -3.29 cgd2= .22 .21
cgs2= .43 vg2d1(k)= -1.00 vl(n)= 1.00
n= 1 k= 3 m= 91 gm1= .0419
gm2= .0438 rds1=187.70 rds2=172.13
vpg1= -.38 vpg2= -.27 cgs1= .41
vg1d1= -4.00 vg2d2= -3.00 cgd2= .23 .20
cgs2= .43 vg2d1(k)= -1.00 vl(n)= 1.00
n= 1 k= 3 m= 136 gm1= .0424
gm2= .0432 rds1=183.08 rds2=176.61
vpg1= -.35 vpg2= -.30 cgs1= .42
vg1d1= -3.71 vg2d2= -3.29 cgd2= .22 .21
cgs2= .43 vg2d1(k)= -1.00 vl(n)= 1.00
n= 1 k= 3 m= 181 gm1= .0437
gm2= .0419 rds1=172.15 rds2=187.68
vpg1= -.27 vpg2= -.38 cgs1= .43
vg1d1= -3.00 vg2d2= -4.00 cgd2= .20 .23
cgs2= .41 vg2d1(k)= -1.00 vl(n)= 1.00
n= 1 k= 4 m= 181 gm1= .0428
gm2= .0428 rds1=179.85 rds2=179.81
vpg1= -.32 vpg2= -.32 cgs1= .42
vg1d1= -4.00 vg2d2= -4.00 cgd2= .20 .20
cgs2= .42 vg2d1(k)= -1.50 vl(n)= 1.00
n= 1 k= 4 m= 226 gm1= .0442

gm2= .0415 rds1=169.01 rds2=190.99
vpg1= -.24 vpg2= -.40 cgs1= .44
vg1d1= -3.29 vg2d2= -4.71 cgd2= .19 .22
cgs2= .41 vg2d1(k)= -1.50 vl(n)= 1.00
n= 1 k= 4 m= 271 gm1= .0447
gm2= .0410 rds1=164.59 rds2=195.74
vpg1= -.20 vpg2= -.44 cgs1= .45
vg1d1= -3.00 vg2d2= -5.00 cgd2= .19 .23
cgs2= .40 vg2d1(k)= -1.50 vl(n)= 1.00
n= 1 k= 4 m= 316 gm1= .0442
gm2= .0415 rds1=168.96 rds2=191.04
vpg1= -.24 vpg2= -.40 cgs1= .44
vg1d1= -3.29 vg2d2= -4.71 cgd2= .19 .22
cgs2= .41 vg2d1(k)= -1.50 vl(n)= 1.00
n= 1 k= 4 m= 361 gm1= .0428
gm2= .0428 rds1=179.78 rds2=179.88
vpg1= -.32 vpg2= -.33 cgs1= .42
vg1d1= -4.00 vg2d2= -4.00 cgd2= .20 .20
cgs2= .42 vg2d1(k)= -1.50 vl(n)= 1.00
cgs2= .46 vg2d1(k)= -1.50 vl(n)= 2.00
n= 2 k= 4 m= 91 gm1= .0394
gm2= .0469 rds1=212.33 rds2=150.03
vpg1= -.54 vpg2= -.07 cgs1= .39
vg1d1= -6.00 vg2d2= -2.00 cgd2= .27 .17
cgs2= .48 vg2d1(k)= -1.50 vl(n)= 2.00
n= 2 k= 4 m= 136 gm1= .0403
gm2= .0456 rds1=202.56 rds2=158.45
vpg1= -.48 vpg2= -.15 cgs1= .40
vg1d1= -5.42 vg2d2= -2.58 cgd2= .24 .18
cgs2= .46 vg2d1(k)= -1.50 vl(n)= 2.00
n= 2 k= 4 m= 181 gm1= .0428
gm2= .0428 rds1=179.88 rds2=179.78
vpg1= -.33 vpg2= -.32 cgs1= .42
vg1d1= -4.00 vg2d2= -4.00 cgd2= .20 .20
cgs2= .42 vg2d1(k)= -1.50 vl(n)= 2.00
n= 2 k= 4 m= 226 gm1= .0456
gm2= .0403 rds1=158.52 rds2=202.48
vpg1= -.15 vpg2= -.48 cgs1= .46
vg1d1= -2.59 vg2d2= -5.41 cgd2= .18 .24
cgs2= .40 vg2d1(k)= -1.50 vl(n)= 2.00
n= 2 k= 4 m= 271 gm1= .0469
gm2= .0394 rds1=150.03 rds2=212.33
vpg1= -.07 vpg2= -.54 cgs1= .48
vg1d1= -2.00 vg2d2= -6.00 cgd2= .17 .27
cgs2= .39 vg2d1(k)= -1.50 vl(n)= 2.00
n= 2 k= 4 m= 316 gm1= .0456
gm2= .0403 rds1=158.42 rds2=202.60
vpg1= -.15 vpg2= -.48 cgs1= .46
vg1d1= -2.58 vg2d2= -5.42 cgd2= .18 .24
cgs2= .40 vg2d1(k)= -1.50 vl(n)= 2.00
n= 2 k= 4 m= 361 gm1= .0428
gm2= .0428 rds1=179.73 rds2=179.93
vpg1= -.32 vpg2= -.33 cgs1= .42
vg1d1= -3.99 vg2d2= -4.01 cgd2= .20 .20
cgs2= .42 vg2d1(k)= -1.50 vl(n)= 2.00
n= 3 k= 1 m= 1 gm1= .0458
gm2= .0402 rds1=157.23 rds2=203.95
vpg1= -.14 vpg2= -.49 cgs1= .46
vg1d1= -1.00 vg2d2= -4.00 cgd2= .20 .33
cgs2= .39 vg2d1(k)= .00 vl(n)= 3.00
n= 3 k= 1 m= 46 gm1= .0417

gm2= .0440 rds1=189.62 rds2=170.30
vpg1= -.39 vpg2= -.25 cgs1= .41
vg1d1= -3.12 vg2d2= -1.88 cgd2= .27 .23
cgs2= .44 vg2d1(k)= .00 vl(n)= 3.00
n= 3 k= 1 m= 91 gm1= .0402
gm2= .0458 rds1=203.95 rds2=157.23
vpg1= -.49 vpg2= -.14 cgs1= .39
vg1d1= -4.00 vg2d2= -1.00 cgd2= .33 .20
cgs2= .46 vg2d1(k)= .00 vl(n)= 3.00
n= 3 k= 1 m= 136 gm1= .0417
gm2= .0440 rds1=189.68 rds2=170.24
vpg1= -.40 vpg2= -.25 cgs1= .41
vg1d1= -3.12 vg2d2= -1.88 cgd2= .27 .23
cgs2= .44 vg2d1(k)= .00 vl(n)= 3.00
n= 3 k= 1 m= 181 gm1= .0458
gm2= .0402 rds1=157.30 rds2=203.87
vpg1= -.14 vpg2= -.49 cgs1= .46
vg1d1= -1.00 vg2d2= -4.00 cgd2= .20 .33
cgs2= .39 vg2d1(k)= .00 vl(n)= 3.00
n= 3 k= 1 m= 226 gm1= .0508
gm2= .0370 rds1=127.91 rds2=240.58
vpg1= .17 vpg2= -.69 cgs1= .56
vg1d1= 1.12 vg2d2= -6.12 cgd2= .17 .33
cgs2= .37 vg2d1(k)= .00 vl(n)= 3.00
n= 3 k= 1 m= 271 gm1= .0532
gm2= .0358 rds1=116.57 rds2=256.75
vpg1= .32 vpg2= -.76 cgs1= .65
vg1d1= 2.00 vg2d2= -7.00 cgd2= .16 .33
cgs2= .36 vg2d1(k)= .00 vl(n)= 3.00
n= 3 k= 1 m= 316 gm1= .0508
gm2= .0370 rds1=127.77 rds2=240.76
vpg1= .17 vpg2= -.69 cgs1= .57
vg1d1= 1.13 vg2d2= -6.13 cgd2= .17 .33
cgs2= .37 vg2d1(k)= .00 vl(n)= 3.00
n= 3 k= 1 m= 361 gm1= .0458
gm2= .0402 rds1=157.09 rds2=204.11
vpg1= -.14 vpg2= -.49 cgs1= .46
vg1d1= -.99 vg2d2= -4.01 cgd2= .20 .33
cgs2= .39 vg2d1(k)= .00 vl(n)= 3.00
n= 3 k= 2 m= 1 gm1= .0447
gm2= .0410 rds1=164.59 rds2=195.74
vpg1= -.20 vpg2= -.44 cgs1= .45
vg1d1= -2.00 vg2d2= -4.00 cgd2= .20 .27
cgs2= .40 vg2d1(k)= -.50 vl(n)= 3.00
n= 3 k= 2 m= 46 gm1= .0408
gm2= .0450 rds1=197.70 rds2=162.80
vpg1= -.45 vpg2= -.19 cgs1= .40
vg1d1= -4.12 vg2d2= -1.88 cgd2= .27 .20
cgs2= .45 vg2d1(k)= -.50 vl(n)= 3.00
n= 3 k= 2 m= 91 gm1= .0394
gm2= .0469 rds1=212.33 rds2=150.03
vpg1= -.54 vpg2= -.07 cgs1= .39
vg1d1= -5.00 vg2d2= -1.00 cgd2= .33 .19
cgs2= .48 vg2d1(k)= -.50 vl(n)= 3.00
n= 3 k= 2 m= 136 gm1= .0408
gm2= .0450 rds1=197.76 rds2=162.75
vpg1= -.45 vpg2= -.19 cgs1= .40
vg1d1= -4.12 vg2d2= -1.88 cgd2= .27 .20
cgs2= .45 vg2d1(k)= -.50 vl(n)= 3.00
n= 3 k= 2 m= 181 gm1= .0447
gm2= .0410 rds1=164.66 rds2=195.66

vpg1= -.20 vpg2= -.44 cgs1= .45
vg1d1= -2.00 vg2d2= -4.00 cgd2= .20 .27
cgs2= .40 vg2d1(k)= -.50 vl(n)= 3.00
n= 3 k= 2 m= 226 gm1= .0495
gm2= .0377 rds1=134.56 rds2=231.66
vpg1= .09 vpg2= -.64 cgs1= .53
vg1d1= .12 vg2d2= -6.12 cgd2= .17 .54
cgs2= .37 vg2d1(k)= -.50 vl(n)= 3.00
n= 3 k= 2 m= 271 gm1= .0518
gm2= .0365 rds1=122.93 rds2=247.53
vpg1= .24 vpg2= -.72 cgs1= .60
vg1d1= 1.00 vg2d2= -7.00 cgd2= .16 .54
cgs2= .36 vg2d1(k)= -.50 vl(n)= 3.00
n= 3 k= 2 m= 316 gm1= .0495
gm2= .0377 rds1=134.42 rds2=231.83
vpg1= .09 vpg2= -.64 cgs1= .53
n= 3 k= 4 m= 136 gm1= .0392
gm2= .0471 rds1=214.43 rds2=148.27
vpg1= -.55 vpg2= -.05 cgs1= .38
vg1d1= -6.12 vg2d2= -1.88 cgd2= .27 .17
cgs2= .48 vg2d1(k)= -1.50 vl(n)= 3.00
n= 3 k= 4 m= 181 gm1= .0428
gm2= .0428 rds1=179.90 rds2=179.76
vpg1= -.33 vpg2= -.32 cgs1= .42
vg1d1= -4.00 vg2d2= -4.00 cgd2= .20 .20
cgs2= .42 vg2d1(k)= -1.50 vl(n)= 3.00
n= 3 k= 4 m= 226 gm1= .0471
gm2= .0392 rds1=148.37 rds2=214.32
vpg1= -.05 vpg2= -.55 cgs1= .48
vg1d1= -1.88 vg2d2= -6.12 cgd2= .17 .27
cgs2= .38 vg2d1(k)= -1.50 vl(n)= 3.00
n= 3 k= 4 m= 271 gm1= .0492
gm2= .0379 rds1=136.14 rds2=229.59
vpg1= .07 vpg2= -.63 cgs1= .53
vg1d1= -1.00 vg2d2= -7.00 cgd2= .16 .33
cgs2= .37 vg2d1(k)= -1.50 vl(n)= 3.00
n= 3 k= 4 m= 316 gm1= .0471
gm2= .0392 rds1=148.22 rds2=214.49
vpg1= -.05 vpg2= -.55 cgs1= .48
vg1d1= -1.87 vg2d2= -6.13 cgd2= .17 .27
cgs2= .38 vg2d1(k)= -1.50 vl(n)= 3.00
n= 3 k= 4 m= 361 gm1= .0428
gm2= .0428 rds1=179.68 rds2=179.98
vpg1= -.32 vpg2= -.33 cgs1= .42
vg1d1= -3.99 vg2d2= -4.01 cgd2= .20 .20
cgs2= .42 vg2d1(k)= -1.50 vl(n)= 3.00

THE OUTPUT OF NL FOR PROGRAM

v2(i3,m)= (.0000000,.0000000) i3=1
v2(i3,m)= (.0000000,.0000000) i3=2
v2(i3,m)= (.0000000,.0000000) i3=3
v2(i3,m)= (.0000000,.0000000) i3=4
v2(i3,m)= (5.000000E-001,.000)i3=5
v2(i3,m)= (-3.5000000,.0000000)i3=6
v2(i3,m)= (5.000000E-001,.0000)i3=7
v2(i3,m)= (.0000000,.0000000) i3=8
v2(i3,m)= (.0000000,.0000000) i3=9
v2(i3,m)= (.0000000,.0000000) i3=10
v2(i3,m)= (.0000000,.0000000) i3=11
v1(n6,m)= (.0000000,.0000000) n6=1
v1(n6,m)= (.0000000,.0000000) n6=2
v1(n6,m)= (.0000000,.0000000) n6=3
v1(n6,m)= (.0000000,.0000000) n6=4
v1(n6,m)= (.0000000,.0000000) n6=5
v1(n6,m)= (-2.0000000,.0000000)n6=6
v1(n6,m)= (.0000000,.0000000) n6=7
v1(n6,m)= (.0000000,.0000000) n6=8
v1(n6,m)= (.0000000,.0000000) n6=9
v1(n6,m)= (.0000000,.0000000) n6=10
v1(n6,m)= (.0000000,.0000000) n6=11
k=1
v11(nc,k+1)= (-4.455097E-006,8.850168E-007)
v11(nc,k+1)= (-5.520520E-005,1.341532E-005)
v11(nc,k+1)= (-7.522283E-004,2.387687E-004)
v11(nc,k+1)= (-3.827024E-002,-5.263928E-002)
v11(nc,k+1)= (-3.058815E-002,1.1205070)
v11(nc,k+1)= (-2.0000000,.0000000)
v11(nc,k+1)= (-3.058815E-002,-1.1205070)
v11(nc,k+1)= (-3.827024E-002,5.263928E-002)
v11(nc,k+1)= (-7.522283E-004,-2.387687E-004)
v11(nc,k+1)= (-5.520520E-005,-1.341532E-005)
v11(nc,k+1)= (-4.455097E-006,-8.850168E-007)
v22(nc2,k+1)= (-2.563900E-005,3.031064E-005)
v22(nc2,k+1)= (-3.143534E-004,3.297422E-004)
v22(nc2,k+1)= (-4.161178E-003,4.002476E-003)
v22(nc2,k+1)= (-3.508301E-001,-2.328017E-001)
v22(nc2,k+1)= (3.1600960,4.7577560)
v22(nc2,k+1)= (-18.6229100,.0000000)
v22(nc2,k+1)= (3.1600960,-4.7577560)
v22(nc2,k+1)= (-3.508301E-001,2.328017E-001)
v22(nc2,k+1)= (-4.161178E-003,-4.002476E-003)
v22(nc2,k+1)= (-3.143534E-004,-3.297422E-004)
v22(nc2,k+1)= (-2.563900E-005,-3.031064E-005)
fu1(i15,k)= (-4.455097E-006,8.850168E-007)
fu1(i15,k)= (-5.520520E-005,1.341532E-005)
fu1(i15,k)= (-7.522283E-004,2.387687E-004)
fu1(i15,k)= (-3.827024E-002,-5.263928E-002)
fu1(i15,k)= (-3.058815E-002,1.1205070)
fu1(i15,k)= (-2.0000000,.0000000)
fu1(i15,k)= (-3.058815E-002,-1.1205070)
fu1(i15,k)= (-3.827024E-002,5.263928E-002)
fu1(i15,k)= (-7.522283E-004,-2.387687E-004)
fu1(i15,k)= (-5.520520E-005,-1.341532E-005)
fu1(i15,k)= (-4.455097E-006,-8.850168E-007)
k=9
v11(nc,k+1)= (5.514198E-007,1.500965E-006)
v11(nc,k+1)= (4.383811E-006,-5.167405E-005)
v11(nc,k+1)= (-1.363936E-003,1.151753E-003)

v11(nc,k+1)= (-1.335640E-003, 2.952672E-002)
v11(nc,k+1)= (3.618348E-001, 2.740419E-001)
v11(nc,k+1)= (-2.0000000, .0000000)
v11(nc,k+1)= (3.618380E-001, -2.740449E-001)
v11(nc,k+1)= (-1.335291E-003, -2.952811E-002)
v11(nc,k+1)= (-1.363875E-003, -1.151880E-003)
v11(nc,k+1)= (4.378474E-006, 5.167407E-005)
v11(nc,k+1)= (5.504500E-007, -1.500583E-006)
v22(nc2,k+1)= (1.155841E-005, 7.783340E-006)
v22(nc2,k+1)= (-2.162895E-004, -3.501831E-004)
v22(nc2,k+1)= (-5.719883E-003, 1.225551E-002)
v22(nc2,k+1)= (9.240143E-003, 2.025092E-001)
v22(nc2,k+1)= (1.9026590, 2.277649E-001)
v22(nc2,k+1)= (-4.2031560, 5.709759E-006)
v22(nc2,k+1)= (1.9026850, -2.277839E-001)
v22(nc2,k+1)= (9.245785E-003, -2.025181E-001)
v22(nc2,k+1)= (-5.719846E-003, -1.225603E-002)
v22(nc2,k+1)= (-2.162776E-004, 3.501620E-004)
v22(nc2,k+1)= (1.155710E-005, -7.785216E-006)
v11(117,k+1)= (3.881269E-009, -1.367766E-009)
v11(117,k+1)= (7.389326E-008, 1.530752E-007)
v11(117,k+1)= (-3.968831E-006, -2.041808E-006)
v11(117,k+1)= (-1.027848E-003, 2.897680E-004)
v11(117,k+1)= (-1.690102E-002, -2.180830E-002)
v11(117,k+1)= (-2.0000000, .0000000)
v11(117,k+1)= (-1.690122E-002, 2.180919E-002)
v11(117,k+1)= (-1.027775E-003, -2.896264E-004)
v11(117,k+1)= (-3.909227E-006, 2.025976E-006)
v11(117,k+1)= (7.014341E-008, -1.531153E-007)
v11(117,k+1)= (3.405205E-009, 1.370836E-009)
v22(km,k+1)= (-7.177368E-008, -2.660281E-007)
v22(km,k+1)= (2.010012E-006, 2.692570E-006)
v22(km,k+1)= (-2.979534E-005, -2.983958E-006)
v22(km,k+1)= (-9.833798E-003, 1.542404E-003)
v22(km,k+1)= (7.744372E-002, 5.813803E-002)
v22(km,k+1)= (-4.3099770, 1.652804E-005)
v22(km,k+1)= (7.744372E-002, -5.813831E-002)
v22(km,k+1)= (-9.833522E-003, -1.541764E-003)
v22(km,k+1)= (-2.979720E-005, 2.983026E-006)
v22(km,k+1)= (2.010231E-006, -2.688990E-006)
v22(km,k+1)= (-7.167273E-008, 2.659044E-007)

k=10

v11(nc,k+1)= (-1.765481E-007, 1.656974E-008)
v11(nc,k+1)= (-1.320329E-005, -6.524463E-006)
v11(nc,k+1)= (3.881221E-005, 3.079399E-004)
v11(nc,k+1)= (-6.289873E-004, -1.824403E-002)
v11(nc,k+1)= (-1.602743E-001, 2.021335E-001)
v11(nc,k+1)= (-2.0000000, .0000000)
v11(nc,k+1)= (-1.602774E-001, -2.021306E-001)
v11(nc,k+1)= (-6.275984E-004, 1.824372E-002)
v11(nc,k+1)= (3.886422E-005, -3.080018E-004)
v11(nc,k+1)= (-1.319958E-005, 6.512798E-006)
v11(nc,k+1)= (-1.772675E-007, -1.606549E-008)
v22(nc2,k+1)= (-9.277728E-007, 1.046657E-006)
v22(nc2,k+1)= (-1.210070E-004, 1.379789E-005)
v22(nc2,k+1)= (1.244771E-003, 1.888121E-003)
v22(nc2,k+1)= (-3.358331E-002, -1.178039E-001)
v22(nc2,k+1)= (5.485002E-001, 1.4787030)
v22(nc2,k+1)= (-3.7689300, 3.306723E-004)
v22(nc2,k+1)= (5.484837E-001, -1.4787090)
v22(nc2,k+1)= (-3.357470E-002, 1.178033E-001)

v22(nc2,k+1)= (1.244534E-003,-1.888225E-003)
v22(nc2,k+1)= (-1.208741E-004,-1.385607E-005)
v22(nc2,k+1)= (-9.281242E-007,-1.046276E-006)
v11(117,k+1)= (3.818911E-009,-1.385018E-009)
v11(117,k+1)= (8.191728E-008,1.390126E-007)
v11(117,k+1)= (-4.265214E-006,-2.042245E-006)
v11(117,k+1)= (7.455259E-004,-2.757665E-004)
v11(117,k+1)= (-2.115755E-001,6.130421E-001)
v11(117,k+1)= (-2.0000000,.0000000)
v11(117,k+1)= (2.115649E-002,-6.130445E-001)
v11(117,k+1)= (7.455227E-004,2.757628E-004)
v11(117,k+1)= (-4.205576E-006,2.026383E-006)
v11(117,k+1)= (7.814106E-008,-1.391049E-007)
v11(117,k+1)= (3.342961E-009,1.388193E-009)
v22(km,k+1)= (-7.261644E-008,-2.610419E-007)
v22(km,k+1)= (2.089611E-006,2.306248E-006)
v22(km,k+1)= (-3.146939E-005,-2.323184E-006)
v22(km,k+1)= (1.239318E-003,-6.172433E-004)
v22(km,k+1)= (4.037076E-001,3.933918E-001)
v22(km,k+1)= (-3.8742280,8.692441E-007)
v22(km,k+1)= (4.037072E-001,-3.933918E-001)
v22(km,k+1)= (1.239173E-003,6.172061E-004)
v22(km,k+1)= (-3.147149E-005,2.322486E-006)
v22(km,k+1)= (2.089946E-006,-2.304517E-006)
v22(km,k+1)= (-7.251066E-008,2.609179E-007)

k=11

v11(nc,k+1)= (6.417624E-007,-9.656231E-008)
v11(nc,k+1)= (-1.174290E-005,7.504756E-006)
v11(nc,k+1)= (2.699122E-004,-1.640738E-004)
v11(nc,k+1)= (-1.094035E-002,-4.498118E-003)
v11(nc,k+1)= (-2.333594E-001,5.973956E-001)
v11(nc,k+1)= (-2.0000000,.0000000)
v11(nc,k+1)= (-2.333573E-001,-5.973977E-001)
v11(nc,k+1)= (-1.094024E-002,4.498215E-003)
v11(nc,k+1)= (2.699833E-004,1.640036E-004)
v11(nc,k+1)= (-1.174695E-005,-7.502089E-006)
v11(nc,k+1)= (6.408122E-007,9.711827E-008)
v22(nc2,k+1)= (4.038654E-006,-4.227445E-006)
v22(nc2,k+1)= (-4.835275E-005,1.002090E-004)
v22(nc2,k+1)= (1.368439E-003,-1.887999E-003)
v22(nc2,k+1)= (-8.100894E-002,3.474305E-003)
v22(nc2,k+1)= (5.175559E-001,3.1091380E-001)
v22(nc2,k+1)= (-3.3851570,2.443060E-006)
v22(nc2,k+1)= (5.175550E-001,-3.1091400E-001)
v22(nc2,k+1)= (-8.100843E-002,-3.473282E-003)
v22(nc2,k+1)= (1.368349E-003,1.887899E-003)
v22(nc2,k+1)= (-4.833781E-005,-1.002084E-004)
v22(nc2,k+1)= (4.036457E-006,4.227154E-006)
v11(117,k+1)= (3.867683E-009,-1.372072E-009)
v11(117,k+1)= (6.597384E-008,1.379826E-007)
v11(117,k+1)= (-4.115282E-006,-1.943437E-006)
v11(117,k+1)= (-1.464970E-005,-1.248749E-003)
v11(117,k+1)= (-2.1161203E-001,5.133925E-001)
v11(117,k+1)= (-2.0000000,.0000000)
v11(117,k+1)= (-2.116605E-001,-5.133961E-001)
v11(117,k+1)= (-1.458079E-005,1.248665E-003)
v11(117,k+1)= (-4.055677E-006,1.927576E-006)
v11(117,k+1)= (6.224036E-008,-1.380795E-007)
v11(117,k+1)= (3.391676E-009,1.375213E-009)
v22(km,k+1)= (-7.176277E-008,-2.649349E-007)
v22(km,k+1)= (1.712968E-006,2.380810E-006)

v22(km,k+1)= (-3.038009E-005,-2.068700E-006)
v22(km,k+1)= (-3.063105E-003,-5.884849E-003)
v22(km,k+1)= (5.600337E-001,3.242393E-001)
v22(km,k+1)= (-3.5267110,1.615459E-006)
v22(km,k+1)= (5.600307E-001,-3.242384E-001)
v22(km,k+1)= (-3.062934E-003,5.884494E-003)
v22(km,k+1)= (-3.038242E-005,2.068002E-006)
v22(km,k+1)= (1.714572E-006,-2.378576E-006)
v22(km,k+1)= (-7.166227E-008,2.648117E-007)
k=12
v11(nc,k+1)= (6.399412E-007,1.071462E-006)
v11(nc,k+1)= (7.273284E-006,-1.355215E-005)
v11(nc,k+1)= (-3.174525E-004,-2.830937E-004)
v11(nc,k+1)= (5.081722E-003,7.259468E-003)
v11(nc,k+1)= (-2.4219323E-001,4.929649E-001)
v11(nc,k+1)= (-2.0000000,.0000000)
v11(nc,k+1)= (-2.4119327E-001,-4.929655E-001)
v11(nc,k+1)= (5.081398E-003,-7.259313E-003)
v11(nc,k+1)= (-3.173568E-004,2.830050E-004)
v11(nc,k+1)= (7.260930E-006,1.355017E-005)
v11(nc,k+1)= (6.390954E-007,-1.070825E-006)
v22(nc2,k+1)= (1.034244E-005,3.774506E-006)
v22(nc2,k+1)= (-1.173590E-005,-1.258623E-004)
v22(nc2,k+1)= (-2.851560E-003,-8.810053E-004)
v22(nc2,k+1)= (5.224088E-002,4.579705E-002)
v22(nc2,k+1)= (5.308871E-001,3.881749E-001)
v22(nc2,k+1)= (-3.7154230,2.938838E-006)
v22(nc2,k+1)= (5.309256E-001,3.881736E-001)
v22(nc2,k+1)= (5.223755E-002,-4.579594E-002)
v22(nc2,k+1)= (-2.851430E-003,8.808585E-004)
v22(nc2,k+1)= (-1.175550E-005,1.257971E-004)
v22(nc2,k+1)= (1.034052E-005,-3.773890E-006)
v11(117,k+1)= (3.815842E-009,-1.357307E-009)
v11(117,k+1)= (7.453309E-008,1.363733E-007)
v11(117,k+1)= (-4.170870E-006,-2.056593E-006)
v11(117,k+1)= (1.466088E-004,-6.902125E-004)
v11(117,k+1)= (-2.215159E-001,5.361161E-001)
v11(117,k+1)= (-2.0000000,.0000000)
v11(117,k+1)= (-2.215103E-001,-5.361231E-001)
v11(117,k+1)= (1.466502E-004,6.901845E-004)
v11(117,k+1)= (-4.111265E-006,2.040702E-006)
v11(117,k+1)= (7.077551E-008,-1.364706E-007)
v11(117,k+1)= (3.339892E-009,1.360490E-009)
v22(km,k+1)= (-7.039671E-008,-2.607846E-007)
v22(km,k+1)= (1.906367E-006,2.284491E-006)
v22(km,k+1)= (-3.092922E-005,-2.596527E-006)
v22(km,k+1)= (-2.131891E-003,-2.472617E-003)
v22(km,k+1)= (5.393307E-001,3.469684E-001)
v22(km,k+1)= (-3.2824990,4.185475E-006)
v22(km,k+1)= (5.393314E-001,-3.469702E-001)
v22(km,k+1)= (-2.131853E-003,2.472531E-003)
v22(km,k+1)= (-3.093132E-005,2.595829E-006)
v22(km,k+1)= (1.907307E-006,-2.282701E-006)
v22(km,k+1)= (-7.029212E-008,2.606646E-007)

*****THE OUTPUT OF ELT.FOR PROGRAM*****
v1(m4)= (.0000000,.0000000)
v1(m4)= (.0000000,.0000000)
v1(m4)= (.0000000,.0000000)
v1(m4)= (.0000000,.0000000)
v1(m4)= (-3.600000E-001,-1.380000E-001)
v1(m4)= (-2.000000,.0000000)
v1(m4)= (-3.600000E-001,1.380000E-001)
v1(m4)= (.0000000,.0000000)
v1(m4)= (.0000000,.0000000)
v1(m4)= (.0000000,.0000000)
v1(m4)= (.0000000,.0000000)
v2(m5)= (.0000000,.0000000)
v2(m5)= (.0000000,.0000000)
v2(m5)= (.0000000,.0000000)
v2(m5)= (.0000000,.0000000)
v2(m5)= (5.400000E-001,-6.200000E-001)
v2(m5)= (-2.500000,.0000000)
v2(m5)= (5.400000E-001,6.200000E-001)
v2(m5)= (.0000000,.0000000)
v2(m5)= (.0000000,.0000000)
v2(m5)= (.0000000,.0000000)
v2(m5)= (.0000000,.0000000)
c2(i3)= (-8.970499E-006,3.006673E-004)
c2(i3)= (-4.777312E-005,2.644584E-004)
c2(i3)= (-6.476045E-005,2.268404E-004)
c2(i3)= (-2.777576E-005,2.353787E-004)
c2(i3)= (1.228601E-005,5.124211E-004)
c2(i3)= (-8.092357E-004,1.540869E-003)
c2(i3)= (-6.546661E-003,1.922071E-003)
c2(i3)= (-2.474931E-002,-1.596844E-002)
c2(i3)= (-1.890698E-002,-1.350269E-002)
c2(i3)= (4.615439E-001,-5.301093E-001)
c2(i3)= (5.405102E-001,.0000000)
c2(i3)= (4.615439E-001,5.301093E-002)
c2(i3)= (-1.890698E-002,1.350269E-001)
c2(i3)= (-2.474931E-002,1.596844E-002)
c2(i3)= (-6.546661E-003,-1.922071E-003)
c2(i3)= (-8.092357E-004,-1.540869E-003)
c2(i3)= (1.228601E-005,-5.124211E-004)
c2(i3)= (-2.777576E-005,-2.353787E-004)
c2(i3)= (-6.476045E-005,-2.268404E-004)
c2(i3)= (-4.777312E-005,-2.644584E-004)
c2(i3)= (-8.970499E-006,-3.006673E-004)
ic2(i8)= (3.320641E-004,1.402388E-004)
ic2(i8)= (4.409976E-004,1.509219E-003)
ic2(i8)= (-4.013813E-003,6.154771E-003)
ic2(i8)= (-3.784296E-002,5.241919E-003)
ic2(i8)= (-1.728308E-002,-1.506743E-002)
ic2(i8)= (1.404769E-005,.0000000)
ic2(i8)= (-1.728308E-002,1.506743E-002)
ic2(i8)= (-3.784296E-002,-5.241919E-003)
ic2(i8)= (-4.013813E-003,-6.154771E-003)
ic2(i8)= (4.409976E-004,-1.509219E-003)
ic2(i8)= (3.320641E-004,-1.402388E-004)
im2(i10)= (-1.829863E-007,-1.600342E-006)
im2(i10)= (3.311038E-007,-1.321137E-006)
im2(i10)= (6.535649E-007,-1.001060E-006)
im2(i10)= (-1.545846E-003,-1.116100E-002)
im2(i10)= (-1.799954E-002,2.066694E-002)
im2(i10)= (1.701076E-003,.0000000)

im2(i10)= (-1.799954E-002,-2.066694E-002)
im2(i10)= (-1.545846E-003,1.116100E-002)
im2(i10)= (6.535649E-007,1.001060E-006)
im2(i10)= (3.311038E-007,1.321137E-006)
im2(i10)= (-1.829863E-007,1.600342E-006)
GM2(ki)= (-1.358986E-007,1.529683E-006)
GM2(ki)= (-4.780293E-007,1.188517E-006)
GM2(ki)= (-6.977469E-007,8.717179E-007)
GM2(ki)= (-8.429587E-007,5.733967E-007)
GM2(ki)= (8.999342E-003,-1.033335E-002)
GM2(ki)= (8.332628E-003,.0000000)
GM2(ki)= (8.999342E-003,1.033335E-002)
GM2(ki)= (-8.429587E-007,-5.733967E-007)
GM2(ki)= (-6.977469E-007,-8.717179E-007)
GM2(ki)= (-4.780293E-007,-1.188517E-006)
GM2(ki)= (-1.358986E-007,-1.529683E-006)
IM1= (1.895428E-007,-7.659518E-007)
IM1= (3.141165E-007,-5.885959E-007)
IM1= (4.012138E-007,-4.310906E-007)
IM1= (1.843115E-003,1.655765E-003)
IM1= (6.000671E-003,2.299927E-003)
IM1= (-2.837886E-002,.0000000)
IM1= (6.000671E-003,-2.299927E-003)
IM1= (1.843115E-003,-1.655765E-003)
IM1= (4.012138E-007,4.310906E-007)
IM1= (3.141165E-007,5.885959E-007)
IM1= (1.895428E-007,7.659518E-007)
GM1= (-7.845462E-008,2.828558E-007)
GM1= (-1.239777E-007,2.187863E-007)
GM1= (-1.549535E-007,1.605600E-007)
GM1= (-1.750328E-007,1.063943E-007)
GM1= (-6.000366E-003,-2.300016E-003)
GM1= (1.666697E-002,.0000000)
GM1= (-6.000366E-003,2.300016E-003)
GM1= (-1.750328E-007,-1.063943E-007)
GM1= (-1.549535E-007,-1.605600E-007)
GM1= (-1.239777E-007,-2.187863E-007)
GM1= (-7.845462E-008,-2.828558E-007)
ZG(J5)= (50.0000000,19.2920800)
ZG(J5)= (50.0000000,24.1151000)
ZG(J5)= (50.0000000,32.1534600)
ZG(J5)= (50.0000000,48.2301900)
ZG(J5)= (50.0000000,96.4603800)
ZG(J5)= (.0000000,.0000000)
ZG(J5)= (50.0000000,-96.4603800)
ZG(J5)= (50.0000000,-48.2301900)
ZG(J5)= (50.0000000,-32.1534600)
ZG(J5)= (50.0000000,-24.1151000)
ZG(J5)= (50.0000000,-19.2920800)

****the output of sms.for program****

v2s(i1)= (7.0000E-004,-4.0000E-004) i1=1
v2s(i1)= (-1.0000E-003,1.0000E-003) i1=2
v2s(i1)= (6.7000E-004,-4.6000E-004) i1=3
v2l(j1)= (7.0000E-004,-4.0000E-004) j1=1
v2l(j1)= (-1.0000E-003,1.0000E-003) j1=2
v2l(j1)= (6.7000E-004,-4.6000E-004) j1=3
vlo(k1)= (3.000000E-001,.0000000) k1=1
vlo(k1)= (-1.0000000,.0000000) k1=2
vlo(k1)= (3.000000E-001,.0000000) k1=3
hn(i)= (-42.4261700,5.818709E-001) i=1
hn(i)= (35.7118900,6.310265E-001) i=2
hn(i)= (8.327312E-001,-2.955627E-003) i=3
hn(i)= (8.363441E-002,1.477814E-003) i=4
hn(i)= (35.7118900,6.310264E-001) i=5
hn(i)= (-63.8960000,4.1649780) i=6
hn(i)= (-7.007213E-001,-1.95089E-002) i=7
hn(i)= (-1.496393E-001,9.754046E-003) i=8
hz(j)= (-17.1770600,-39.4558900) j=1
hz(j)= (14.3796500,33.2677200) j=2
hz(j)= (9.326480E-001,-1.558207E-001) j=3
hz(j)= (3.367599E-002,7.791035E-002) j=4
hz(j)= (14.3796500,33.2677200) j=5
hz(j)= (-45.7268900,-27.5795000) j=6
hz(j)= (-7.858225E-001,1.291780E-001) j=7
hz(j)= (-1.070887E-001,-6.45889E-002) j=8
hp(k)= (-2.0936620,-18.9739600) k=1
hp(k)= (1.7414850,15.9824200) k=2
hp(k)= (9.918432E-001,-7.485911E-002) k=3
hp(k)= (4.078419E-003,3.742956E-002) k=4
hp(k)= (1.7414850,15.9824200) k=5
hp(k)= (-35.1370200,-13.2170800) k=6
hp(k)= (-8.354238E-001,6.190669E-002) k=7
hp(k)= (-8.228809E-002,-3.09534E-002) k=8
w(i4)= (1.0023260,1.436681E-001) i4=1
w(i4)= (-2.239846E-001,5.18227E-002) i4=2
w(i4)= (8.070803E-001,-1.35880E-001) i4=3
w(i4)= (-4.277574E-001,8.10704E-001) i4=4
w(i4)= (2.899844E-001,-7.60724E-001) i4=5
w(i4)= (2.3482540,16.2448000) i4=6
w(i4)= (1.4254670,16.4888900) i4=7
x(i5)= (-1.164442E-001,-1.12037E-001) i5=1
x(i5)= (1.06284E-001,-2.04117E-001) i5=2
x(i5)= (-5.83651E-001,-4.27559E-001) i5=3
x(i5)= (1.1814410,-6.415530E-001) i5=4
x(i5)= (3.509959E-001,6.331479E-001) i5=5
x(i5)= (-2.80673E-001,-5.22705E-001) i5=6
x(i5)= (1.1258620,-1.762876E-001) i5=7
y(i6)= (8.807388E-004,-1.07634E-001) i6=1
y(i6)= (3.518301E-001,-1.72556E-001) i6=2
y(i6)= (-5.000122E-001,2.146057E-001) i6=3
y(i6)= (1.2032940,-5.208696E-001) i6=4
y(i6)= (-6.880510E-002,5.331118E-001) i6=5
y(i6)= (-3.699307E-001,-4.53145E-002) i6=6
y(i6)= (1.1079780,-1.210009E-001) i6=7
z(i7)= (1.2246380,1.986153E-001) i7=1
z(i7)= (-1.600388E-001,3.755910E-001) i7=2
z(i7)= (1.0659410,1.296020E-002) i7=3
z(i7)= (1.326324E-001,1.9693520) i7=4
z(i7)= (-9.629891E-001,-4.58684E-001) i7=5
z(i7)= (1.3851150,-3.380157E-002) i7=6

$z(17) = (1.806440E-001, 2.8929410)$ 17=7
 $rid(m2) = (-7.254416E-004, -9.597019E-005)$
 $rid(m2) = (-7.558672E-004, 6.178369E-004)$
 $rid(m2) = (1.153930E-004, 2.664649E-004)$
 $ridl(m3) = (3.190971E-003, 3.427561E-003)$
 $ridl(m3) = (-3.516196E-003, 3.315000E-006)$
 $ridl(m3) = (3.190971E-003, -3.427561E-003)$

the output of roots.for program

vm=0.6 vg2s=-1. vg1s=-3.
v1(-)=-3.027902E-004 5.4774586611545E-004
v1(0)=-2.445992E-003 1.5808337308411E-003
v1(+) =2.267022E-003 -1.5382378175276E-003
v2(-)=7.037981E-004 -4.7722440223511E-004
v2(0)=-9.431413E-004 9.5135354932782E-004
v2(+) =6.788749E-004 -4.6998471369058E-004

vm=1. vg2s=-1. vg1s=-2.
v1(-)=1.034799E-003 1.4838357941733E-003
v1(0)=-1.839563E-003 7.2658734833433E-004
v1(+) =1.750501E-003 -6.4190642303031E-004
v2(-)=2.627621E-004 8.3315669037591E-004
v2(0)=3.118846E-004 -1.3690371638143E-003
v2(+) =1.229682E-003 -1.1133892317142E-003

vm=1.2 vg2s=-2.5 vg1s=-4.
v1(-)=3.190030E-003 -4.6690935807742E-004
v1(0)=2.941187E-004 -9.7911350305821E-004
v1(+) =-4.962147E-003 3.8544170715134E-004
v2(-)= 2.751364E-003 -1.0402598757015E-003
v2(0)=-3.484556E-004 -1.5934573346000E-003
v2(+) =-5.069612E-003 6.9650649735357E-004

vm=0.8 vg2s=-1.5 vg1s=-3.
v1(-)=-1.509933E-003 6.6988904264821E-004
v1(0)=1.328337E-003 -7.8439959105888E-004
v1(+) =7.719222E-006 1.0321715859388E-003
v2(-)=1.902613E-003 -1.5341939661654E-003
v2(0)=8.775928E-003 -4.8183218478357E-004
v2(+) =3.448912E-004 5.8557092550113E-003

BIOGRAPHY

A. Hakimi DARSINOOIEH was born in Rafsanjan, Iran on August 1, 1961. He graduated from the Shahid Ansari High School in Rafsanjan in 1979.

He received the B.Sc degree in 1986 from Technical College of Shahid Bahonar University of Kerman, Iran in the field of Electronics Engineering.

Using the scholarship which was granted by YÜKSEK-ÖĞRETİM KURULU, in 1987 he has been studing for the degree of M.Sc in the Faculty of Electrical and Electronic at the Istanbul Technical University.